Direct Plasma Interaction

with Living Tissue

A Thesis
Submitted to the Faculty
of
Drexel University
by
Gregory Fridman
in partial fulfillment of the
requirements for the degree
of
Doctor of Philosophy

September 2008

© Copyright 2008

Gregory Fridman. All Rights Reserved

ACKNOWLEDGEMENTS

I would like to sincerely thank my thesis advisors for all their help throughout the time of my doctoral studies. My colleagues, coworkers, and friends were also an integral part of my development and without the help of all who surround me I would have never been able to complete this work.

I would especially like to thank all the people at Drexel University's School of Biomedical Engineering, College of Engineering, College of Medicine, Drexel's Machine Shop staff, University of Pennsylvania's Micro-Fabrication Facility staff, and UPenn School of Veterinary Medicine. Much appreciated is the valuable advice from the members of Drexel University's Institutional Animal Care and Use Committee (IACUC), Institutional Review Board (IRB), representatives of the Food and Drug Administration (FDA), Drexel's office of Technology Commercialization, Knoble Yoshida & Dunleavy LLC, and Woodcock Washburn LLP.

Finally, I would like to acknowledge the financial support this work received from the Ben Franklin Technology Partners, Wallace H. Coulter Foundation, National Science Foundation (NSF), Defense Advanced Research Projects Agency (DARPA), and Bayshore Holdings LLC.

ABSTRACT

Direct Plasma Interaction with Living Tissue
Gregory Fridman
Dr. Gary Friedman, Dr. Kenneth Barbee

For some time, plasma has been used in medicine to cauterize or cut tissue using heat and mechanical energy. In the recent decade, some researchers around the world have started to investigate how gas jets that pass through thermal plasma can be employed in medicine. This thesis presents the first investigation of biomedical uses of non-thermal plasma discharge which comes in direct contact with living tissue. It is demonstrated that the direct application of non-thermal plasma in air can cause rapid deactivation of bacteria on surfaces of tissues without causing any visible tissue damage. Medical need for such a device is discussed. Construction and operation of various types of non-thermal plasma power supplies and many types of treatment electrodes are presented as well. Application of this plasma to living organisms is shown to be safe from both the electrical perspective and from the biological perspective. Biological safety is revealed through a series of differential skin toxicity trials on human cadaver tissue, live hairless mouse skin tissue, live pig skin tissue, and finally in an open wound model on pigs. Direct non-thermal plasma in air is shown to deactivate bacteria about 100 times faster than indirect application using jets. A series of experiments reveal that this effectiveness is due to the ability of direct discharge to bring charges to tissue surfaces. It is demonstrated that neither ultraviolet (UV) radiation nor neutral active species such as hydroxyl radicals or ozone produced in plasma are responsible for the main effect on bacteria. Although

much additional work remains on establishing detailed mechanism by which charges from plasma achieve this effect, the work carried out in this thesis clearly demonstrates that direct application of non-thermal plasma in air can be a very useful tool in medicine.

CONTENTS

Acknowledgements ii

Abstract iii

List of Figures viii

List of Tables xv

Chapter 1. Direct Non-Thermal Plasma Medicine versus Conventional Thermal and Jet Plasma Treatment of Living Tissue 1

1.1. Sterilization of Non-Living Objects for Medical Applications: a Review 5

1.2. Plasma-Assisted Wound Healing and Tissue Regeneration: Discharge Systems for Air-Plasma Surgery and Nitrogen Oxide (NO) Therapy 9

1.3. Non-Thermal Plasma Treatment of Various Diseases 14

1.3.1. Non-Equilibrium Pulsed Spark Plasma Jet 14

1.3.2. Non-Equilibrium “Plasma Needle” Treatment 17

1.3.3. Indirect 6-Electrode Thermal Microwave Plasma Torch System 19

1.4. Review Summary of Non-Equilibrium Plasma Applications in Medicine 21

Chapter 2. Device for Direct Non-Damaging Application of Plasma to Living Tissue: Floating Electrode Dielectric Barrier Discharge (FE-DBD) 23

2.1. Principle of Operation of the Floating Electrode Dielectric Barrier Discharge. 24

2.2. Application of FE-DBD Plasma to Biological Objects 26

2.3. Observation of the FE-DBD Plasma 28

Chapter 3. Direct Non-Equilibrium Plasma Application for Skin Sterilization; Effectiveness of Direct versus Indirect (Jet) Plasma Treatment 31

3.1. Quantitative Direct Sterilization on Agar 31

3.2. Comparison of Direct and Indirect Sterilization in Open Air 34

3.2.1. Direct and Indirect Plasma Setup Employing Mesh to Separate the Effect 38

3.2.2. Direct and Indirect Plasma Setup Employing Gas Flow (Blower) to Separate the Effect 41

3.2.3. Results of Direct and Indirect Treatment in Ambient Air 42

3.3. Effects of UV Radiation, Applied Electric Field, Thermal Energy, and Other Indirect Plasma Effects 50

3.4. Direct and Indirect Plasma Treatment in Various Gases 54

3.5. Effect of Localized High Electric Fields and Effect of Heating 56

3.6. Summary of Direct with Indirect comparison of FE-DBD Plasma Application to Tissue 65

Chapter 4. Direct Non-Damaging Treatment by Non-Equilibrium Plasma of Living Tissue: Toxicity Trials 67

4.1. Skin Toxicity Trials on Human Cadaver Tissue 69

4.2. Skin Toxicity Trials on Live Hairless Mice 72

4.3. Skin Toxicity Trials on Live Regular Swine 78

4.4. Wound Toxicity Trials on Live Regular Swine 83

4.5. FE-DBD Treatment of Living Tissue: Next Steps 90

Concluding Remarks 95

List of References 97

Vita 119

LIST OF FIGURES

Figure 1. Photograph of the Floating Electrode Dielectric Barrier Discharge (FE-DBD) plasma in direct contact with living tissue. 3

Figure 2. A principal schematic of the plasma needle setup [18]. 18

Figure 3. A void created in a cell culture, grown on a Petri dish. At the incidence of the plasma needle, the cells are removed (suspended in the medium and washed away) [18]..19

Figure 4. Microwave plasma torch schematic (left) and plasma output photo (right) [105]. 20

Figure 5. Bacterial cultures on agar plates after 2 minutes of plasma treatment. Left: methicillin-resistant Staphyolococcus aureus (gram positive) Right: Burkholderia cepacia (gram negative) [104].....21

Figure 6. Histological images of skin samples, treated ex-vivo. After 2 minutes no changes could be observed with respect to the untreated control sample. Vacuolization of keratinocytes can be observed after 10 minutes [104]. 21

Figure 7. Simplified electrical schematic of a) electrode itself, b) electrode near the treated object, and c) plasma discharge on the treated object. 25

Figure 8. General schematic of the plasma treatment experimental setup.....27

Figure 9. Principal schematic of the FE-DBD treatment setup with removable meshes and windows. In this setup either agar with bacteria (shown), cell culture, or living tissue can be treated. 28

Figure 10. Side view of plasma over the surface of water at different exposure times. 29

Figure 11. Water electrode setup schematic. 30

Figure 12. 0.004 sec (left) and 0.2 sec (right) exposures of the FE-DBD plasma in dry air (from gas tank) at 3 slpm flow rate with sinusoidal excitation wave.....30

Figure 13. Photograph of the blood agar Petri dish following 24 hour incubation period of bacterial sample treated by FE-DBD plasma for 10 seconds: plasma-agar contact area is completely clean of bacterial colonies, area outside of plasma shows partial inactivation, and the rest of the Petri dish shows complete coverage with bacterial colonies.....34

Figure 14. A 3-dimentioan representation and schematic of the electrode with controlled atmosphere. 39

Figure 15. Schematic of treatment of bacteria on blood agar and the electrode footprint generated by this method. 39

Figure 16. Schematic of the direct/indirect treatment setup in the “direct” mode without the grounded mesh: plasma contacts bacteria directly.....40

Figure 17. Schematic of the direct/indirect treatment setup in the “indirect” mode with the grounded mesh: plasma is bound by the mesh and only the plasma afterglow can reach the surface of bacteria. 41

Figure 18. Schematic of the direct/indirect treatment setup with blower used to create the indirect treatment effect of the plasma afterglow. 42

Figure 19. Photograph of the setup used for direct/indirect experiment with using the blower to move air through plasma.....42

Figure 20. Using a blower to shift sterilization region does not affect plasma and shows little effect of the afterglow: 15 seconds of treatment with (a) blower off and (b) blower on

(air flows up). Note: arrow is painted on the back of the dish and shows through on the photograph. 46

Figure 21. Zoomed in photograph of the bacterial growth results following plasma treatment and incubation (photograph is converted to black and white for increased contrast). Note: arrow is painted on the back of the dish and shows through on the photograph. 46

Figure 22. Results of measurement of light intensity in the visible spectrum for no mesh, fine mesh, and coarse mesh.....48

Figure 23. Results of measurement of light intensity in the ultraviolet spectrum measured at three peaks (239.5 nm, 263.54 nm, and 284.03 nm) without mesh (taken as 100%) and with mesh. 49

Figure 24. Direct application of plasma yields to better sterilization efficiency than treatment by plasma afterglow: (a) 5 seconds and (b) 15 seconds of direct plasma compared with (c) 30 seconds and (d) 2 minutes of plasma jet. 50

Figure 25. Emission from DBD plasma over the cell surface in UV range.....51

Figure 26. No effect on bacteria protected from plasma by MgF_2 slide (10 mm square in the center) is observed.....52

Figure 27. Grounded mesh placed directly on bacteria (no space) generates interesting pattern: only mesh openings are sterilized (magnified area is color-corrected for clarity). 53

Figure 28. Identification of different areas under the FE-DBD electrode following the plasma treatment and 24-hour incubation: (1) under the electrode, (2) outside of the electrode but inside of the treatment area bound by legs, (3) inside of the gas channel, (4)

immediately outside of the gas channel, and (5) outer parts of the dish not in the direct gas path. 55

Figure 29. Avalanche transition to streamer [162]. 57

Figure 30. Rotational and vibrational temperature measurements from a model fit to 2nd positive Nitrogen system; please note, "modeled data" curve was intentionally raised, otherwise it is invisible since the curve-fit is nearly perfect. 60

Figure 31. Photograph of plasma through water electrode. 1/3 second (0.33 sec) shutter open time. 60

Figure 32. Photograph of plasma through water electrode. 1/320 second (0.0031 sec) shutter open time. 61

Figure 33. Oscillogram of the nanosecond pulse voltage and current. Voltage rises to ~ 30 kV in ~ 10 ns, or 3,000 V/ns. 63

Figure 34. Diagram of a setup to capture a *single* pulse of Dielectric Barrier Discharge plasma on photographic film. 63

Figure 35. Image produced on black and white photographic film (100 ISO sensitivity negative film) by a single nanosecond pulse of DBD plasma. 64

Figure 36. Image produced on black and white photographic film (100 ISO sensitivity negative film) by a single microsecond pulse of DBD plasma. 65

Figure 37. Photograph of the FE-DBD treatment electrode with a "jacket" which allows for control of distance between electrode and treatment target. 69

Figure 38. Photographs and schematics of the results of 2 minutes of FE-DBD plasma treatment at 1.6 W/cm^2. Skin is laying on metal surface which leads to uncontrollable results: uniform treatment is some cases (top) and non-uniform in others (bottom). 70

Figure 39. Schematic of the tissue treatment setup with vacuum suction and zoom photographs of the vacuum holder perforations.....70

Figure 40. Vacuum suction treatment setup in operation during plasma treatment.....71

Figure 41. Photos (top) and tissue histology (bottom) of cadaver skin samples after FE-DBD treatment: control (left), 15 seconds of treatment (center), and 5 minutes of treatment (right) – no visible damage is detected. 72

Figure 42. Photograph of a regular mouse during hair shaving procedure. Post shaving the skin appears to be quite irritated and thus the model is not usable for a skin toxicity trial. 73

Figure 43. Photograph of a Charles River Laboratories SKH1 hairless mouse immediately after arrival at the animal care facility. 74

Figure 44. Photograph of two power supplies (microsecond pulsed and continuous sinusoidal) with the small 10 mm diameter electrode for treatment of mouse skin. 75

Figure 45. Schematic of the 10 mm diameter copper electrode with attached perforated spacer for controlled treatment of a mouse. 75

Figure 46. Photograph of an animal immediately following treatment. The perforated spacer is left on the area of treatment to mark it for later sample harvesting. Areas 1 and 2 have already been treated, in this particular case for 75 seconds at 0.3 Watt/cm^2 surface power density by microsecond pulsed power supply. No damage to skin is observed visually. 76

Figure 47. Histology of toxic and non-toxic to SKH1 skin plasma doses, compared to untreated skin. 77

Figure 48. Animal remains fine immediately after a high plasma dose (more than 10 times higher than needed for skin sterilization). 77

Figure 49. Animal remains fine two weeks following a high plasma dose (more than 10 times higher than needed for skin sterilization). 78

Figure 50. 3D schematic of the electrode used for swine skin experiments. 79

Figure 51. Photograph of the modified FE-DBD electrode attached to animal skin using tape. 80

Figure 52. Photograph of the animal skin prior (left) and immediately following a 10-minute FE-DBD treatment at low frequency Setting #1 (right). A mild skin inflammation is visible immediately after the treatment (shown) which disappears within a few minutes following the treatment (not shown). Black markings on the skin indicate position of the edge of the treatment electrode (for skin sample harvesting purposes). 81

Figure 53. H&E histological stain of the skin sample treated for 10 minutes at low frequency Setting #1 (Figure 52). No microscopic damage to skin can be seen. 82

Figure 54. Photograph of the animal skin immediately following treatment by Bovie® knife (positive control) – excessive skin damage, desiccation, and inflammation are clearly visible. 83

Figure 55. Photograph of a process of making a partial thickness skin wound with a dermatome knife (left) and a zoomed in photograph of the resulting wound immediately prior to the FE-DBD plasma treatment. 85

Figure 56. Photograph of a positive control treatment with Bovie® knife (left) where the tissue is clearly desiccated and blood is clotted but the tissue damage is quite extensive. Compared to a photograph of a wound treated by FE-DBD plasma for 15 minutes in low power Setting #1 (right) where no significant tissue damage is observed and a layer of coagulated blood is formed over the wound surface.....86

Figure 57. Results of H&E histological stain for samples described in Table 6. 88

Figure 58. Results of H&E histological stain for samples described in Table 7. 90

LIST OF TABLES

Table 1. Dependence of the current density and ion concentration of the Xenon plasma flow on the distance [22].....15

Table 2. Results of Staphylococcus inactivation by air plasma [22]. 15

Table 3. Bacteria sterilization results (in cfu/mL) 32

Table 4. Results of treatment of bacteria by FE-DBD plasma in different gases. Areas of treatment are identified in Figure 28. Note: all experiments are repeated in triplicate and the results presented here are averaged. 55

Table 5. Plasma power supply settings used in the swine skin treatment experiments. 80

Table 6. Results and analysis of FE-DBD plasma treatment of wound surface. 86

Table 7. Results and analysis of FE-DBD plasma treatment of wound surface. 88

CHAPTER 1. DIRECT NON-THERMAL PLASMA MEDICINE VERSUS CONVENTIONAL THERMAL AND JET PLASMA TREATMENT OF LIVING TISSUE

In physical sciences, “plasma” refers to the forth state of matter; while in medicine and biology “plasma” is mostly known as the non-cellular fluid component of blood. Interestingly, the term plasma has been coined by Irving Langmuir to emphasize that the characteristics of ionic liquids ubiquitous in biology and medicine are analogous to those of ionized gas [1]. Despite this historical connection, few applications of plasma in medicine have been explored until recently [2]. This situation is rapidly changing, and in this thesis we will discuss a new non-thermal atmospheric pressure plasma system which can effectively inactivate bacteria on human tissue without damaging it.

Plasma can exist in a variety of forms and can be created in different ways. In many technological applications, for example, plasma exists at low gas pressures. Lightning, on the other hand, is an example of atmospheric pressure thermal plasma. For the purpose of this work it is important to distinguish between thermal and non-thermal plasma. In all plasmas supported by electric field, electrons receive the external energy much faster than much heavier ions. Electrons have the opportunity to heat up to several thousands of degrees before their environment heats up. In *non-thermal* plasma, cooling of ions and uncharged molecules can be highly effective compared with the energy transfer from electrons. As a result, gas remains at low temperature. Since electrons and gas are at very different temperatures, non-thermal plasma is also called non-equilibrium plasma. In *thermal* plasma, on the other hand, energy flux from electrons to heavy particles

equilibrates the energy flux from heavy particles to the environment only when temperature of heavy particles becomes almost equal to the electron temperature. Of course the terms thermal and non-thermal, equilibrium and non-equilibrium are not very precise. Sometimes even a few tens of degrees difference in the temperature of the heavier species can play a substantial role. This is particularly important when various plasma-chemical processes are considered. It is certainly important when plasma is used to treat heat sensitive objects.

Some of the earlier applications of plasma in medicine relied mainly on the thermal effects of plasma. Heat and high temperature have been exploited in medicine for a long time for the purpose of tissue removal, sterilization and cauterization (cessation of bleeding) [3]. Warriors have cauterized wounds by bringing them in contact with red hot metal objects since ancient times. Electrocautery is a more modern technique which applies controlled heat to surface layers of tissue by passing sufficiently high current through it [4]. However, contact of tissue with metal surface of a cautery device often results in adhesion of charred tissue to the metal. Subsequent removal of the metal can peel the charred tissue away re-starting bleeding. Some of the earlier applications of plasma in medicine provided an alternative to metal contact electrocautery. In argon plasma coagulation (APC, also sometimes called argon beam coagulation) highly conductive plasma replaced the metal contacts in order to pass current through tissue avoiding the difficulties with tissue adhesion. Hot plasma is also being employed to cut tissue [3, 5-8], although the exact mechanism by which this cutting occurs remains unclear. Heat delivered by plasma has also been employed recently for cosmetic re-structuring of tissue [9-11].

What differentiates more recent research on applications of plasma in medicine is the exploitation of non-thermal effects. Why are non-thermal effects of plasma so interesting and promising? The main reason is that non-thermal plasma effects can be tuned for various sub-lethal purposes such as genetic transfection [12-14], cell detachment [15-18], wound healing [19-23], and others (i.e., [2, 24, 25]). Moreover, non-thermal effects can be selective in achieving a desired result for some living matter, while having little effect on the surrounding tissue (Figure 1). This is the case, for example, with recent plasma blood coagulation and bacteria deactivation which does not cause toxicity in the surrounding living tissue [19, 20].

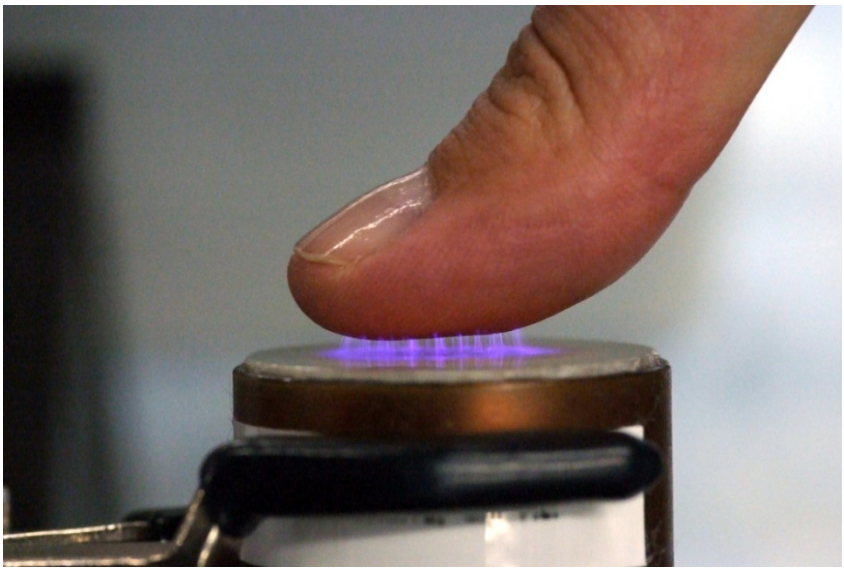


Figure 1. Photograph of the Floating Electrode Dielectric Barrier Discharge (FE-DBD) plasma in direct contact with living tissue.

Most of research focusing on the use of non-thermal plasma effects in medicine can be fit into two major categories: that are *direct* plasma treatment and *indirect* plasma treatment. Direct plasma treatment has been pioneered at Drexel University (see Fridman, Shekhter,

Vasilets, et al, 2008 [26]). In direct plasma treatment living tissue or organs play the role of one of the plasma electrodes. Voltage does not need to be directly connected to this living tissue electrode, but some current may flow through living tissue in the form of either a small conduction current, displacement current or both. Conduction current should be limited in order to avoid any thermal effects or electrical stimulation of the muscles. Direct plasma treatment may permit a flux of various active uncharged species of atoms and molecules as well as UV radiation to the surface of the living tissue. These active uncharged species generated in plasma will typically include ozone (O_3), NO, OH radicals, etc. However, the most important distinguishing feature of the direct plasma treatment is that a significant flux of charges reaches the surface of the living tissue. These charges may consist of both electrons as well as positive and negative ions.

In contrast, indirect plasma treatment employs mostly uncharged atoms and molecules that are generated in plasma, but involves small, if any, flux of charges to the surface. In indirect treatment the active uncharged species are typically delivered to the surface via flow of gas through a plasma region.

Both indirect and direct non-thermal plasma treatments permit some degree of tuning of the plasma properties [27]. For example, the amount of NO vs. ozone produced in plasma can be tuned. It is also possible to tune micro-structure of the plasma discharge which can be particularly relevant in direct treatment. The fact that direct plasma treatment involves substantial charge flux provides greater flexibility in tuning the non-thermal plasma effects. Indirect plasma treatment, on the other hand, may have an advantage when the plasma device needs to be at a substantial distance from the surface.

In this chapter we will discuss current status of various plasma systems from many research groups around the world in their applications to medicine. The mode of operation of these plasmas will be specifically pointed out: is the plasma thermal or not, how is it generated, and what are some of the benefits and drawbacks.

1.1. Sterilization of Non-Living Objects for Medical Applications: a Review

Traditionally, sterilization or treatment of non-living objects like metals, plastics, fabrics, and other surfaces have been carried out either by temperature (i.e., autoclaves [28-31]), liquid or gaseous chemistry (i.e., by ethylene oxide [32, 33], ozone [34, 35], chlorine [36, 37], etc.), or at reduced pressure by non-equilibrium plasmas [38, 39]. Details of such approaches are widely available in literature. Here we will focus on medical application of non-equilibrium plasma at atmospheric pressure and surface sterilization of materials cannot then be overlooked because, after all, these materials later come in contact with living tissue either as implants, dressings, tools, etc.

Drs. Alexeff and Laroussi and their colleagues reported a rather interesting modification of a conventional dielectric barrier discharge – a Resistive Barrier Discharge (RDB) [2, 40, 41]. Main feature of the RDB is that is can function in both DC and AC modes, and rather than a dielectric a wetted high resistivity material is used. RDB has been shown to be effective in sterilization of *E. coli*, *B. subtilis*, and other organisms [2, 41, 42] without significant damage to the surface being processed. Going back to a more traditional DBD system, Laroussi and his colleagues [43-46] show that a barrier discharge in helium with

small additions of oxygen is not only able to sterilize bacteria but is able to influence metabolic changes in the organisms surviving the treatment [44]. This raises an intriguing question – can plasma-resistant bacteria emerge? Due to synergetic effect of plasma constituents on bacteria, plasma-resistance might not be possible or statistically probable, however, the authors think that this issue might become rather important in the near future and should be addressed. Two more discharges are studied by Dr. Laroussi and colleagues: plasma plume (a helium jet) [47, 48], and an arc-like discharge between metal and water in air [49, 50]. Both discharges are also reported to efficiently inactivate various micro-organisms.

Dr. Massines and her colleagues propose a DBD discharge in N_2/N_2O mixture for micro-organism inactivation (i.e., *B. subtilis* spores) [51-53]. Operated at atmospheric pressure, her results indicate a very high dependence of the inactivation efficiency on UV, which is somewhat contrary to results presented by other groups [51]. In fact, the difference is attributed to the fact that the gas composition necessary to achieve the best results is in a very narrow concentration range of the oxidant molecule, which might have simply been overlooked previously. Though this study offers good information on UV, a real-life environment might need a system that is slightly less picky as to the gas mixture concentration ranges. However, one needs to account for effects of ultraviolet radiation on bacteria as apparently they cannot be neglected, even in plasmas where doses of UV are lower than in that proposed by Dr. Massines [51].

Microplasmas have recently been gaining momentum in bio-medical applications. These systems of 10-500 μm characteristic dimensions capable of generating diffuse atmospheric

pressure plasmas offer an interesting solution in, for example, medical diagnostics and environmental sensing. Dr. Becker and colleagues [54, 55] offer a few different microplasma sources suitable for remediation of gaseous waste streams, removal of volatile organic compounds (VOCs), detection of trace contaminants in gas flow, generation of high intensity ultraviolet (UV) radiation, and sources suitable for micro-sized plasma-reactors. Though the temperature of these discharges can be at or near room temperature in noble gases, when a molecular gas (i.e., air) is used plasma temperatures can be high, on the order of 2,000 K. Dr. Becker et al. show efficient inactivation of *B. subtilis* spores (1 log reduction in ~100 seconds) and *B. stearothermophilus* spores (1 log reduction in ~90 seconds) without damage to the substrate; more interestingly they are able to inactivate bio-films of *Chromobacterium violaceum* CV026 achieving 2 log reduction in ~ 5 minutes and 3 log reduction in ~60 minutes of plasma afterglow treatment [54]. In general, these microplasmas have not yet found a niche in medicine directly through many potential applications are clearly possible and the reader is encouraged to take a look at a review of the recent developments in that field [55].

Dr. Roth and his colleagues have developed a one atmosphere uniform glow discharge plasma (OAUGDP) system capable of addressing a broad range of potential applications [56-62]. OAUGDP is a DBD-like bipolar RF plasma discharge operated in air or other gases. The list of potential applications where experimental evidence is very favorable includes increasing surface energy and wettability of fabrics, films, and solid surfaces; sterilization of various surfaces for healthcare and food processing; decontamination of surfaces compromised by chemical or biological warfare agents; a sterilizable air filter to

deal with the sick building syndrome [63]; removal of soot and volatile organic compounds from Diesel engine exhaust; mercury-free atmospheric pressure fluorescent lamps; stripping of photoresist and directional etching in microelectronics; plasma assisted chemical vapor deposition; and plasma aerodynamic flow control. For details on these applications reader is encourages to consult a recent publication by Dr. Roth et al. [60]. Of note, however, is a less recent publication from Dr. Roth's group comparing sterilization efficiency of their system against a multitude of bacteria, yeasts, and viruses [57]. D-values, or time to 90% reduction in micro-organism load, are ranging from 6 seconds for *E. coli* bacteria to 6.8 minutes for Bacteriophage Phi X 174 virus. Additionally survivability of these organisms on different substrates is addressed comparing glass, agar, and polypropylene with the later showing highest survival times. In general, OAUGDP was not reported to be used in medicine directly; however, sterilization of medical instruments and other surfaces found in the hospital as well as air sterilization in an operating room is on the list of potential medical applications [60].

Dr. Kong and his colleagues have investigated inactivation of various organisms by pulsed electric field [64], and, primarily, by He/O_2 RF plasma afterglow (or jet) [65-74]. Ability of their plasma setup to inactivate *B. subtilis* spores [65, 69] and various *E. coli* mutants [70] does not come as a surprise, however the results on inactivation of biofilm-forming bacteria are quite intriguing. Dr. Vleugels et al. [72] have successfully achieved inactivation of biofilm-forming *Pantoea agglomerans* in sterilization of foods, specifically of bell peppers (*Capsicum annuum*). He/O_2 plasma afterglow was shown to effectively inactivate the biofilm without causing unacceptable levels of discoloration to the peppers

[72]. Detailed analysis of this system reveals that the primary role in inactivation is played by reactive oxygen species (e.g. atomic oxygen and OH) with minor aid from UV photons, charged particles, heat, and electric fields [65, 68, 70, 71, 73, 74]. Another interesting idea is not only sterilization of various surfaces but complete decontamination of them with removal not only of bacterial load but of the remaining protein debris. Deng et al. show that this RF plasma jet treatment can effectively remove proteins from surface of medical instruments, achieving up to 4.5 log reduction [66, 67]; here, again, reactive oxygen species are deemed to be the major inactivation factors.

1.2. Plasma-Assisted Wound Healing and Tissue Regeneration: Discharge Systems for Air-Plasma Surgery and Nitrogen Oxide (NO) Therapy

Effective use of hot plasma in surgery has been first demonstrated in 1960s: plasma afterglow jet of an inert gas has been applied for tissue sectioning with instant blood coagulation. Because of that plasma-surgical devices got a long-standing name of “plasma scalpel” in the hospitals (see, for example, Glover et al. [75]). An example plasma of a thermal plasma used in surgery for wound healing and tissue regeneration is the “Plazon” system based on the jet of hot air plasma rapidly quenched which provides relatively high NO concentration with significant therapeutic effect [76, 77]. This plasma device is used in two modes. In the first “hot mode” plasma jet is used for rapid coagulation and sterilization of wound surfaces, destruction and desiccation of dead tissue and pathologic growths, dissection of biological tissues. In the second “cold mode” NO-containing plasma gas flow

with temperature of 20 to 40°C is used for stimulation of regenerative processes and wound healing.

The “Plazon” generators [21, 76, 77] are the DC arcs with different configurations of the exit channels corresponding to the different applications (blood coagulation, tissue destruction, therapeutic manipulation/stimulation). Main and common elements of the system construction are the liquid-cooled cathode, intra-electrode insert, and anode. Atmospheric air enters the manipulator through the built-in micro-compressor, passes through the plasma arc, heats up and thus accelerates, and exits through the hole in the anode of the plasma-generating module. Plasma temperature at the anode exit differs in different configurations of the device, corresponding to different medical applications. Further away from the anode, temperature drops rapidly, and at 30-50 mm from the anode, the flow is composed simply of the warm gas, and the plasma-generated NO. Nitrogen oxide content in the gas flow is mainly determined by the quenching rate. The necessary quenching rate for effective operation of the medical device is about $\sim 10^7$-10^8 K/sec. Commonly, the cooling rate of plasma jets is on the order of $\sim 10^6$ K/sec. Thus, to achieve the cooling rate of $\sim 10^7$-10^8 K/sec, it is necessary to utilize additional cooling of the plasma jet, which has been achieved by special construction of the plasma nozzles.

The therapeutic manipulator-stimulator configuration of the “Plazon” discharge system is used solely for therapeutic treatment by exogenic nitrogen oxide. The principle difference of this manipulator is that the air-plasma jet does not freely exit into the atmosphere, but rather it exits the anode into the two-step cooling system, gas channels of which are created in a maze scheme to force-cool the jet by the liquid circulating from the cooling system.

This construction allows one to obtain NO-containing gas flow (NO-CGF) with sufficiently low temperature, and optimal concentration of nitrogen oxide molecules, which makes it possible to apply this manipulator for treatment of external body surfaces by using the cooling hose of 150 mm length (temperature of NO-CGF at the exit ~36 °C). Of course, NO content in the gas flow depends on the distance from the exit channel. Additionally, for laparoscopic operation, a special manipulator of 350 mm length and 10 mm diameter is utilized.

The possible operating regimes of the apparatus are defined by the characteristics of the gas flow exiting from the manipulator, main parameters of which are its temperature and the nitrogen oxide content. First group of regimes – regimes of free-flowing plasma off-gas exiting the manipulator; second group of regimes – regimes of treatment of bio-tissues by completely cooled (20ºC) NO-containing gas flow, to obtain which a manipulator is connected to the internal gas cooler, and delivery of NO-CGF to bio-tissues is achieved through a silicone tube with an attached tip of 130 or 390 mm length, and the exit channel diameter of 0.7 mm. This allows not only direct treatment of the bio-tissues by NO, but also its delivery to a pathologic center through drainage tubes, puncture needles, or any endoscopic devices (gastroscope, broncoscope, cystoscope, rectascope, etc).

The Nobel Prize in medicine and biology was awarded in 1998 to R. F. Furchgott, L. J. Ignarro, and F. Murad for their work in investigation of function of nitrogen oxide as a signal molecule [78]. Today it is well known that in a human organism, NO serves a multitude of essential biological functions – it regulates blood vessel tone (via relaxation of flat epithelial cells) and blood coagulation, immune system and early apoptosis, neural

communication and memory, relaxation of flat bronchial and gastrointestinal muscles, hormonal and sex functions, NO offers antimicrobial and antitumor defense, etc. In pathology, NO plays a major role in adaptation, stress, tumor growth, immunodeficiency, cardiovascular, liver, and gastrointestinal tract disease, etc. This explains wide possibilities of the plasma-generated exogenic NO in multiple medical applications.

Importance of exogenic NO in infection and inflammation processes is also well studied and is linked with antimicrobial effects; stimulation of macrophages; induction of cytokines, T-lymphocytes, and many immunoglobulins; interaction with oxygen radicals; and influence on microcirculation, cytotoxic and cytoprotective role in different conditions. During inflammation, macrophages and some other cells (i.e. aibroblasts, epithelial cells, etc.) produce NO via inducible NO-synthase (iNOS) in quantities significantly greater (2 orders of magnitude) than normal when NO is formed via constructional NOS: endothelial (eNOS) and neuronal (nNOS).

Exogenic NO is also crucial in trauma wound processes. Activity of inducible NO-synthase (iNOS) grows substantially in trauma wounds, burn wound tissues, bone fracture site tissues, and others in the inflammatory and proliferation phases of the healing process. Activation of iNOS was also discovered in cultivation of wound fibroblasts. Macrophage activation in a wound, cytokine synthesis and proliferation of fibroblasts, epithelization and wound healing processes are all linked with the activity levels of iNOS. In animal models, injection of iNOS inhibitors disrupts all of these processes and especially the synthesis of collagen, while NO synthesis promoters increase the rate of these processes.

Animals with iNOS deficiency demonstrate significant decrease in wound healing rate, however this can be reversed by injection of iNOS gene. In complicated wound models, for example in experimentally-induced diabetes, protein deficiency, injection of corticosteroids or immunosuppressants, and also in patients with tropic ulcers, lowered activity of iNOS is usually discovered which correlates to slowed healing processes. Exogenic delivery of NO-donors (nitrogen-containing compounds) to the wound promotes and speeds up healing processes in animals with complicated wounds and in animals with inhibited iNOS. This knowledge, coupled with theoretical and experimental data on NO generation in air plasmas, served as a basis for a series of bio-medical experiments focused on use of the plasma-generated exogenic NO, delivered directly to the pathologic site, for control of inflammatory processes and increase in the rate of wound healing.

Possibility of directing of the plasma-generated NO-containing gas flows through puncture needles, vent lines, and endoscopic instruments, and also the inhalation method of action considerably enlarges prospects for the plasma NO-therapy in treatment of the ulcero-necrotic, erosive and inflammatory processes in the pleural and abdominal cavities, lungs, stomach and bowels, ear nose and throat (ENT) organs (purulent sinusitis, purulent otitis media, paratonsillar abscesses), etc. Effectiveness of the plasma NO-therapy is already at present shown with a number of diseases in pulmonology [79], phthisiology [80], traumatology and orthopedics [21, 81], gynecology [82-84], dentistry [85], maxillofacial surgery [21], ophthalmology [86], otorhinolaryngology [87], dermatology [88], gastroenterology [89], purulent peritonitis [81], and in other applications discussed in further detail in our recent review [26].

1.3. Non-Thermal Plasma Treatment of Various Diseases

1.3.1. Non-Equilibrium Pulsed Spark Plasma Jet

A special micro-plasma jet system has been developed by our collaborators for local medical treatment of skin diseases, and especially for treatment of corneal infections (see Fridman, Shekhter, Vasilets, et al, 2008 [26]). The device allows generation of plasma flows with average gas temperature not exceeding 30-40°C [22, 26]. It consists of a coaxial cathode and needle-like anode, which is fixed in metal capillary. The gas is fed through the capillary to the discharge gap. The anode is connected with the positive lead of the power source and the cathode is grounded. The discharge appears on the nozzle output if the pressure on the nozzle input is higher than the atmospheric pressure. The discharge is a specific plasma sphere with the diameter ~4 mm, atmospheric air or xenon are fed through the capillary at 0.2-0.5 atm, the discharge voltage is 1-3 kV, the pulse duration is about 50 μs, the total power was kept on the order of 1-2 W.

The medical micro-plasma operated in Xe radiates intensively in the UV range, and operated in air it generates excited oxygen species, ozone, oxides of nitrogen, and OH radicals [22]. Both regimes have bactericidal effects and air plasma is able also to aid in tissue regeneration via the NO-therapy mechanisms discussed above. UV-radiation of Xe plasma in this case is: UVA (315-400 nm) 180 $\mu W/cm^2$, UVB (280-315 nm) 180 $\mu W/cm^2$, and UVC (200-280 nm) 330 $\mu W/cm^2$. UV-radiation of air plasma is: UVA (315-400 nm) 53 $\mu W/cm^2$, UVB (280-315 nm) 25 $\mu W/cm^2$, and UVC (200-280 nm) 90 $\mu W/cm^2$. Results

of probe measurements of current density, velocity, and ion concentration at different distances from the exit nozzle are shown in Table 1.

Table 1. Dependence of the current density and ion concentration of the Xenon plasma flow on the distance [22].

Distance, mm	1	1.3	2	3
Current density, mA/cm^2	2040	2000	240	60
Velocity, cm/sec	$2\cdot10^4$	$1.8\cdot10^4$	$1.2\cdot10^4$	$7\cdot10^3$
Ion concentration, cm^{-3}	$6.4\cdot10^{14}$	$3.7\cdot10^{14}$	$1.5\cdot10^{14}$	$5.3\cdot10^{13}$

Ability of the medical micro-plasma system to sterilize surface has been demonstrated by Misyn et al. [90-93]. Staphylococcus cultures in liquid media (~$2\cdot10^6$ cfu/ml) have been treated by the air plasma plume of 3 mm diameter, incubated for 24 hours, and counted (Table 2).

Table 2. Results of Staphylococcus inactivation by air plasma [22].

Culture volume, ml	Plasma exposure time, sec			
	0 (control)	25	50	100
1	$2\cdot10^6$ cfu	0 cfu	0 cfu	0 cfu
2	$4\cdot10^6$ cfu	25 cfu	0 cfu	0 cfu
3	$6\cdot10^6$ cfu	$1\cdot10^6$ cfu	680 cfu	460 cfu

A 6-log reduction in viable bacteria is achieved in 25 seconds of treatment; however the sterilization efficiency drops off with increasing volume of liquid which inhibits UV penetration and diffusion of active species generated in plasma. Nevertheless, the micro-plasma system should be a good solution for treatment of living human and animal skin as the bacteria are normally at much lower concentrations on skin ($<<10^5$ cfu/cm^2 of skin surface [94]).

A series of in vitro experiments on bacterial cultures and in vivo experiments on rabbit eyes [93] affirm the strong bactericidal effect of the micro-discharge with minimal and reversible changes, if any, in biological tissues, even in such delicate tissues as cornea. During the investigation of plasma treatment of ulcerous dermatitis of rabbit cornea two important observations were made: 1) plasma treatment has a pronounced and immediate bactericidal effect, and 2) the treatment has an effect on wound pathology and the rate of tissue regeneration and wound healing process.

These results offered a strong ground for application of the medical micro-plasma system for treatment of human patients with complicated ulcerous eyelid wounds, which is shown in [93]. Necrotic phlegm on the surface of the upper eyelid was treated by air plasma plume of 3 mm diameter for 5 seconds once every few days. By the 5^{th} day of treatment (two 5-second plasma treatment sessions) the eyelid edema and inflammation were reduced; and by the 6^{th} day (third session) the treated area was free of edema and inflammation and granular tissue appeared. Three more plasma treatments were administered (six total), and the patient was discharged from the hospital six days following the last treatment. The micro-plasma treatment is being further developed for stimulation of reparative processes in various topical wounds, tropic ulcers, chronic inflammatory complications, and other diseases of soft tissues and mucous membrane [93].

1.3.2. Non-Equilibrium "Plasma Needle" Treatment

A radio frequency plasma source, a *plasma needle*, was recently developed by E. Stoffels et al. [18, 95-97]. Plasma needle is a flexible hand-held device (Figure 2) consisting of a 0.3 mm diameter needle, 0.8 mm diameter Perspex tube, 10 cm in length. The plasma is generated at the end of the needle at the applied frequency of 13.56 MHz. This device was successfully demonstrated in treatment of various cell lines and inactivation of bacteria. Though the final goal of this plasma treatment is in treatment of dental cavities, localized and precise inactivation of cancerous tissues, and in other medical applications, at the moment deeper understanding of biological mechanisms of plasma-cell interaction mechanisms is being pursued [98]. Dr. Stoffels and her colleagues have thus-far worked with the following eukaryotic cells and bacteria [18]:

- fibroblasts: Chinese hamster ovarian cells (CHO-K1) [99], 3T3 mouse fibroblasts,
- muscle cells: rat aortic smooth muscle cells (SMC) (A7r5) [100],
- endothelial cells: bovine aortic endothelial cells (BAEC) [100],
- epithelial cells: human MR65 cells originating from non-small cell lung carcinoma (NSCLC) [101],
- gram-positive bacteria: *Streptococcus mutans*,
- gram-negative bacteria: *Escherichia coli* [102, 103], and
- artery sections obtained from Swiss mouse (carotid and uterine arteries) [18].

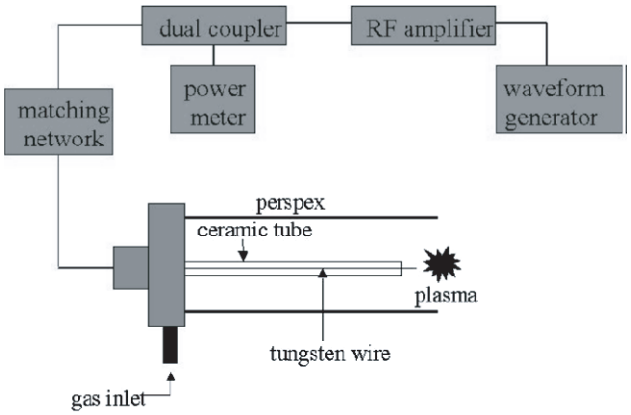


Figure 2. A principal schematic of the plasma needle setup [18].

Treatment by plasma needle of various cell lines causes these cells to lift off from the substrate and float away, without necrosis of these cells (Figure 3) [18]. The penetration depth of this treatment is usually limited to a single cell layer when no necrosis is observed while deeper treatment is possible at higher doses where cell necrosis is also observed. In addition to a well-localized detachment, apoptosis-like behavior was observed in the detached cells; however, the level of apoptosis appears to be not too significant as about 3% of the human epithelial cells underwent apoptosis while 100% were detached [18]. Dr. Stoffels hypothesizes that the dosage requirement induction of apoptosis are very narrow and further investigation onto the biochemical mechanisms of apoptosis induction are necessary. In treatment of *E. coli* roughly a 2-log reduction in bacterial load was achieved in 60 seconds of plasma treatment at 100 mW, 1 cm away from the sample [18, 103].

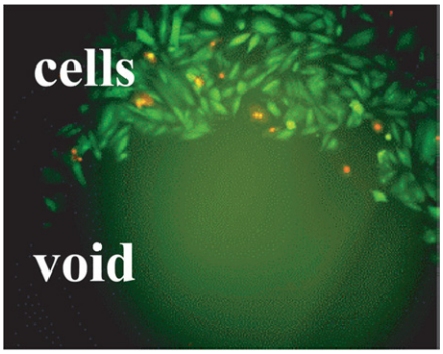


Figure 3. A void created in a cell culture, grown on a Petri dish. At the incidence of the plasma needle, the cells are removed (suspended in the medium and washed away) [18].

1.3.3. Indirect 6-Electrode Thermal Microwave Plasma Torch System

Treatment of chronic foot and leg ulcers was shown to be possible using a microwave argon plasma torch which is, as above, rapidly cooled by fast gas flow (Figure 4) [104, 105]. Argon is passed at 3 slpm through a 135 mm tube with six aluminum electrodes to which 2.45 GHz microwave power is allied. This torch operates at roughly 100 Watt [105]. Interestingly, the plasma afterglow generated in this way is able to sterilize many types of bacteria in minutes of treatment. Some of the bacteria tested were *Staphylococcus epidermidis*, *Escherichia coli*, *Streptococcus pyogenes*, *Bacillus cereus*, *Pseudomonas aeruginosa*, etc. Additionally *Candida albicans* yeast was tested. While the torch was effective in inactivation on all the organisms tested, the dose requirements and the size of the inactivation area varied by organism [104].

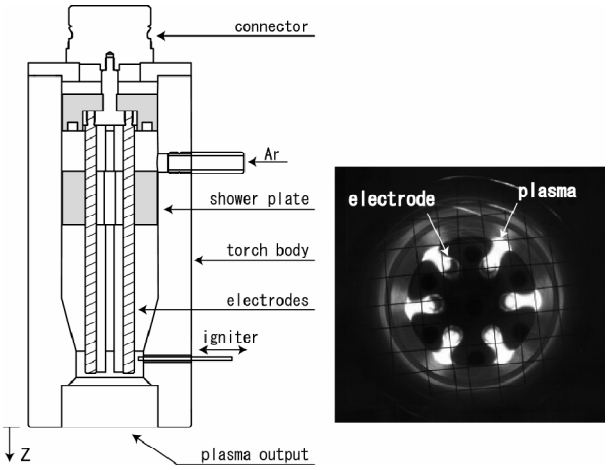


Figure 4. Microwave plasma torch schematic (left) and plasma output photo (right) [105].

Figure 5 shows an example of the results of a 2 minute treatment of bacteria. An inactivation circle is clearly visible and is much larger than the diameter of the nozzle. Similar effects are observed on other types of bacteria as well [104, 105]. While the effect on bacteria is quite evident, Morfill et al. do not observe any effect on human blood or skin tissue (Figure 6) [104]. Histological evaluation of the treated tissue revealed no or little difference as compared with untreated skin. Only after 10 minutes of treatment vacuolization of keratinocytes of the basal epidermis becomes evident; curiously, these effects are observed in vitro on dead skin, only minutes following removal from live patient [104]. In any case, no effect is observed on blood or tissue in 2 minutes of treatment which is quite sufficient to significantly reduce bacterial load.

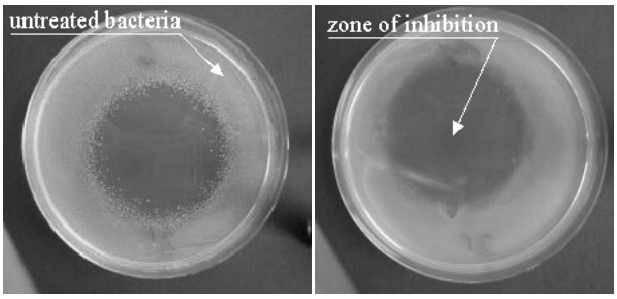


Figure 5. Bacterial cultures on agar plates after 2 minutes of plasma treatment. Left: methicillin-resistant Staphyolococcus aureus (gram positive) Right: Burkholderia cepacia (gram negative) [104].

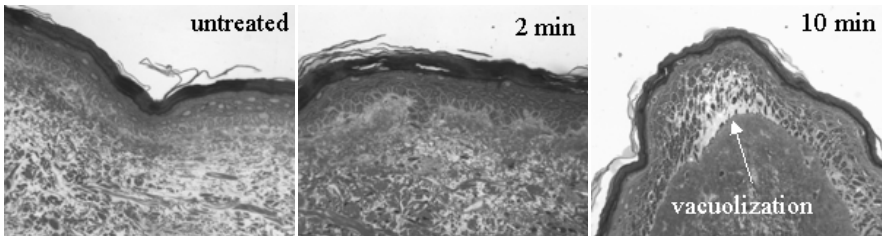


Figure 6. Histological images of skin samples, treated ex-vivo. After 2 minutes no changes could be observed with respect to the untreated control sample. Vacuolization of keratinocytes can be observed after 10 minutes [104].

1.4. Review Summary of Non-Equilibrium Plasma Applications in Medicine

The above review of current applications of non-equilibrium plasmas in medicine, as our recent more detailed review [26], clearly demonstrates limitations of indirect application of plasma. Thermal plasma afterglow is mainly affecting tissues and cells through temperature-related effects while non-thermal plasmas are limited in their effectiveness when applied indirectly. Plasma was not, prior to this work, been put in direct contact with tissue and this thesis presents such application. In the following chapters we will discuss this and show that non-equilibrium cold plasma can be applied directly to living tissue without physical or biological damage to this tissue. We will also show that such treatment

can lead to rapid pathogen inactivation (sterilization) on this tissue at doses far below those required for damage.

CHAPTER 2. DEVICE FOR DIRECT NON-DAMAGING APPLICATION OF PLASMA TO LIVING TISSUE: FLOATING ELECTRODE DIELECTRIC BARRIER DISCHARGE (FE-DBD)

As can be seen from Chapter 1, there is a clear need for less damaging plasma systems. Safety, however, becomes a very important issue when the treatment target is alive. The device needs to, most importantly, not kill the patient immediately. This is discussed in Section 2.1 where we show that in the case of the FE-DBD plasma all the power is deposited in the discharge and does not penetrate into the tissue. Additional safety in case of FE-DBD is maintained by limiting current to below 5 mA which is considered to be safe by the U.S. Occupational Safety and Health Administration (OSHA) [106].

Once the device is electrically (physically) safe, a more subtle question arises of how to apply this plasma in the most efficient way. Various electrode configurations are discussed in Section 2.2 and the power supplies in 2.3. Importance of using different plasma electrodes is clear: an electrode to stop micro-capillary bleeding during brain surgery should be quite different from a catheter-like electrode to be used during gastroenterological surgery. What is not immediately obvious is the need for different plasma power supplies or the frequency, peak voltage, polarity, and waveform at which they operate – this will be discussed in more detail in Section 2.3.

2.1. Principle of Operation of the Floating Electrode Dielectric Barrier Discharge.

Principal of operation of FE-DBD plasma can be explained with the help of a relatively simple model. Let us model the insulated electrode as a sphere of diameter D_{el}, while the object whose surface is being treated is modeled as a sphere of diameter D_{ob}. In the absence of the object the electrode capacitance with respect to the far away (located at infinity) ground is given by the well-known formula $C_{el} = 2\pi\varepsilon_0 D_{el}$ (where ε_0 is permittivity of free space). Now, if the object being treated has a relatively high dielectric constant (like that of water), it effectively expels most of the electric field from its interior when it is brought close to the electrode. From that point of view this object behaves like a good conductor and, therefore, its capacitance with respect to the far away ground can also be modeled by $C_{og} = 2\pi\varepsilon_0 D_{ob}$. The region between the object and the electrode can be modeled roughly as a parallel plate capacitor with the value $C_{gap} = \frac{\pi\varepsilon_0 D_{el}^2}{2g}$ (where g is gap distance) if the gap is significantly smaller than the electrode diameter. Note that $\frac{C_{gap}}{C_{og}} = \frac{D_{el}^2}{4gD_{ob}}$ is significantly smaller than 1 for the typical choices of characteristic sizes.

In the absence of any conduction current, the electrical models of the electrode by itself, and the electrode near the treated object are well approximated by the circuits in Figure 7 a) and b). When the electrode is well removed from the ground, the magnitude of the applied voltage V is insufficient to create electric field strong enough to cause the breakdown and discharge. However, when the object with a high dielectric constant is sufficiently close to the electrode, most of the applied voltage appears across the gap. This

is because the capacitance of the object with respect to ground is much larger than the gap capacitance, and the voltage divides across these capacitors proportionally to the inverse of their size. This results in a strong electric field in the gap which can now lead to breakdown and discharge.

The electrical circuit model can be further refined by taking into account non-linear resistance and capacitance of the plasma created in the gap. The resulting circuit refinement is shown in Figure 7 c). The refined circuit does not change the main conclusion that most of the applied voltage appears across the plasma gap.

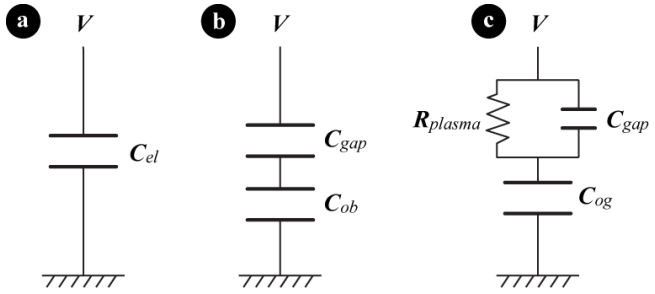


Figure 7. Simplified electrical schematic of a) electrode itself, b) electrode near the treated object, and c) plasma discharge on the treated object.

At about 10 kHz, the following circuit parameters typical for our experiments can be estimated assuming that body diameter is roughly 1 meter, the electrode diameter is about 25 mm, and the gap is about 1 mm.

$$C_{gap} = \frac{\pi D_{el}^2 \varepsilon_0}{4g} \approx 4 \times 10^{-12} F = 4 \text{ pF}$$

$$\frac{1}{\omega C_{gap}} \approx 4.2 \text{ M}\Omega$$

$$R_{plasma} = \frac{V^2}{Power} \approx 5 - 10 \text{ M}\Omega$$

$$C_{og} = 2\pi\varepsilon_0 D_{body} \approx 50 \times 10^{-12} F = 50 \text{ pF}$$

$$\frac{1}{\omega C_{og}} \approx 300 \text{ k}\Omega$$

Electrical safety of the object being treated by plasma is ensured because current the power supply delivers is under 5 mA. Although such currents may cause some mild discomfort, they do not cause muscle or cardiovascular malfunction in a human and, therefore, are deemed safe by the U.S. Occupational Safety and Health Administration (OSHA; see [106] for example).

2.2. Application of FE-DBD Plasma to Biological Objects

FE-DBD system is based on a conventional dielectric barrier discharge and is basically a system driven by alternating current high voltage applied between two conductors where one or both are covered with a dielectric to limit the current and to prevent transition to an arc. In this setup, amplitude and waveform of the high voltage signal are quite important (this will be discussed in the next section).

A simplified schematic of the treatment setup is shown in Figure 8. Here, the signal of any frequency, amplitude, and waveform is current-amplified and then voltage is stepped up in the transformer which is then connected to the “powered electrode”. The electrode is, basically, a conductor covered by a dielectric. Plasma is then generated between the surface of the dielectric and the treatment target.

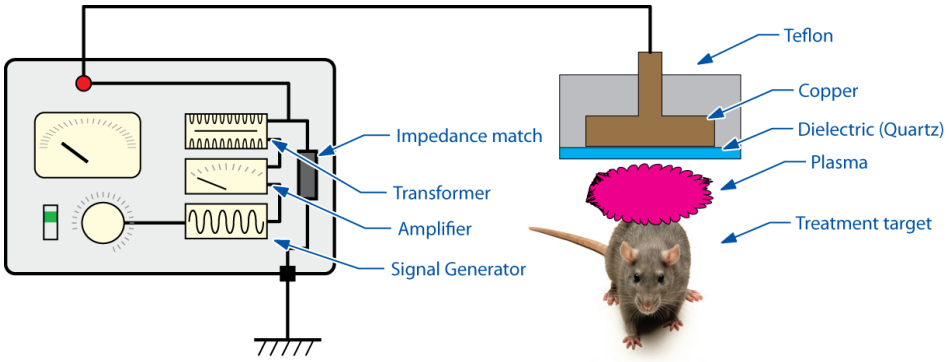


Figure 8. General schematic of the plasma treatment experimental setup.

The distance between electrodes plays one of the key roles in generation of plasma and thus for repeatable experimental results the distance needs to be precisely controlled. To accomplish this we simply connect the round electrode to a stage that can move in Z direction (up/down). This allows for one to repeatably measure and fix the distance between the substrate and the electrode. Figure 9 shows a schematic of such a setup where the electrode can be held by a "jacket" providing for the possibility of a controlled atmosphere (use of different gases or vacuum suction); insertion or removal of a grounded mesh which can separate plasma from the treatment target (which will be discussed in Chapter 4); insertion of, for example MgF_2 or quartz glass which will allow only ultraviolet photons but not the rest of plasma through; and/or other additions.

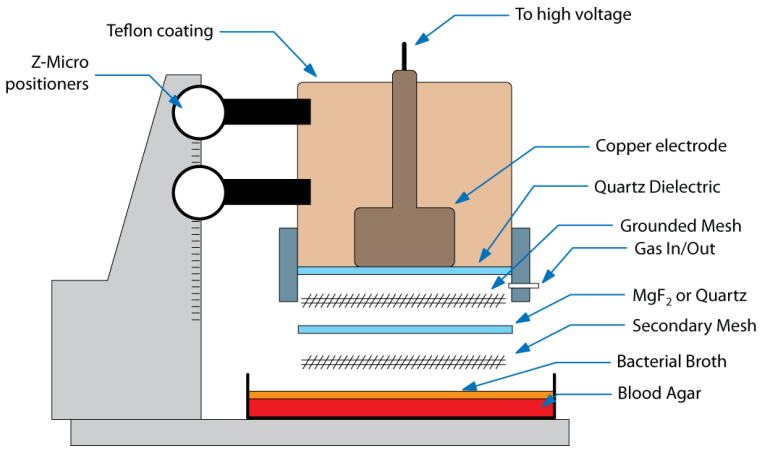


Figure 9. Principal schematic of the FE-DBD treatment setup with removable meshes and windows. In this setup either agar with bacteria (shown), cell culture, or living tissue can be treated.

2.3. Observation of the FE-DBD Plasma

When the system is operating, plasma can be clearly seen by an observer, should they look between the electrodes. Figure 10 shows one of such situations where photographs are taken at different exposure times (camera shutter is left open for 1, 2, 3, 5, 10, and 30 seconds while all other parameters are kept constant). Here plasma over the water surface is shown; tap water is used as it is conductive and it is grounded on the bottom.

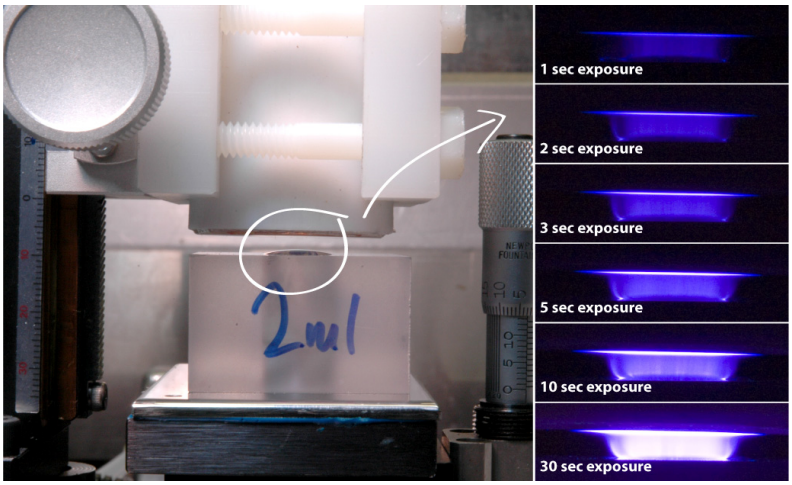


Figure 10. Side view of plasma over the surface of water at different exposure times.

More interesting is the observation of plasma as the treatment target sees it. Figure 11 shows a setup where water is used as the powered electrode. Water is clear, so plasma can be observed directly but dielectric heating effects at our operating frequencies [107, 108] create the need for cooling which is accomplished by flowing water through the electrode and into the ice bath. It is important to note that degasifying water improves visibility through the electrode as does using distilled water with NaCl addition to desired conductivity.

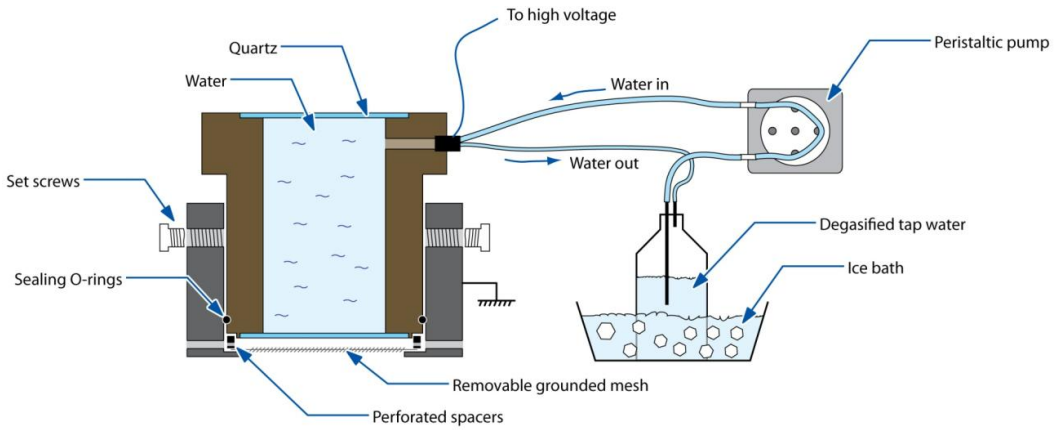


Figure 11. Water electrode setup schematic.

This setup allows for many different types of observations. For example, Figure 12 shows one such observation where medical-grade dry air is flown from a gas tank at 3 slpm through sinusoidal excitation wave discharge. Interestingly, even though plasma is instantaneously (1/250 sec) quite non-uniform, filaments cover practically the entire area after less than 0.2 seconds.

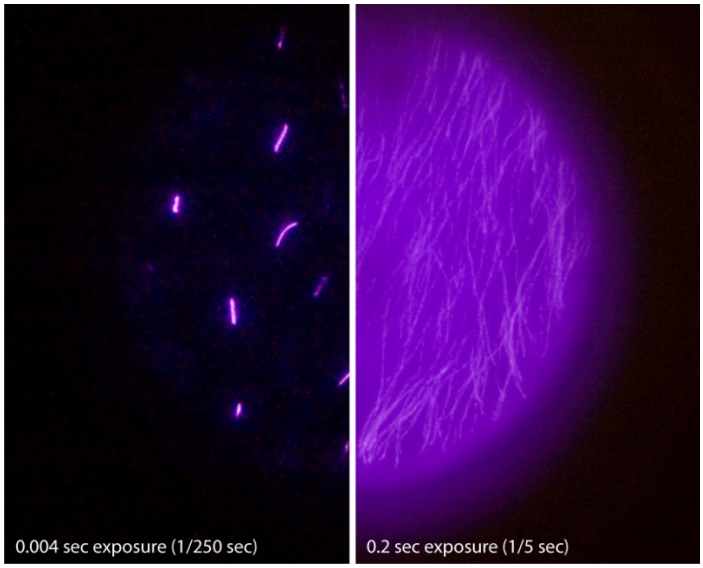


Figure 12. 0.004 sec (left) and 0.2 sec (right) exposures of the FE-DBD plasma in dry air (from gas tank) at 3 slpm flow rate with sinusoidal excitation wave.

Of note about Figure 12 is that we observe microfilament movement. These filaments are approximately 0.1 mm in diameter and at these flow rates we should see them as stationary dots. Calculating the distance the filament traveled in 1/250 sec and comparing it with approximate flow velocity we find that they are comparable [109]. Further research is being performed on this subject currently (see [110] for initial results and discussion).

CHAPTER 3. DIRECT NON-EQUILIBRIUM PLASMA APPLICATION FOR SKIN STERILIZATION; EFFECTIVENESS OF DIRECT VERSUS INDIRECT (JET) PLASMA TREATMENT

3.1. Quantitative Direct Sterilization on Agar

Careful sample preparation is required before carrying out the plasma experiments. Since our interest is primarily in sterilization of skin of an animal or human, bacterial samples were collected from de-identified skin samples from human cadavers at the Hahnemann Hospital (Philadelphia, PA). Identification of the bacterial species was performed using standard methodology at the Hahnemann Hospital's Clinical Microbiology Labs. Bacteria from skin samples consisted of staphylococci, streptococci, and Candida species of yeast. To collect these micro-organisms, six skin samples were swabbed twice each by sterile cotton-tipped applicators pre-wetted with 10X Phosphate Buffered Saline (PBS). These applicators were then transferred into 5 mL of 10X PBS and placed into an ultrasonic bath for 10 minutes to lift off the bacteria from the swab. The resulting solution was transferred onto the blood agar plate (Trypticase™ Soy Agar with 5% Sheep Blood) and incubated in air at 37 °C for 24 hours. The resulting colonies were collected and re-inoculated onto fresh blood agar plates and again incubated for 24 hours. These steps were repeated to obtain large quantities of bacteria. In the end of this preparation, bacteria were collected from the plates and diluted in 10X PBS to approximately 10^9 colony forming units (CFU) per mL. Bacterial concentration was assessed by a standard dilution assay [111, 112].

Since the results of the plasma treatment are characterized below in terms of appearance of the blood agar surface after the treatment, it is important to normalize the results by establishing how the agar surface would look for different concentrations of colony

forming units (CFUs) on its surface. To do that we exposed an agar-covered Petri dish with bacteria cultured on its surface from samples prepared as described above to the DBD plasma for different times at fixed plasma power levels [19]. The exact plasma set-up, surface power density, and other plasma parameters used for these normalization experiments are the same as those used in the experiments described later that compare direct and indirect treatment.

To quantify sterilization efficiency, 20 μL drops of 10^9 cfu/mL bacteria were placed on agar surface, left to dry for 5 minutes, and finally treated by plasma. This volume was selected as it spread to ~1 cm^2 over the agar surface; thus, the area covered by the bacterial sample drop was entirely within the area covered by the insulated plasma electrode. Following the treatment the drop was spread over the entire agar surface and incubated in air at 37 °C for 24 hours. Bacterial colonies (CFUs) were then counted and the results are presented in Table 3. There is a clearly visible difference in agar appearance between untreated, partially sterilized, and completely sterilized agar. Based on this difference, it is reasonable to classify the appearance of the bacterial surface into 5 categories: 1) untreated (10^9 cfu/mL), 2) partially disinfected (10^9 to 10^7 cfu/mL) 3) disinfected (10^7 to 10^4 cfu/mL), 4) partially sterilized (1,000 to 10 cfu/mL), and 5) completely sterilized (zero cfu/mL). Note that the definitions of sterilization and disinfection follow those that are accepted in the literature [19, 43, 51, 103, 113-115].

Table 3. Bacteria sterilization results (in cfu/mL)

Original Concentration	5 sec of FE-DBD	10 sec of FE-DBD	15 sec of FE-DBD
10^9	850 ±183	9 ±3	4 ±4

10^8	22 ±5	5 ±5	0 ±0
10^7	6 ±6	0 ±0	0 ±0

To quantify the *extent of sterilization*, 1 mL of 10^9 cfu/mL was poured over the entire agar surface. These samples were left to dry for 3 hours and then treated by plasma. Here plasma only covered a portion of the Petri dish. Following the 24 hour incubation period, the extent of sterilization was clearly visible – areas where bacteria were killed looked like uncontaminated agar while areas that received no treatment changed color and appearance significantly as bacteria grew there. The complete sterilization area is easiest to identify – it corresponds to the agar area that is completely clear from bacteria (for examples, see Figure 13 or [19]). Partial sterilization is also relatively easy to define since the number of CFUs is relatively small and can be counted. Disinfection is more difficult to assess because of the difficulty of counting the large number of CFUs. As can be seen from Figure 13, the complete sterilization gradually fades into untreated areas, forming a "grey-scale" fade that gradually increases from 0 cfu/mL in the sterile zone to 10^9 cfu/mL in the untreated zone much like in the quantitative experiments described in the previous paragraph.

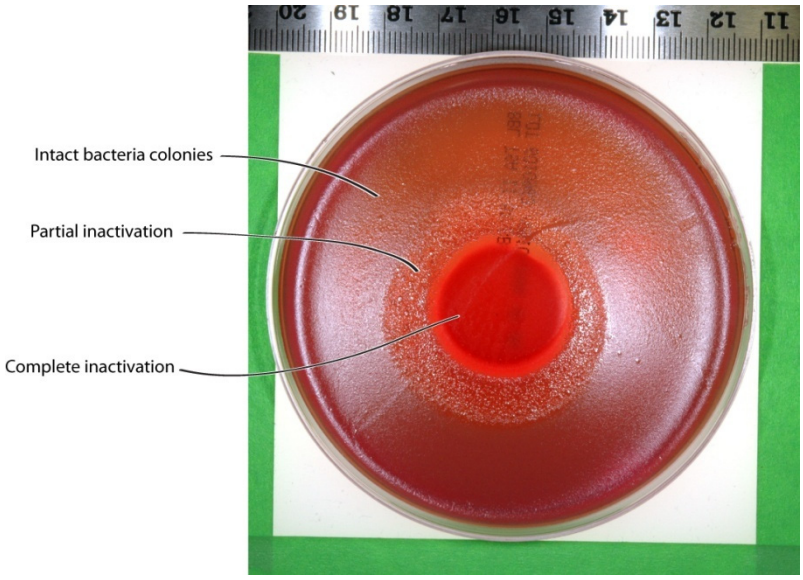


Figure 13. Photograph of the blood agar Petri dish following 24 hour incubation period of bacterial sample treated by FE-DBD plasma for 10 seconds: plasma-agar contact area is completely clean of bacterial colonies, area outside of plasma shows partial inactivation, and the rest of the Petri dish shows complete coverage with bacterial colonies.

3.2. Comparison of Direct and Indirect Sterilization in Open Air

Over the past few years new non-thermal atmospheric pressure plasma (APP) devices have emerged with several important applications in medicine. These applications involve possibly-selective inactivation of unhealthy cells [5, 12, 17, 19, 113, 116-118], blood coagulation [3, 5, 19, 119], and killing of parasites, bacteria, fungi and viruses on living tissue [8, 16, 17, 19, 48, 115, 120-128]. Another attractive application is sterilization of various surfaces [17, 43, 44, 103, 113, 115, 120, 129-131]. Two different approaches have been suggested for atmospheric pressure non-thermal plasma-based sterilization of living tissues. These two approaches can be classified as indirect and direct. *Indirect* treatment uses a jet of products (plasma afterglow) generated in remotely located plasma discharge.

Direct treatment, by contrast, uses the tissue itself as an electrode that participates in creating the plasma discharge, as illustrated below. Plasma in this case is contained between the quartz surface of the powered high voltage electrode and the surface of bacteria or tissue being treated. It is important to stress that the distinction between these two approaches is not only related to the proximity of the plasma and the tissue, but that direct contact with plasma brings *charged energetic particles* to the plasma-tissue interface. By contrast, no charged particles are usually taken out of the plasma region by a jet even if the plasma region is located only a fraction of a millimeter away. The question arises: Is there a substantial difference between the two types of treatment? In other words, is the transport of charged particles to the surface being treated as important or is the effect of plasma due mainly to long-living active molecules and longer wavelength ultraviolet radiation (as short wavelength "vacuum" UV is absorbed by air at atmospheric pressure within microns) [43, 132-135].

Here we compare effectiveness of direct and indirect sterilization treatment by non-thermal APP generated using the same discharge setup, and demonstrate that the direct treatment can achieve sterilization much faster without any thermal effects. Specifically, we employ the same Dielectric Barrier Discharge (DBD) to compare both types of treatment. To do that, we carried out two types of experiments. In one set of experiments we employed a surface covered by bacteria as a DBD electrode, placed a second smaller area DBD electrode over it and compared the areas of sterilization with air flow parallel to the surface and without the air flow. In another set of experiments we again employed a surface

covered by bacteria as one DBD electrode and compared the rate of sterilization to the case when this surface was separated from the DBD discharge by a grounded mesh electrode.

Here we attempt to compare direct and indirect application of plasma for sterilization. Since we are comparing two different modalities to each other, difference between them needs to be kept to a bare minimum. The basic idea is to somehow separate the effect of direct plasma from indirect effect of plasma afterglow. We achieve this in two setups: 1) we separate plasma from bacteria by a grounded metal mesh; and 2) we blow pair through plasma which is in direct contact with bacteria, thus creating a "tail" of afterglow effect.

From the previous chapters it is clear that non-thermal plasma, specifically the Floating Electrode Dielectric Barrier Discharge, is able to achieve a medically-relevant therapeutic effect when it is applied to living tissue. We show that FE-DBD plasma is able to sterilize surface from bacteria while causing no visible or microscopic damage to this surface. A question then arises: What in plasma could potentially be responsible for sterilization and how does the effect of FE-DBD compare to application of other types of plasmas? Different cold plasmas also show therapeutic effect, see for example Dr. Stoffels' et al "plasma needle" [18, 97, 98, 118, 136-138], Dr. Laroussi's et al "plasma plume" (or "plasma pencil") [2, 25, 42, 44, 47, 139], or Dr. Coulombe's et al "atmospheric pressure glow discharge torch (APGD-t)" [12, 14, 140-142], etc.

There are two modes of application of FE-DBD to the surface being treated: 1) where the tissue or cells are used as a second active electrode – plasma then is bound between the dielectric surface of the powered electrode and the surface of the tissue being treated; or 2)

where plasma is separated from the tissue by a grounded metal mesh and gas is blown through the discharge to carry active species outside of the plasma. We call the first method a "direct" and the second an "indirect" application of plasma to tissue. It was previously shown that direct application of plasma yields to roughly a two orders of magnitude improvement in rate of bacteria inactivation as compared to indirect application, even when the plasma is removed from tissue only a fraction of a millimeter away [27].

Effects of direct application of dielectric barrier discharges in air to bacteria can be separated into four major categories:

1. Effects of Ultraviolet (UV) radiation. In addition to the longer wavelength UV (180-340 nm) we also need to account for contribution of deeper UV, or Vacuum UV[1] (110-180 nm) as the plasma is in direct contact with tissue.
2. Global effects of increased gas temperature in the discharge gap and of the applied electric field (field of the electrodes, not the self-generated field gradients at the streamer head).
3. Effect of neutral active species generated in plasma; for example the long-living ozone, NO, HO_2, etc, or the short-living OH, atomic oxygen, electronically excited oxygen $O(^1D)$, $O_2(^1\Delta g)$, etc.
4. Effects of charged species: electrons and positive and negative ions.

---

[1] VUV is absorbed in air in microns and thus cannot travel outside of the discharge zone, however in the direct plasma treatment this plasma is in direct contact with tissue and thus if the more energetic VUV photons are generated they can, in fact, reach the treatment target.

Below, we will show that all the effects of direct plasma on bacteria are negligible compared to the effects of charges. In short, leaving only UV radiation (removing plasma by use of quartz (UV) or magnesium fluoride (VUV) windows) removes the ability of plasma to sterilize. Global gas temperature and applied electric fields are also negligible as the gas temperature rise is insufficient to achieve sterilization and the frequency and waveform utilized is out of the range for effective electroporation (see [26, 27, 143-146] for further details). Effects of neutral active species cannot be ignored. Neutrals by themselves, given enough time, are able to sterilize as well as direct plasma treatment and they are also responsible for many interesting biological effects; i.e. effect of NO in tissue regeneration [21, 26, 76].

3.2.1. Direct and Indirect Plasma Setup Employing Mesh to Separate the Effect

For the first setup we employ what we call a "spider" electrode (Figure 14). The electrode itself in this setup is the same as described above; however, it is covered with a "jacket" which can be grounded and into which we can insert spacers to precisely control distance. The jacket is supplied with gas feed lines to allow for controlled atmosphere.

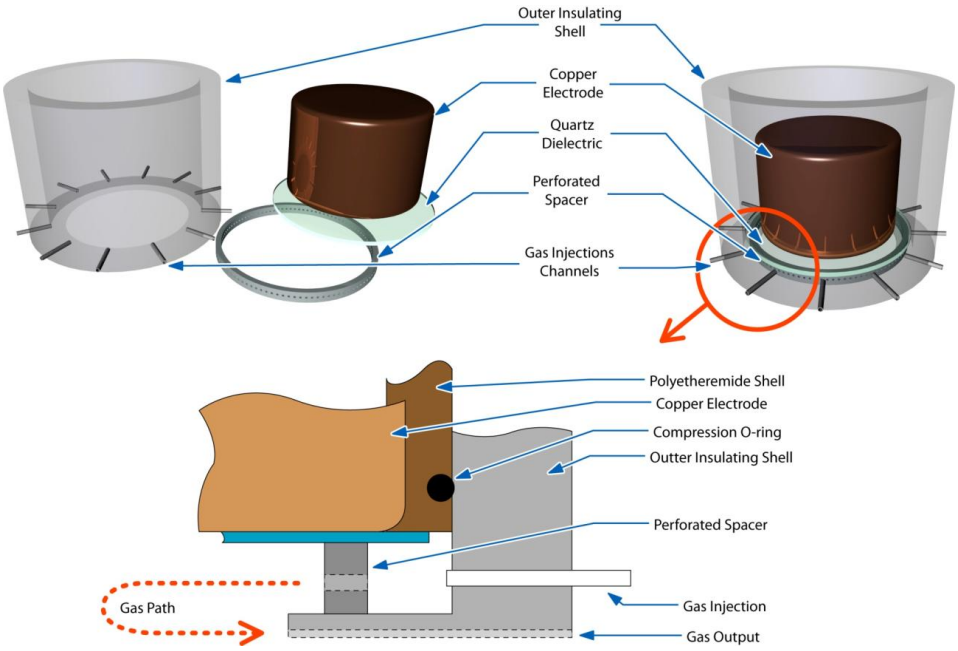


Figure 14. A 3-dimentioan representation and schematic of the electrode with controlled atmosphere.

Illustrated in Figure 15 is such an electrode in use. During the treatment the entire setup, including bacteria-covered agar, is placed upside down so the agar is in full contact with the jacket and is kept down by its own weight. The electrode footprint can be clearly seen on agar post-incubation (Figure 15) where gas output channels are visible.

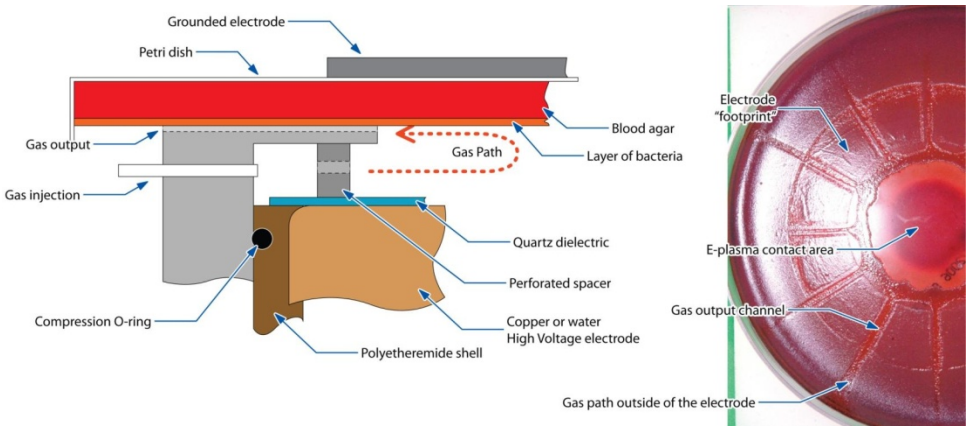


Figure 15. Schematic of treatment of bacteria on blood agar and the electrode footprint generated by this method.

In this setup, when plasma is turned on, we get essentially the same FE-DBD system described above and shown schematically below in Figure 16. Let us call this setup "direct" treatment as plasma is clearly in direct contact with bacteria. The step on the metal jacket is 0.5 mm and the spacer is 1.5 mm tall. Thus, the distance between bacteria and quartz is 2 mm. We can also place a grounded metal mesh between the perforated spacer and the step on the metal jacket as is shown in Figure 17. If we then replace the 1.5 mm spacer with a 2 mm spacer we get two setups which generate nearly identical plasmas (with the exception of bacteria at the boundary in the first case and metal mesh in the second, but this difference cannot be avoided in this setup and will be addresses below). We call this an indirect treatment as plasma is separated from bacteria by the mesh. We can now flow gas through this setup. In the case of the first setup this does not much alter plasma, but in the case of the second one longer-living active species and radicals are carried out of plasma while charged species (electrons and ions) are captured by the mesh.

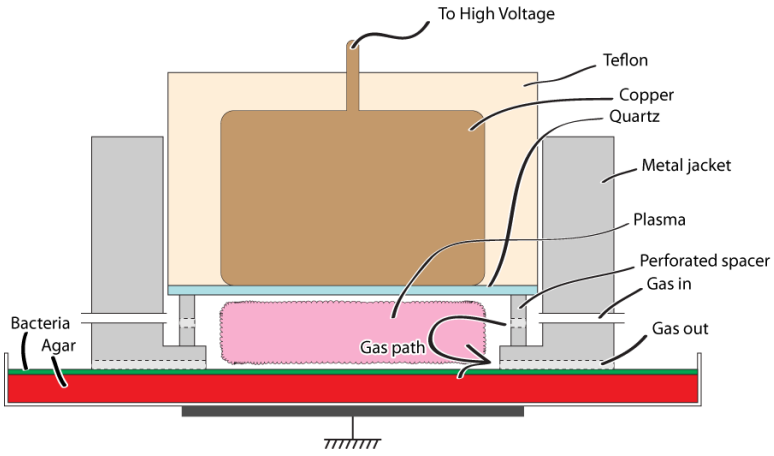


Figure 16. Schematic of the direct/indirect treatment setup in the "direct" mode without the grounded mesh: plasma contacts bacteria directly.

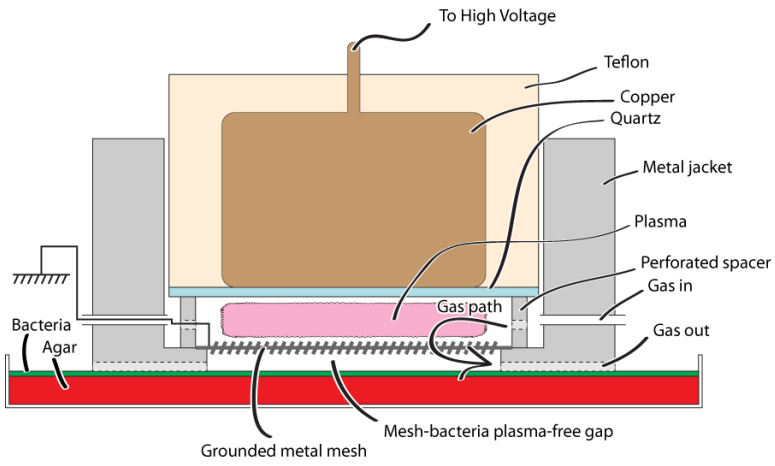


Figure 17. Schematic of the direct/indirect treatment setup in the "indirect" mode with the grounded mesh: plasma is bound by the mesh and only the plasma afterglow can reach the surface of bacteria.

3.2.2. Direct and Indirect Plasma Setup Employing Gas Flow (Blower) to Separate the Effect

Even though the setup presented above is able to show us clear difference between direct and indirect application of plasma, one could argue that the plasma characteristics are changed by introducing a metal mesh rather than moist bacteria on surface of a moist hydrogel. For this reason and to compare the results we have introduced a second system where only direct plasma is used but we flow air through the discharge creating the plasma "jet" effect on the other side (Figure 18 and Figure 19). The setup is the same as above but we have removed the jacket and added a fan to move air through plasma essentially creating the afterglow effect on the opposite side.

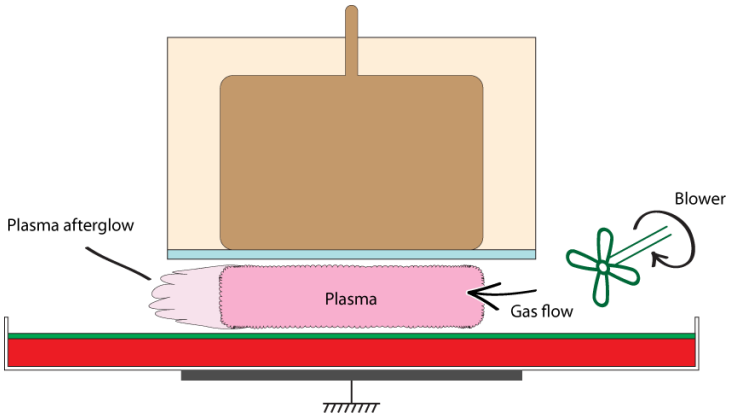


Figure 18. Schematic of the direct/indirect treatment setup with blower used to create the indirect treatment effect of the plasma afterglow.

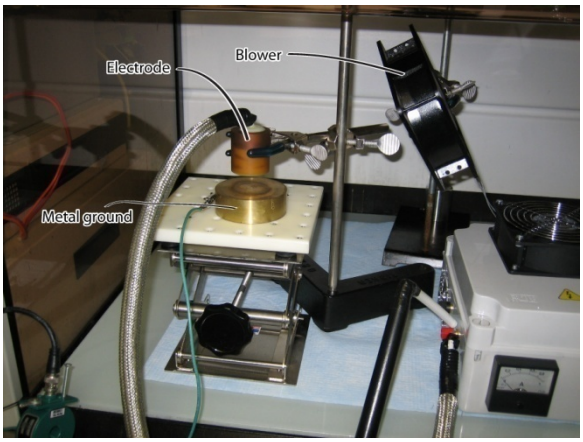


Figure 19. Photograph of the setup used for direct/indirect experiment with using the blower to move air through plasma.

3.2.3. Results of Direct and Indirect Treatment in Ambient Air

We now describe the first of the two types of experiments that compare direct and indirect plasma treatments. The setup is illustrated in Figure 16 and Figure 17 and discussed above. To test the sterilization treatment, we used an agar-covered Petri dish with bacteria spread on its surface from the earlier prepared samples of 10^9 cfu/mL concentration. Specifically,

one milliliter of such bacterial sample was transferred onto the blood agar and spread over the entire plate. The plates were dried for 3 hours in a Class II biological safety cabinet (SterilchemGard™ SG-4TX, The Baker Company) prior to the plasma treatment. After the plasma treatment, the samples were incubated in air at 37 °C for 24 hours to assess the ability of the DBD plasma to sterilize. Control experiments with gas flow only were performed for all gas flows shown here. Bacteria were completely unaffected by flowing room air in up to 30 minutes (maximum time tested) as these bacteria were at a surface of a hydrogel (agar) which takes over 3 days to dry. When exposed to dry air, agar surface begins to show signs of drying, beginning at 10 minutes, but bacteria were unaffected by this even after 30 minutes of dry air[2].

When placed on a metal substrate, the agar dish with bacteria on its surface acts as one of the DBD electrodes – bacteria are at the plasma-agar interface. The other smaller area DBD electrode is made of 2.5 cm diameter solid copper disc separated from the plasma by a 1 mm thick quartz dielectric. The plasma gap, or the distance between quartz-plasma and agar-plasma interfaces was set to 1.5 mm. Alternating polarity sinusoidal voltage of 35 kV magnitude (peak to peak) and 12 kHz frequency was applied between the copper electrode and the aluminum substrate under the agar Petri dish. A standard 120 mm high speed fan (Multicomp MC1122HBT, 120x120x25 mm, 40 slps) was placed ~20 cm away from the discharge and the angle of the fan was adjusted to allow for maximum air flow parallel to the substrate through the plasma gap. Flow speed for this experiment was measured

[2] Also of note is that the humidity in the incubator is maintained at >80% so if the agar dries outside, once placed in the incubator, bacteria get all the moisture and nutrients necessary for their proliferation.

between the electrode and the substrate, directly outside of the electrode, to be 0.8 ±0.3 m/s (EXTECH Instruments model 407123 Hot Wire Thermo-Anemometer) (see Figure 18 and Figure 19).

The power surface density delivered into the plasma discharge was measured by two methods. One was the more traditional electrical measurement method involving voltage across the discharge and current into it. This measurement was performed using a high speed high voltage probe (PVM-4 1000:1, North Star High Voltage, Marana, AZ) and high speed current probe (1 V/Amp +1/-0% sensitivity, 10 ns usable rise time, 35 MHz bandwidth, Model 4100 Current Monitor, Pearson Electronics, Palo Alto, CA). Signals from the probes were measured and integrated using a high speed oscilloscope (500 MHz bandwidth, $5x10^9$ samples/s, TDS5052B, Tektronix, Inc, Richardson, TX). These electrical measurements were confirmed using custom-built calorimetric measurement set-up. Both electrical and calorimetric measurements indicated the power of 0.8 ±0.2 W/cm^2.

When there is no air flow parallel to the surface, the area directly under the second smaller electrode is exposed simultaneously to charged particles, UV, and the plasma afterglow containing longer living active plasma components such as ozone (O_3), nitric oxide (NO), hydroxyl radicals (OH), and other excited molecular and atomic species. In the presence of the airflow, the area under the second smaller electrode experiences practically the same conditions as without the flow. However, in the presence of flow the plasma afterglow will also impinge on the areas of the substrate that are not directly under the second smaller electrode as it is illustrated in Figure 18.

It should be stressed that, even in the absence of any flow, the sterilization region is not confined to the diameter of the copper electrode. With increasing treatment time, this region extends several millimeters outside the electrode [20, 27]. There are two reasons for this: first, due to the existence of surface discharge near the base of DBD filaments, the "footprint" of a micro-channel is substantially larger than its diameter [19, 147]. Second, since the field lines originating near the edge of the insulated electrode tend to spread out slightly, the discharge filaments also spread out beyond the area of the top electrode. The flow, however, is not expected to change the shape of the plasma discharge region because it is not capable of moving the filaments further than a fraction of a millimeter, as was observed with high speed photography (not shown) as well as theoretically [147, 148]. However, such effects are expected to be confined to within millimeters from the edge of the copper electrode, while the longer living active species and radicals can spread much further with gas flow [43, 97, 103, 147-149].

The results comparing the sterilization with and without flow are illustrated in Figure 20 and zoomed in version in Figure 21. As can be seen from these figures, complete sterilization by direct plasma treatment under the insulated electrode is achieved in 15 seconds. If air is passed parallel to the substrate through the plasma region, the disinfection area shifts by several millimeters, but a "tail" of disinfection appears. Even though complete sterilization is not observed in this "tail", different degrees of disinfection are evident. Locations closer to the plasma region have greater degree of disinfection. This suggests that plasma "afterglow", or the gas carried through and outside of plasma, does contain active species and radicals that have bactericidal effects, although direct plasma is

substantially more potent as a sterilizing agent. Complete sterilization, however, did not extend to the region reachable by the plasma afterglow in as much as 5 minutes of treatment. This clearly demonstrates that longer living active species generated in plasma are much less effective than direct plasma where charged particles participate in the process.

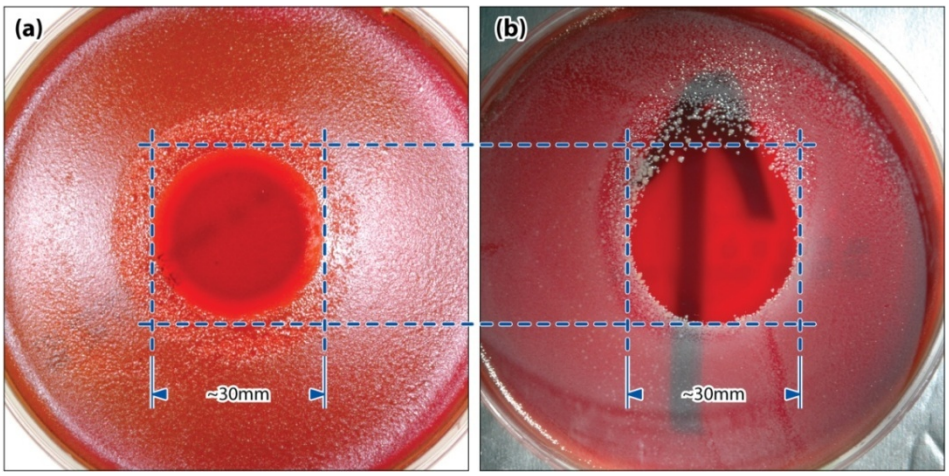


Figure 20. Using a blower to shift sterilization region does not affect plasma and shows little effect of the afterglow: 15 seconds of treatment with (a) blower off and (b) blower on (air flows up). Note: arrow is painted on the back of the dish and shows through on the photograph.

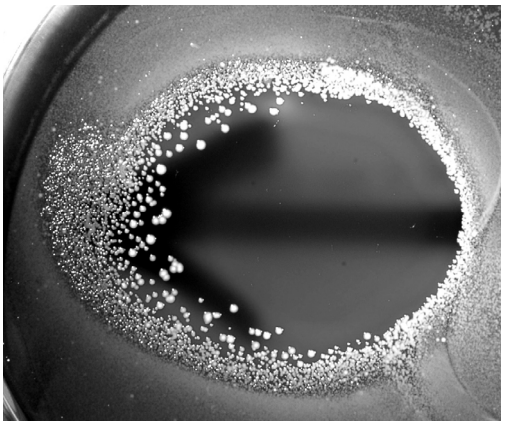


Figure 21. Zoomed in photograph of the bacterial growth results following plasma treatment and incubation (photograph is converted to black and white for increased contrast). Note: arrow is painted on the back of the dish and shows through on the photograph.

In the first type of experiments described above, effects of plasma "afterglow" were separated from the effects of charged particles and from the UV radiation. In the second type of experiments described below, plasma afterglow together with UV is compared against the direct plasma, involving also charged particles. The direct treatment is obtained similarly to the first type of experiments described above. However, instead of creating airflow parallel to the substrate, provisions were made to allow introduction of air at different flow rates into the discharge gap (see Figure 16 and Figure 17). To obtain indirect treatment including UV effects, agar surface covered by bacteria was again employed as one DBD electrode; however, this surface was separated from the DBD discharge by a mesh electrode, as illustrated in Figure 17. With a grounded mesh in place, bacteria are no longer at the plasma interface, as plasma is bound between the grounded mesh and the quartz-covered electrode. The mesh (22.04 wires per cm, 0.1016 mm wire diameter, 0.351 mm opening, 60% open area, weaved mesh) is placed 1 mm above the surface of the agar, which permits only the passage of ultraviolet radiation and longer wavelength photons (not vacuum UV), gas, radicals and other longer living particles created in the plasma gap between the mesh and the quartz-insulated electrode above it. The second electrode used with the mesh was the same electrode that was employed in the direct treatment setup illustrated Figure 16. The gap between the mesh and the second electrode is set at 1.5 mm, just as in the plasma gap of the direct treatment setup. The setup used to introduce air into the discharge gap at 3 different flow rates (1, 5, and 10 slpm, corresponding to flow speeds of 0.078, 0.393, and 0.853 m/s through the mesh) is illustrated in Figure 17. The air was introduced into the discharge gap to enhance extraction of the plasma afterglow through

the mesh. In both direct (without the mesh) and indirect (with the mesh) situations the same air flow rates were employed and the discharge was calibrated to the same plasma power for both cases.

To ensure that both setups, with and without the mesh, produce the same UV radiation, we correct for the UV transparency of the mesh using separate measurements. Regular paper is placed over the light source in these measurements to diffuse the light and a spectrum is measured using TriVista Spectrometer System with Princeton Instruments PIMAX intensified CCD camera with only paper, and with paper and mesh. It turns out that the mesh cuts off roughly ~40% of visible light and ~20-40% of UV light depending on the wavelength of UV (Figure 22 – graph in visible light range and Figure 23 – measurements in ultraviolet range).

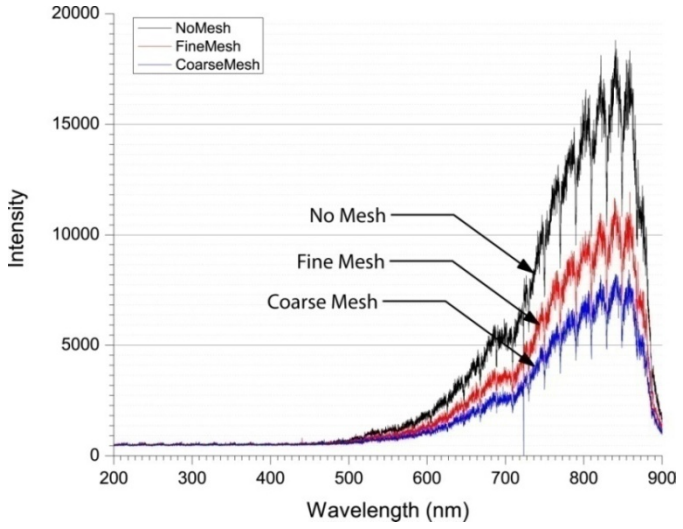


Figure 22. Results of measurement of light intensity in the visible spectrum for no mesh, fine mesh, and coarse mesh.

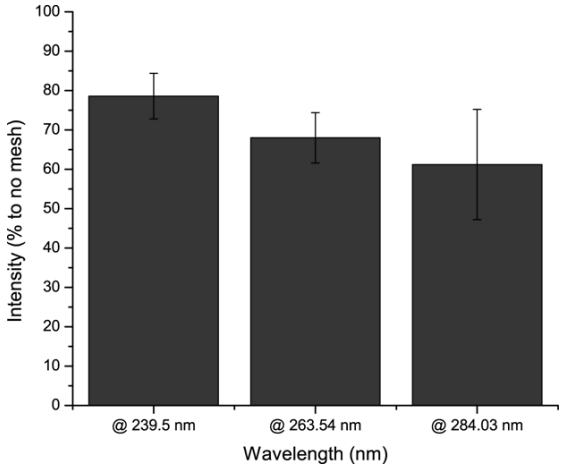


Figure 23. Results of measurement of light intensity in the ultraviolet spectrum measured at three peaks (239.5 nm, 263.54 nm, and 284.03 nm) without mesh (taken as 100%) and with mesh.

The results comparing direct (without the mesh) and indirect (with the mesh) sterilization are illustrated in Figure 24. It is clearly visible that plasma that comes in direct contact with bacteria is able to sterilize significantly faster than afterglow or jet. Only 5 seconds of direct plasma treatment results in the appearance of inactication region (spot near the center). Complete sterilization occurs within 15 seconds when direct treatment is employed and only partial disinfection can be achieved within the same time frame with indirect treatment. Over 5 minutes of indirect treatment is required to achieve sterilization results similar to direct treatment obtained within 15 seconds. Therefore, even with substantial UV radiation, indirect plasma treatment is significantly weaker than direct plasma which includes bactericidal effects due to charged particles.

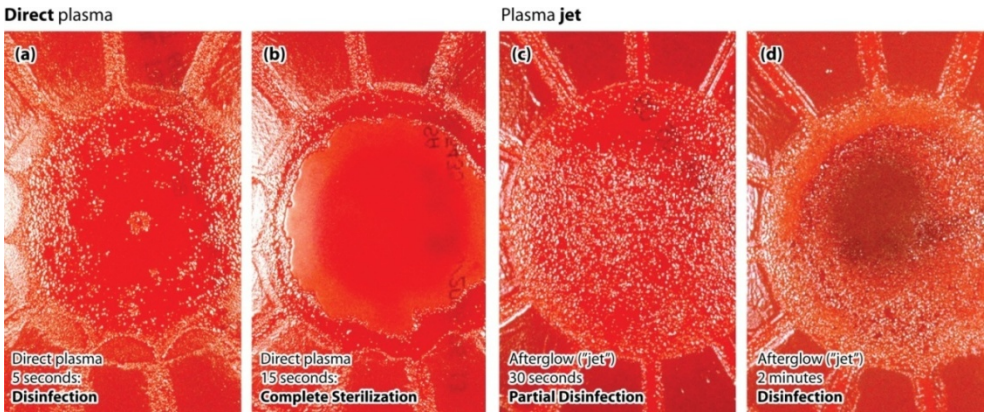


Figure 24. Direct application of plasma yields to better sterilization efficiency than treatment by plasma afterglow: (a) 5 seconds and (b) 15 seconds of direct plasma compared with (c) 30 seconds and (d) 2 minutes of plasma jet.

3.3. Effects of UV Radiation, Applied Electric Field, Thermal Energy, and Other Indirect Plasma Effects

Several possibilities exist that might explain why bacteria inactivation, disruption of membrane's normal functions, or disruption of normal metabolism functions occurs only in the presence of the DBD discharge. One possibility is that UV radiation (probably in the UV-C band) works in synergy with chemically active species produced by direct plasma in the liquid surrounding the organisms to break the integrity of cellular membranes (Figure 25 – emission spectra from plasma in UV range). Photon energy of the UV-C radiation (about 4-6 eV) is sufficient to break some chemical bonds in bio-molecules [150]. More energetic VUV-photons, however, are unable to penetrate deep through the layer of liquid and through bacterial membrane [151-153]. The UV-C radiation can be effectively delivered to the membrane, but its energy can be sufficient also for structural reorganization of the bio-molecules (including fatal but slow DNA changes), and

disruption of hydrogen bonds responsible for the integrity of the membrane's lipid bi-layer. Such disruption of the lipid bi-layer may open the membrane to penetration of multiple active plasma species, particularly such strong oxidants as atomic oxygen, peroxide radicals, singlet oxygen, NO, and positive ions [24]. Thus, deep penetration of the strong plasma treatment effect can possibly be attributed to synergy of UV-C radiation with plasma-generated active chemical oxidants.

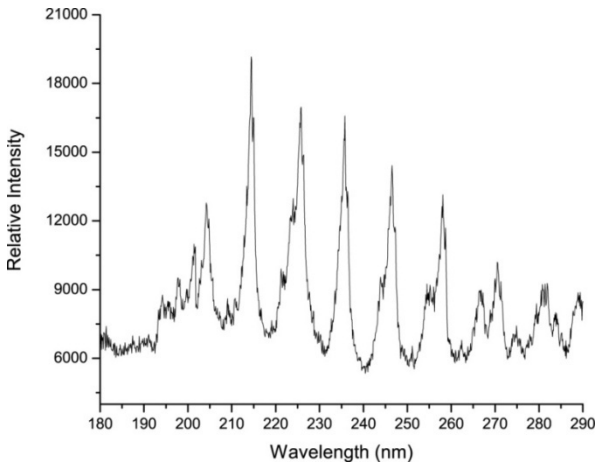


Figure 25. Emission from DBD plasma over the cell surface in UV range.

Although the UV and highly energetic VUV radiation have been linked to efficient cell inactivation rates [132, 154, 155] we show that this effect is negligible in sterilization of bacteria. We are able to separate effects of UV by inserting a quartz slide between the bacteria and plasma, and effects of VUV by use of magnesium fluoride (MgF_2) slide. Quartz is transparent to UV photons of >200 nm wavelengths and MgF2 is transparent to VUV photons of >140 nm wavelengths [152]. This way only UV/VUV photons generated in plasma reach bacteria. Even though we observe no visible effect on bacteria by UV/VUV photons (Figure 26), it cannot be discounted completely as UV, especially VUV,

is known for its synergetic effect in interaction and destruction of model polymers [151-153].

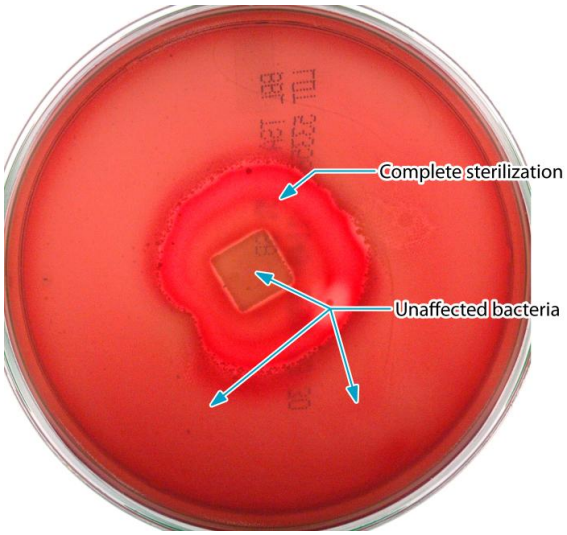


Figure 26. No effect on bacteria protected from plasma by MgF_2 slide (10 mm square in the center) is observed.

When grounded mesh is placed directly onto agar, an interesting (but expected) pattern emerges where only the areas in the openings of the mesh are sterilized and not under the mesh itself (Figure 27). This is indicative that the bacteria are protected by the mesh – whatever is produced in plasma and is possibly embedded/diffused into the agar does not exit the areas that were originally open. The wire diameter in the woven mesh on Figure 27 is ~150 μm and the opening width is ~240-300 μm – if something was diffusing or penetrating under the wires or under the open areas in the weave pattern one should be also to see it more clearly than what is seen in the photo.

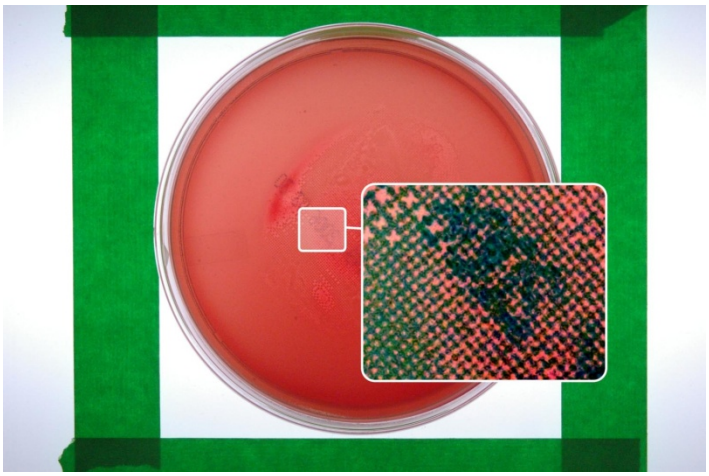


Figure 27. Grounded mesh placed directly on bacteria (no space) generates interesting pattern: only mesh openings are sterilized (magnified area is color-corrected for clarity).

High electric fields, especially pulsed electric fields are known to inactivate bacteria in solution [64, 156-158]. The field strength required for this, however, is on the order of a megavolt per centimeter – significantly higher than the applied electric field we are employing which is on the order of 10 to 30 kV. Experimentally, if we apply electric field at the strength just below the breakdown potential we observe absolutely no effect on bacteria as the agar looks complete unaffected by this following 24 hour incubation. We cannot, however, completely discount the effect of the electric field. In the head of a developing streamer, the electric field are much higher and can be estimated to be:

$$E_m = E_0 \cdot \left(3 + \left(\frac{l}{r}\right)^{0.92}\right) = 2.6 \cdot 10^6 \text{ V/cm}$$

where E_m is the field at the head of a needle-streamer of length l (0.2 cm) and radius r (0.1 cm) at the applied field E_0 of 35 kV. Field needed to destroy a chemical bond is

on the order of $3V/3Å \approx 10^8$ V/cm; to break a Hydrogen bond $\approx 10^7$ V/cm; and to break Van der Waals bond $\approx 10^6$ V/cm. It is also known that ~1 Volt applied across a cell membrane (~ 3 nm thick) is able to depolarize and break it [156, 159-161]. Field needed for this is $1V/3nm = 3 \cdot 10^6$ V/cm. Thus, electric field at the head of streamer as it reaches the bacteria surface is sufficient to open the membrane and thus potentially lead to leakage of cellular contents out and various substances detrimental to the organism into the cell.

3.4. Direct and Indirect Plasma Treatment in Various Gases

Additional experiments were performed to analyze behavior of plasma and its sterilization ability in different gases. Five areas were observed following the treatment: (1) right under the electrode, (2) outside of the electrode but inside of the treatment area bound by legs, (3) inside of the gas channel, (4) immediately outside of the gas channel, and (5) outer parts of the dish not in the direct gas path (Figure 28). Effect of treatment was observed following the 24-hour incubation and rated from 0 (no visible effect) to 5 (complete sterilization). For example, Petri dish in Figure 28 would be rated as 1-2 (visible disinfection in area right under the electrode), 2-1, 3-1, 4-1, and 5-0. Detailed results for various gases are presented in Table 4. Dry gas was obtained from the cylinder or bubbled through sterile deionized water to increase humidity. Humidity was measured to 80% when air was used (both for 1, 3, and 10 slpm flow rates) and not measured for other gases. Basic conclusion of this study is that oxygen is required for fast and effective

inactivation of bacteria and inactivation rate depends little on the exact gas composition, purity (determined by gas flow rate and, of course, the grade used), or humidity.

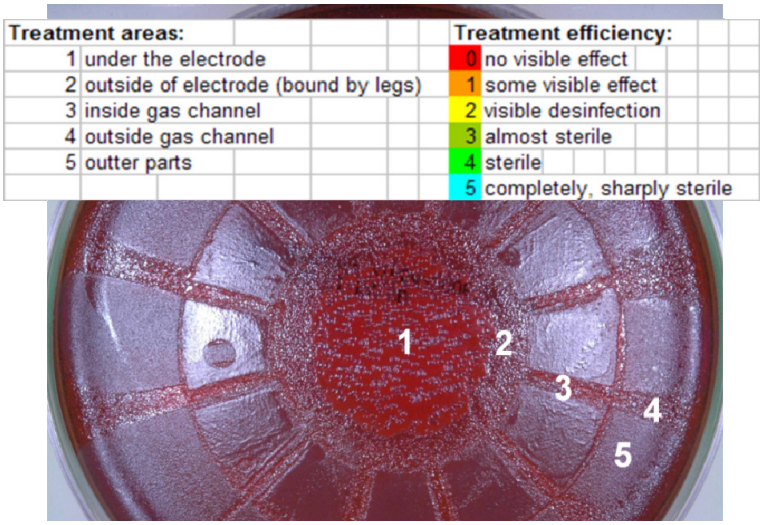


Figure 28. Identification of different areas under the FE-DBD electrode following the plasma treatment and 24-hour incubation: (1) under the electrode, (2) outside of the electrode but inside of the treatment area bound by legs, (3) inside of the gas channel, (4) immediately outside of the gas channel, and (5) outer parts of the dish not in the direct gas path.

Table 4. Results of treatment of bacteria by FE-DBD plasma in different gases. Areas of treatment are identified in Figure 28. Note: all experiments are repeated in triplicate and the results presented here are averaged.

Dry or Wet	Gas	Time (sec)	Flow (slpm)	Area 1	2	3	4	5
Dry	air	5	1	1	1	0	0	0
Dry	air	10	1	2	1	1	0	0
Dry	air	30	1	5	1	2	1	0
Dry	Ar	5	1	0	0	0	0	0
Dry	Ar	10	1	1	0	0	0	0
Dry	Ar	30	1	1	0	0	0	0
Dry	He	5	1	0	0	0	0	0
Dry	He	10	1	1	0	0	0	0

Dry or Wet	Gas	Time (sec)	Flow (slpm)	Area 1	2	3	4	5
Dry	N2	5	10	1	0	0	0	0
Dry	N2	10	10	1	0	0	0	0
Dry	N2	30	10	1	0	0	0	0
Dry	N2-NO	5	10	1	0	0	0	0
Dry	N2-NO	10	10	1	0	0	0	0
Dry	N2-NO	30	10	2	1	0	0	0
Dry	O2	5	10	2	1	2	2	0
Dry	O2	10	10	2	1	2	2	1

Dry	He	30	1	1	0	0	0	0
Dry	N2	5	1	1	0	0	0	0
Dry	N2	10	1	2	0	0	0	0
Dry	N2	30	1	2	0	0	0	0
Dry	N2-NO	5	1	1	0	0	0	0
Dry	N2-NO	10	1	2	0	0	0	0
Dry	N2-NO	30	1	2	0	0	0	0
Dry	O2	5	1	3	1	2	2	0
Dry	O2	10	1	3	1	2	2	0
Dry	O2	30	1	3	2	2	2	1
Dry	air	5	10	2	1	2	2	0
Dry	air	10	10	3	1	2	2	0
Dry	air	30	10	3	2	2	2	0
Dry	Ar	5	10	0	0	0	0	0
Dry	Ar	10	10	0	0	0	0	0
Dry	Ar	30	10	1	0	0	0	0
Dry	He	5	10	0	0	0	0	0
Dry	He	10	10	1	0	0	0	0
Dry	He	30	10	1	0	0	0	0

Dry	O2	30	10	3	1	3	2	1
Wet	air	5	3	2	1	2	1	0
Wet	air	10	3	3	1	3	2	0
Wet	air	30	3	4	1	3	3	0
Wet	Ar	5	3	0	0	0	0	0
Wet	Ar	10	3	0	0	0	0	0
Wet	Ar	30	3	1	0	0	0	0
Wet	He	5	3	0	0	0	0	0
Wet	He	10	3	1	0	0	0	0
Wet	He	30	3	1	0	0	0	0
Wet	N2	5	3	0	0	0	0	0
Wet	N2	10	3	1	0	0	0	0
Wet	N2	30	3	1	0	0	0	0
Wet	N2-NO	5	3	0	0	0	0	0
Wet	N2-NO	10	3	1	0	0	0	0
Wet	N2-NO	30	3	2	0	0	0	0
Wet	O2	5	3	2	1	2	2	0
Wet	O2	10	3	3	2	3	3	0
Wet	O2	30	3	3	2	3	3	1

3.5. Effect of Localized High Electric Fields and Effect of Heating

It turns out that the way the voltage is delivered to the electrode can be quite important. The main issue here is the rise time of the voltage [147, 148, 162]. In dielectric barrier discharges at atmospheric pressure, breakdown occurs following the so-called spark breakdown mechanism [163, 164]. The initial electron avalanche transitions to streamer in approximately 20 – 60 nanoseconds (Figure 29). Thus, if the voltage is increased slowly, as is the case with sinusoidal excitation wave (~ 1 V/nsec), the number of streamers occurring during a single cycle can be quite high. Since the initial streamer forms a pre-ionized channel, probability of the next streamer to strike in the same position is increased. So, in the case of a sinusoidal excitation wave, multiple streamers strike in the same position creating a rather energetic channel called microfilament. Among other things, temperature in this channel can get to quite high values (see Figure 30). To solve this, we

have employed pulses rather than sinusoidal wave allowing for voltage rise time of ~ 5 V/nsec and pulse duration of a few microseconds [143, 165]. Time between pulses is sufficient for the gas to return to the initial conditions so that during the next pulse streamers again strike randomly [147, 148, 162]. Of course, decreasing the pulse duration even further would lead to even better conditions for surface treatment; we will discuss this later in this section.

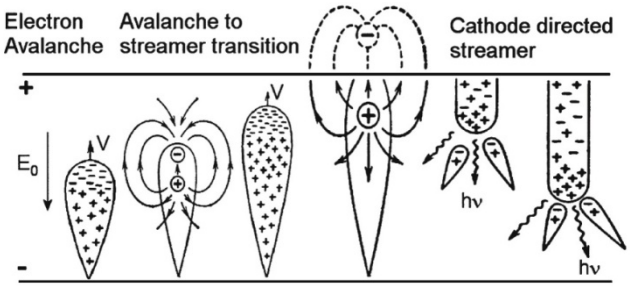


Figure 29. Avalanche transition to streamer [162].

These power supply systems operate on the basis of voltage amplification: a low voltage pulse or a sinusoidal wave is generated, then the current is amplified, and is finally passed through a transformer with high turns ratio. High voltage signal is then taken from the transformer's secondary coil and collected to the load [19]. For power analysis of these systems (plasma in continuous sinusoidal wave or pulsed mode) we measure current passing through plasma and the voltage drop in the gap. For current analysis we utilized a magnetic core current probe (1 Volt/Ampere +1/-0% Sensitivity, 10 nanoseconds usable rise time, 35 MHz bandwidth, Model 4100 Pearson Current Monitor, Pearson Electronics, Palo Alto, CA). Voltage was measured using a wide bandwidth voltage probe (PVM-4 1000:1, North Start High Voltage, Marana, AZ). Signals were acquired and recorded by a

Digital Phosphor Oscilloscope (500 MHz bandwidth, $5 \cdot 10^9$ samples/s, TDS5052B, Tektronix, Inc, Richardson, TX). Acquired data was then integrated in MATLAB. Due to the limitations of the probes, this system cannot be used to analyze the power deposited into nanosecond pulsed plasma.

In general, DBD plasmas are deemed "non-thermal" as the temperature of ions is significantly lower than that of electrons. However, especially in more filamentary regimes, temperature in the filament can grow above room temperature and potentially damage the surface being treated, particularly in the case of sensitive surfaces like in polymer surface treatment or in biological applications [24, 162]. For this reason we have employed emission spectroscopy to measure the vibrational and rotational temperatures in plasma. The temperature measurements were made utilizing the 375.4 nm and 380.4 nm vibrational lines and the rotational structure in those regions of the second positive system of nitrogen. An experimentally obtained spectrum was compared to the simulated spectrum to obtain vibrational and rotational temperatures (this procedure has been described in detail previously [149, 166, 167]). A fiber-optic bundle (Princeton Instruments-Acton, 10 fibers – 200 μm core) was utilized to acquire the emission from the discharge and to transmit it to a spectrometer (Acton Research SpectraPro 500i with Roper Scientific model 7430 CCD camera) and spectra were digitally acquired with approximately 0.6 nm resolution. Temperature of the camera was set to -25°C. Typical acquisition time for the spectra was 10 s. Background images (with the discharge turned off) were subtracted and a low pressure mercury lamp was used to determine the slit function of the spectrometer. Entrance slit width was set to 85 μm

when acquiring emission from the discharge and/or the mercury lamp. The room temperature was 22°C throughout the spectroscopic measurements.

As seen in Figure 30, the temperatures within the filaments of "continuous" and "pulsed" FE-DBD were found to be about 500 K and 300 K respectively by model fit to 2nd positive Nitrogen system. This method measures temperature based on radiation from the discharge. Since radiation is highest from the microfilament area we assume that the measured temperatures come from that region while gas temperature outside of the microfilament remains at room temperature.

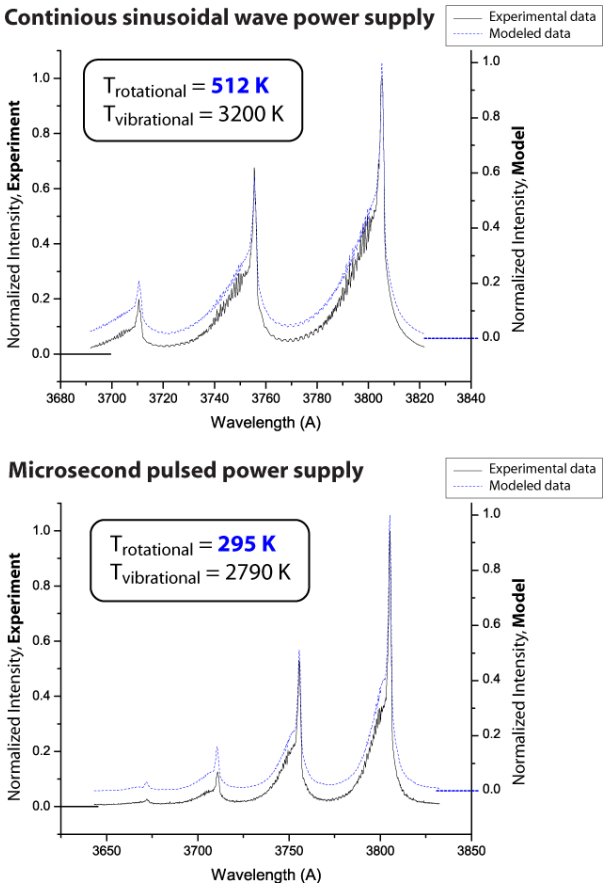


Figure 30. Rotational and vibrational temperature measurements from a model fit to 2nd positive Nitrogen system; please note, "modeled data" curve was intentionally raised, otherwise it is invisible since the curve-fit is nearly perfect.

As can be seen from Figure 30, during a microsecond pulse the gas does not heat up. However, there is sufficient time for streamer formation and development into filaments (see Figure 29). This way the discharge is more uniform than in the case of a sinusoidal excitation wave but still non-uniformity is observed as can be seen from the short exposure photograph through the water electrode below (Figure 31 and Figure 32). This way the treated surface is covered fairly uniformly in as little as a third of a second and below. However, for some applications a more uniform plasma treatment might be needed. For this we have developed a different power supply with shorter pulse duration.

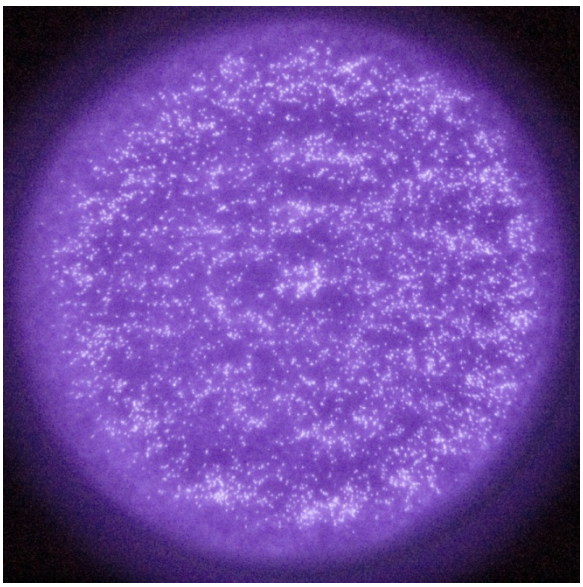


Figure 31. Photograph of plasma through water electrode. 1/3 second (0.33 sec) shutter open time.

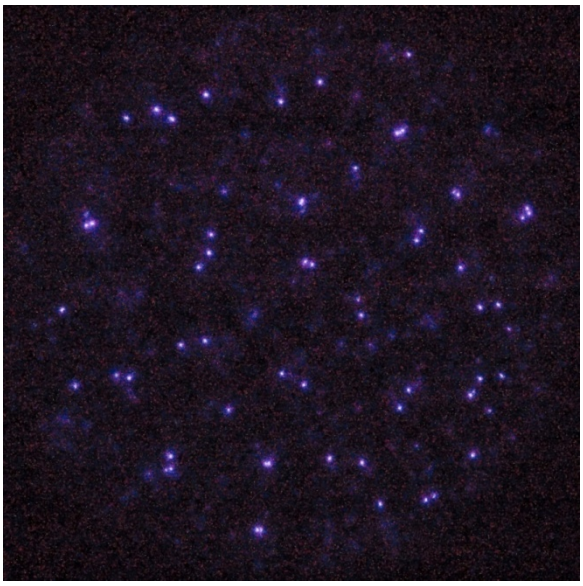


Figure 32. Photograph of plasma through water electrode. 1/320 second (0.0031 sec) shutter open time.

We have designed a system for the generation of high voltage, pulsed, periodic dielectric barrier or corona discharges capable of being used in the presence of conductive liquid droplets and over contaminated surfaces. This system can be used, for example, in different devices for generation of uniform dielectric barrier discharge plasma for treatment and sterilization of various uneven and contaminated surfaces. One of the main difficulties in the development of high voltage short pulsed power supplies is the matching of energy of the pulse generated by the power supply with the energy dissipated in the load. The other important problem is switching off of the high voltage switcher after the pulse subsides. Our so-called nanosecond-pulsed system solves both of these problems and gives us possibility to produce high efficiency generator of extremely short pulses with using reliable and simple pulse switcher like an uncontrolled spark gap.

The system is based on controllable fast charging of a capacitor and then discharging of this capacitor through a series of two spark gaps. This system was discussed in detail previously (see [165]) but the basic principle of operation is as follows. There are two spark gaps and the load connected in parallel with the second spark gap. When the first spark gap discharges, the voltage is applied then simultaneously to the second spark gap and the load. Thus, the voltage applied to the load is defined by the primary spark gap and the duration of the pulse is defined by the second spark gap. Additionally, time between these pulses is defined by the rate of charging of the capacitor. The result of the method is the formation of high voltage pulses with an extremely short rise time, for example, up to 5-20 nanoseconds, and with high pulse repetition frequency, for example, up to 2,000 Hz. The high voltage pulses facilitate maximum efficiency plasma chemical oxidation of detrimental impurities, and increase the range of stable discharge operation in the presence of droplets of water or other conductive liquids in the discharge zone. Details of construction and operation of such a device have already been discussed earlier (see [168]).

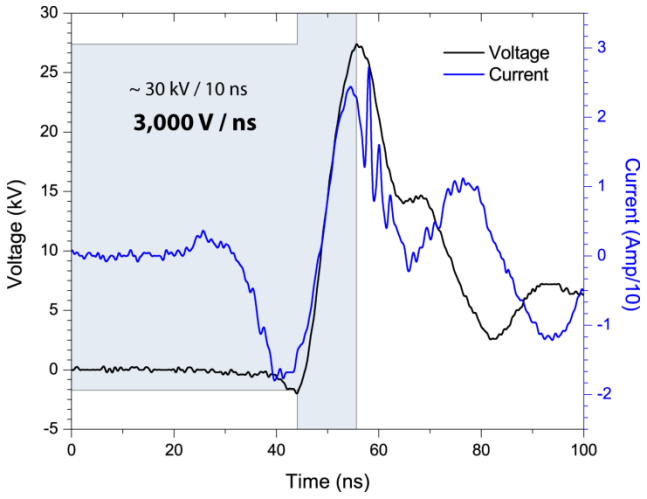


Figure 33. Oscillogram of the nanosecond pulse voltage and current. Voltage rises to ~ 30 kV in ~ 10 ns, or 3,000 V/ns.

Figure 35 shows a result of application of ultra-short high voltage pulses to the FE-DBD setup in Figure 34. This setup allows to quickly move photographic film through plasma discharge. When the discharge is in pulsed mode and the time between pulses is kept sufficiently long (a few hundred Hz) we are able to get an image of a single pulse of plasma on the film plane. The result is a Lichtenberg figure of a completely uniform plasma field. Thus, this setup is able to generate a completely uniform and filament-free plasma at atmospheric pressure and temperature in open air, which can potentially be important for many applications where plasma discharge uniformity is of concern, for example in sterilization of living human tissue or in other applications (see, for example, [19, 26]).

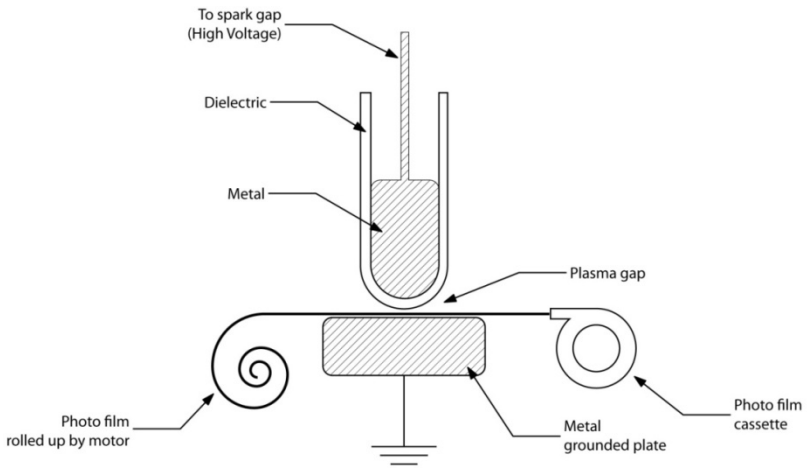


Figure 34. Diagram of a setup to capture a *single* pulse of Dielectric Barrier Discharge plasma on photographic film.

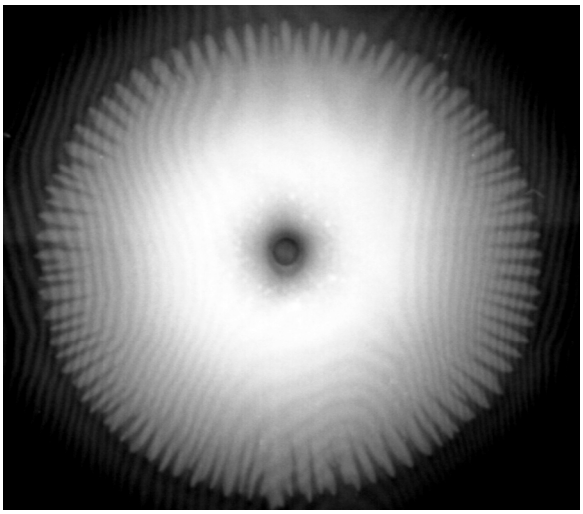


Figure 35. Image produced on black and white photographic film (100 ISO sensitivity negative film) by a single nanosecond pulse of DBD plasma.

For comparison with the uniform plasma pulse produced by the nanosecond excitation (Figure 35) we are able to run the same experiment using the microsecond excitation pulses. The resulting Lichtenberg figure is shown in Figure 36. The microfilament pattern produced on film is identical to that predicted theoretically and observed experimentally in the past, and thus we can assume that we are in fact observing non-uniform plasma [147, 148, 162]. Continuous excitation wave plasma looks similar on the film however since the plasma is on for a significant portion of the time the image on film results in something that is difficult to decipher unless the film movement speed is beyond that of the capabilities of our experimental setup.

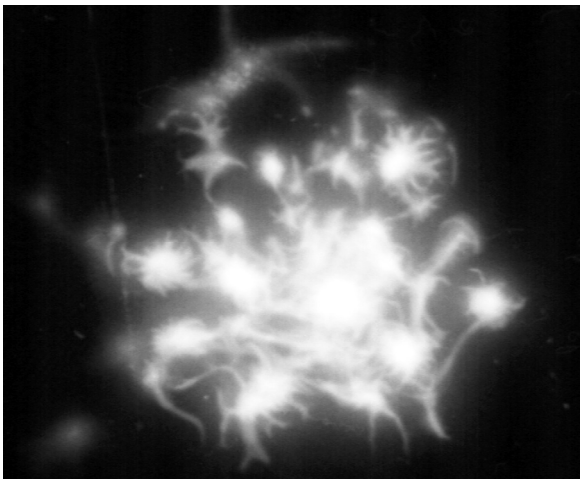


Figure 36. Image produced on black and white photographic film (100 ISO sensitivity negative film) by a single microsecond pulse of DBD plasma.

3.6. Summary of Direct with Indirect comparison of FE-DBD Plasma Application to Tissue

By this point we have discussed the need for a *non-thermal* plasma treatment in Chapter 1 and introduced such a system in Chapter 2. Various modifications of dielectric barrier discharges have already been used by other research groups in the past for surface modification without excessive damage to this surface (see [59, 61, 119, 124, 169-177] for examples). Our task, though, requires direct contact of plasma not with some polymer surface but with a living object. We showed that plasma can safely be put in contact with living tissue where charges are brought to the surface of the organism. This direct treatment was shown to achieve desired effect of sterilization orders of magnitude faster than in the case on indirect treatment by the plasma affluent. Here we understood by what means plasma is able to achieve this desired effect and showed that charged species

(electrons and positive and negative ions) are responsible for the effect. Neutral and excited species also must play an important role in inactivation of bacteria but the presence of charges is essential in achieving the desired effect, at least when the bacteria are treated in room conditions on skin or skin-like surfaces. In the following chapter we will discuss application of the FE-DBD plasma system in non-damaging skin sterilization of human cadavers, and live mice and pigs.

CHAPTER 4. DIRECT NON-DAMAGING TREATMENT BY NON-EQUILIBRIUM PLASMA OF LIVING TISSUE: TOXICITY TRIALS

A topical tissue treatment which induces damage would have a questionable medical use. Our goal in this chapter is to discuss the extent of damage, if any, FE-DBD plasma causes to tissue that it comes in contact with. Some medical treatments, i.e. sterilization of intact skin before surgery or needle insertion, would require no damage to skin, while other treatments, i.e. tattoo removal or removal of necrotic tissue from ulcer surface, would require some degree of precisely controlled damage. We also envision sterilization of open wounds and ulcerating wounds as one of the possible uses of FE-DBD plasma and thus extent of toxicity of the treatment under such conditions needs to be evaluated.

To evaluate the extent of damage FE-DBD plasma treatment causes to tissue, we employ a method known as the "differential skin toxicity trial" [178-182]. In this method, we locate the dose at which damage can be clearly observed both visually and microscopically and then reduce the dose. Once the maximum dose at which no damage is observed is located, more treatments are made around that dose and statistical information is collected. Dose is determined by the combination of plasma power and treatment time; i.e. high power short treatment or low power long treatment. For example, if at 1 Watt/cm^2 of plasma surface power density we observe no damage starting from 60 seconds of treatment then we repeat treatments on 3 samples each at 55, 60, and 65 seconds. If no damage is observed at 55 and 60 seconds while some minor damage is visible at 65 seconds, then 60 second treatment at 1 Watt/cm^2 is deemed the maximum acceptable dose (here dose is 60 sec x 1 Watt/cm^2 =

60 sec·Watt/cm^2). It is a well-known fact in plasma surface processing that dose response is non-linear in most cases [61, 62, 119, 163, 174, 176, 183, 184]. We speak of "dose", but we mean a combination of time and power; i.e. results obtained after 60 seconds of treatment at 1 Watt/cm^2 may be drastically different from the results obtained after 30 seconds of treatment at 2 Watt/cm^2. Additionally, dose rate plays a significant role as well, meaning continuous application of plasma for 60 seconds compared with repeat bursts of 6 seconds, 10 repetitions, with 60 second pause in between; or in the case of a pulsed plasma – the pulse frequency. Although those results were obtained and recorded they are not presented here and can be found in [19, 26, 185].

Initially, all experiments were performed on human cadaver skin tissue samples and discarded skin tissue[3]. The maximum acceptable treatment times were located for different plasma powers. These doses were then employed as the basis for our animal trials. First, we analyzed toxicity on SKH1 hairless mice, and then on regular swine. Following intact skin toxicity trials we moved on to a wound model on swine as their skin closely resembles that of human skin [178, 186-189]. In Section 3.1 we will discuss human cadaver skin trials, mice trials in 3.2, pig intact skin in 3.3 and wound model in 3.4.

---

[3] Discarded tissue, according to our IRB protocol and agreement with the hospital is tissue which was removed from the patient and approved medical doctor deems no longer necessary for any tests. Examples of such tissues include skin tissue discarded during abdominal surgery, placenta tissue not wanted by the patient, tissue removed during plastic surgeries, wound debris, etc.

4.1. Skin Toxicity Trials on Human Cadaver Tissue

Although human cadaver skin is a dead tissue, it does closely resemble skin of a living patient for the purpose of our initial physical investigation [190-192] – in our initial experiments we sought to find conditions under which a not perfectly polished skin-like substrate is not thermally or chemically disintegrated. At first we simply applied plasma to skin which was laying on a metal surface, but have quickly realized that such a setup leads to uncontrollable and rarely repeatable results. Figure 38 shows one such example where two different samples were treated at high power for 2 minutes each (Figure 37 – setup). The first sample (top) remained flat during treatment (as observed by eye during the treatment process); the second sample "bunched up" and touched the electrode in the center leading to a very non-uniform result. Obviously such a result is unacceptable, so we have devised a setup allowing for repeatable experiments (see below).



Figure 37. Photograph of the FE-DBD treatment electrode with a "jacket" which allows for control of distance between electrode and treatment target.

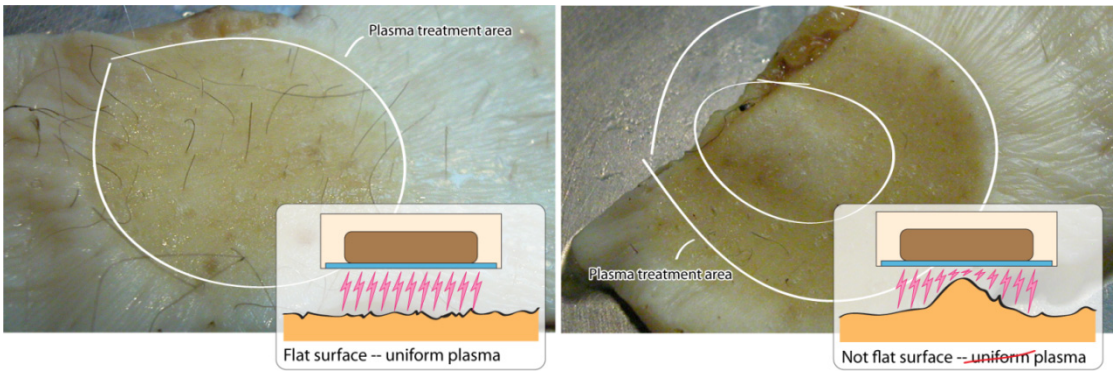


Figure 38. Photographs and schematics of the results of 2 minutes of FE-DBD plasma treatment at 1.6 W/cm^2. Skin is laying on metal surface which leads to uncontrollable results: uniform treatment is some cases (top) and non-uniform in others (bottom).

Modification of the above setup where tissue sample is held in place by vacuum suction was introduced and allowed us to obtain repeatable results. Figure 39 shows a schematic of the setup with the photographs of the perforations on the vacuum skin holder (circular skin sections were cut with a specialized tool we have manufactured for this purpose; it is similar to a basic cookie-cutter with very sharp edges). Figure 40 shows this setup in operation. The photo is dark to allow us to clearly see plasma.

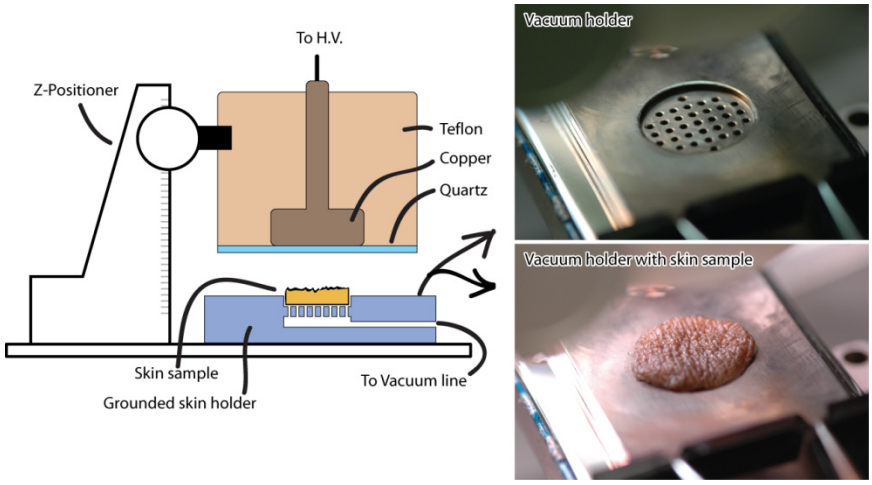


Figure 39. Schematic of the tissue treatment setup with vacuum suction and zoom photographs of the vacuum holder perforations.

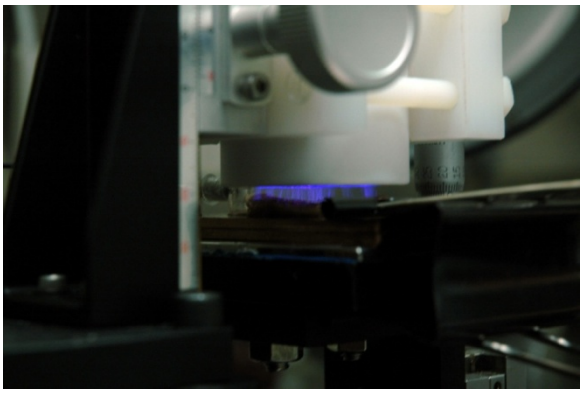


Figure 40. Vacuum suction treatment setup in operation during plasma treatment.

Our results confirm that there is no gross (visible) or histological (microscopic) damage to the treated skin and organ samples in as much as 5 minutes of treatment (Figure 41) while complete hospital-grade sterilization is achieved in less than 6 seconds of plasma treatment. Skin samples treated by plasma show no visible damage (Figure 41, top) and histological analysis shows no microscopic damage (Figure 41, bottom).

For treatment of human skin, explanted tissues and organs, two models were constructed. In the first model, skin samples and organs were harvested from human cadavers; in the second model, tissues and organs discarded during surgery were used. Neither model offers an insight into interaction of plasma with *living* organisms but provides us with data on plasma's ability to physically damage tissue and/or sterilize bacteria from its surface. In all experiments the copper or water electrode was fixed at a controlled distance from the treated tissue or organ either by means of micro-positioners, where available, or by spacers glued to a hand-held electrode. All tests were performed as soon as the samples were obtained. Treated samples were photographed then stored in Formaldehyde and submitted to the Pathology lab

where the samples were fixed in paraffin, sectioned, and stained by Hematoxylin & Eosin (H&E) for microscopic analysis. Additionally, a small section of the sample was frozen in liquid nitrogen and stored at -80°C in case further analysis might be desirable.

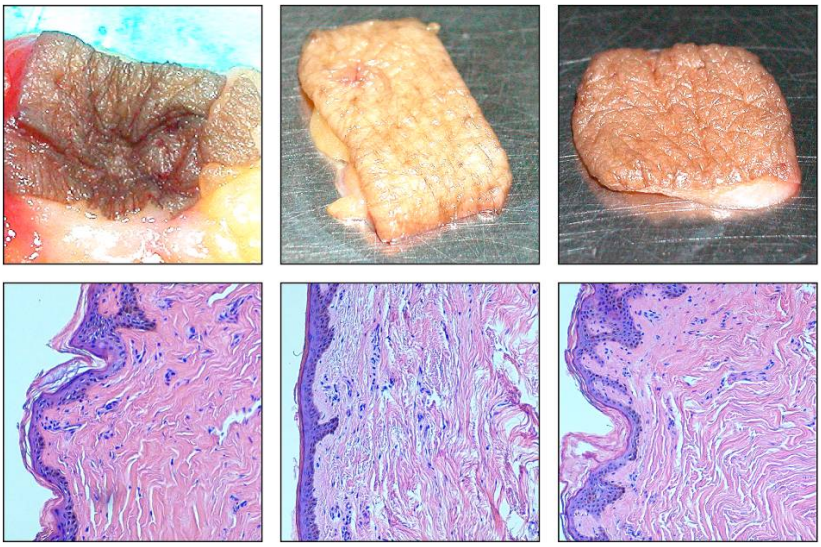


Figure 41. Photos (top) and tissue histology (bottom) of cadaver skin samples after FE-DBD treatment: control (left), 15 seconds of treatment (center), and 5 minutes of treatment (right) – no visible damage is detected.

4.2. Skin Toxicity Trials on Live Hairless Mice

Following the investigation on cadaver tissue we initiated our first live animal trial. Although mouse skin is not as close to human skin as that of a pig, we have selected mice for the initial trial following a suggestion from a representative of Food and Drug Administration (FDA) and the Institutional Animal Care and Use Committee (IACUC) members – since a pig model was also planned at that time, to minimize the overall

experimental matrix, the use of a smaller animal model was recommended to us prior to toxicity trial on larger species.

Regular healthy mice were selected at first; however, we quickly found out that shaving them causes noticeable skin irritation and thus introduces further experimental variability (Figure 42). SKH1 mice from Charles River Laboratories proved then to be an excellent experimental subject. They are not immunodeficient – some mouse models with suppressed immune systems are hairless as a side effect of genetic modification while SKH1 mice are simply hairless but otherwise quite healthy and immunocompetent (Figure 43).

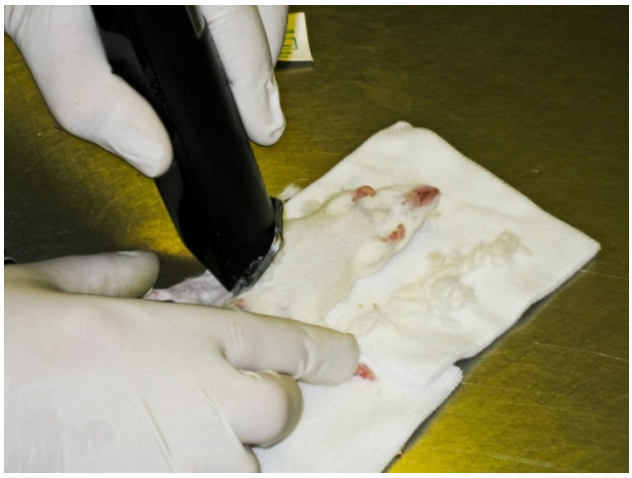


Figure 42. Photograph of a regular mouse during hair shaving procedure. Post shaving the skin appears to be quite irritated and thus the model is not usable for a skin toxicity trial.

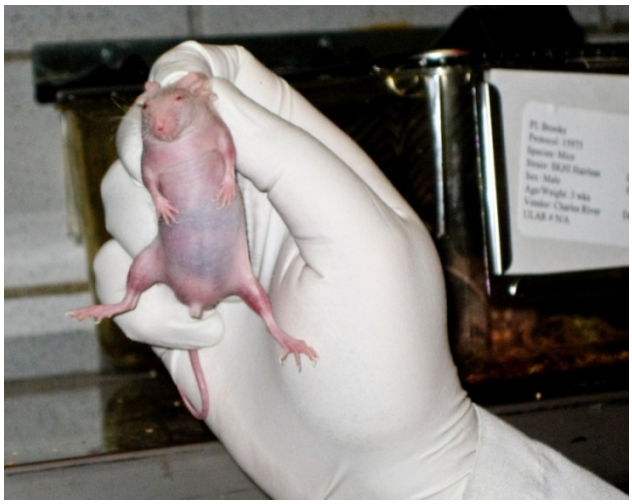


Figure 43. Photograph of a Charles River Laboratories SKH1 hairless mouse immediately after arrival at the animal care facility.

Mice were anesthetized using Isoflurane gas inhalation and remained anesthetized throughout the procedure. Some animals were euthanized by CO_2 asphyxiation while others were placed on a warming blanket and allowed to wake up for post-surgery observation. During plasma treatment animals were fixed using tape to minimize movement and the plasma electrode was attached to a flexible holder which can be adjusted in all dimensions and then fixed in desired position. We have also attached a fixed-thickness perforated ceramic spacer to the electrode to ensure precise distance between the animal and the electrode (Figure 44 – power supplies, Figure 45 – general schematic of the electrode setup, and Figure 46 – example photograph of the animal immediately following treatment).

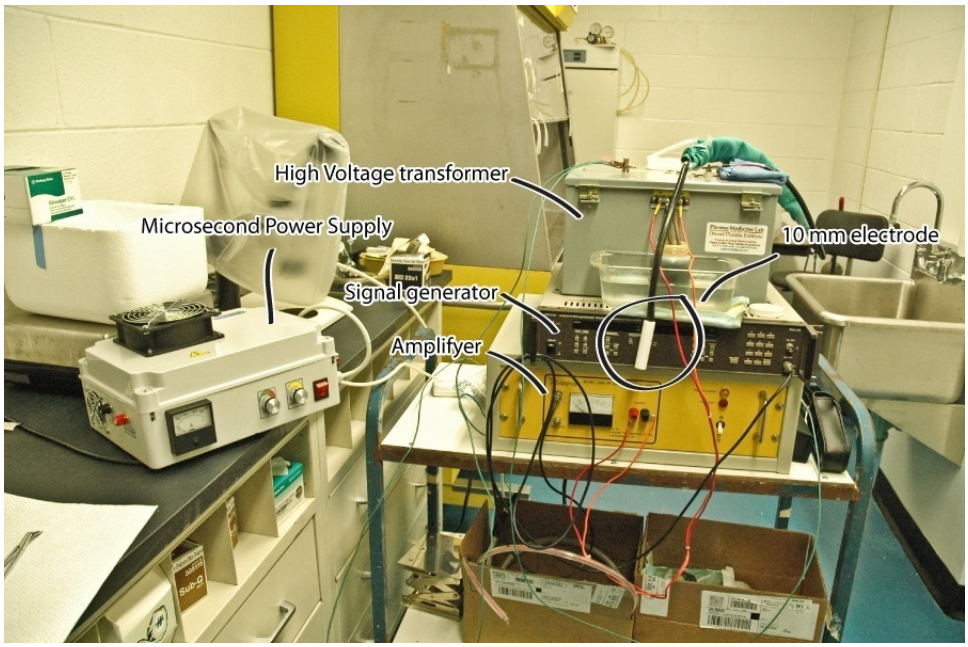


Figure 44. Photograph of two power supplies (microsecond pulsed and continuous sinusoidal) with the small 10 mm diameter electrode for treatment of mouse skin.

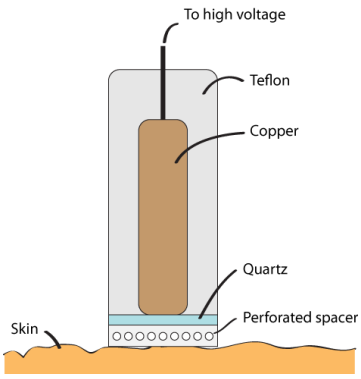


Figure 45. Schematic of the 10 mm diameter copper electrode with attached perforated spacer for controlled treatment of a mouse.



Figure 46. Photograph of an animal immediately following treatment. The perforated spacer is left on the area of treatment to mark it for later sample harvesting. Areas 1 and 2 have already been treated, in this particular case for 75 seconds at 0.3 Watt/cm^2 surface power density by microsecond pulsed power supply. No damage to skin is observed visually.

Based on the experimental matrix, a dose of 10 minutes at 0.6 Watt/cm^2 was determined as maximum acceptable prolonged treatment and a dose of 40 seconds at 2.3 Watt/cm^2 was determined as maximum acceptable high-power treatment. Histological (microscopic) comparison of control SKH1 skin sample with toxic and non-toxic plasma doses show regions where plasma dose is high while the animal remains unaffected (Figure 47 – histological samples, Figure 48 – animal after the treatment). Of note is that sterilization was achieved at 2 to 4 seconds at high-power treatment of 0.8 ±0.2 Watt/cm^2 and at 10 ±4.4 seconds at half that power.

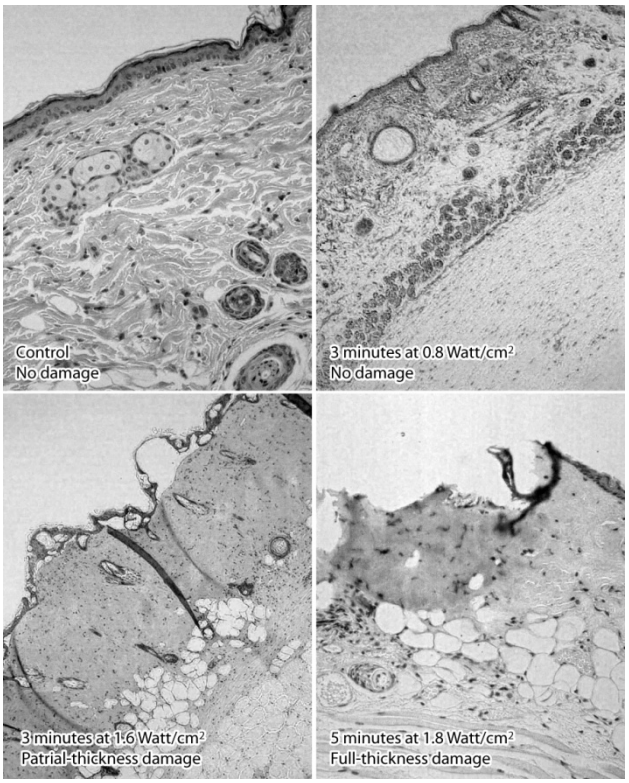


Figure 47. Histology of toxic and non-toxic to SKH1 skin plasma doses, compared to untreated skin.

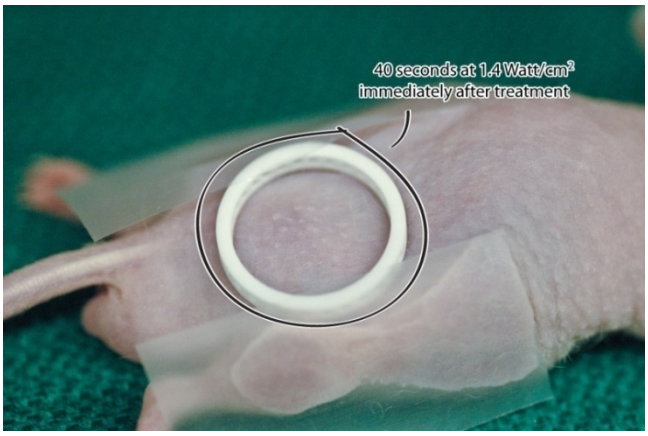


Figure 48. Animal remains fine immediately after a high plasma dose (more than 10 times higher than needed for skin sterilization).

To test if the treatment has some longer-term effect which is not immediately visible we have left a portion of animals alive for up to two weeks. Figure 49 shows the same animal

from Figure 48 two weeks following the treatment. There is no apparent visible change to the treated area and histological samples show no damage to skin as well.



Figure 49. Animal remains fine two weeks following a high plasma dose (more than 10 times higher than needed for skin sterilization).

4.3. Skin Toxicity Trials on Live Regular Swine

Following the toxicity trial on mice we moved on to a large animal model utilizing for it regular swine. Pig skin resembles closely that of humans and thus makes for a good animal model of skin toxicity [178, 186-189]. The experimental setup is essentially the same as for mice, the main difference being that we made a much lighter electrode and taped it to the animal rather than positioning it using a 3D holder as was done for mice and cadaver tissue (Figure 50).

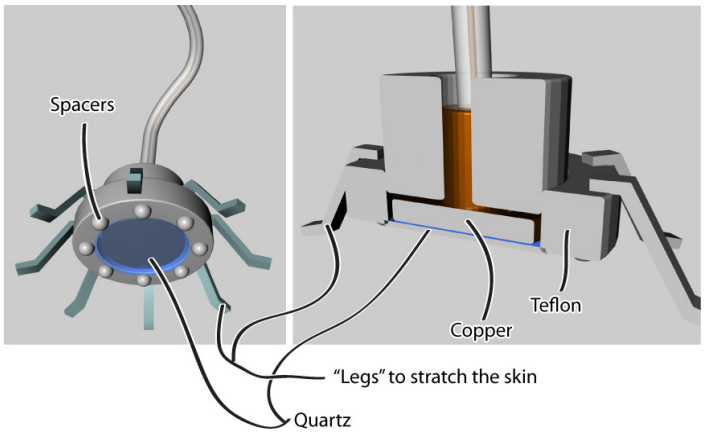


Figure 50. 3D schematic of the electrode used for swine skin experiments.

The electrode design based on the initial idea shown in Figure 50 has proven to be too heavy to be held up to animal skin by tape and thus we have removed Teflon coating replacing it (for electrical safety) with a layer of glue (Figure 51). This small modification does not change the results this electrode is able to achieve as the plasma remains the same, but the electrode weight is reduced enough so that it can be securely attached to the animal skin by tape. This becomes useful mainly for the cases of prolonged treatment (over 30 seconds). This also offers an insight into future electrode designs. When the treatment will be performed on an actual human patient, especially if he or she is not anesthetized and is able to move freely, the treatment time needs to be kept below a few seconds for a hand-held electrode. For treatments longer than that the system needs to be designed to securely hold the electrode to the patient allowing him or her to move freely while the skin-to-electrode distance remains fixed.



Figure 51. Photograph of the modified FE-DBD electrode attached to animal skin using tape.

Based on our experience with SKH1 hairless mice described in the previous section we have performed a series of similar experiments on intact skin of regular swine. For all treatments we have selected a microsecond pulse plasma excitation power supplies. To assess dose rate dependence of these treatments we have utilized four different pulse frequencies identified in Table 5. We refer to these later in the text as ranging from high dose rate ("Setting 4", 1,500 Hz) to low dose rate ("Setting 1", 500 Hz).

Table 5. Plasma power supply settings used in the swine skin treatment experiments.

Label	Pulse frequency	Surface power density
Setting 1	500 Hz	0.13 Watt/cm^2
Setting 2	800 Hz	0.19 Watt/cm^2
Setting 3	1,000 Hz	0.25 Watt/cm^2
Setting 4	1,500 Hz	0.31 Watt/cm^2

A good example of a high dose treatment (low dose rate, Setting #1, but long time) wound be treating an animal for 10 minutes. At this dose rate we observe inactivation of bacteria

on agar, human cadaver skin, and on mice in under 10 seconds (5 seconds leads to 7 log reduction in viable bacteria) [26]. Treatment for longer than 10 seconds would show it to be not only effective but also safe. We were able to treat animal skin for up to 10 minutes without any damage to it apart from mild inflammation that disappears within a few minutes following treatment. For this we locate healthy section of the tissue (Figure 52), shave it, mark the location where the electrode will be attached, take the electrode to the tissue and turn on the plasma. Immediately following the treatment we do observe a slight skin inflammation which can be seen in Figure 52 on the right as compared to Figure 52 on the left which is a photograph of the same section of the skin but prior to treatment. The time between these two photographs is approximately 10 minutes and 15 seconds – as soon as the initial photo is taken the electrode is attached and the plasma treatment commences; the after treatment photograph is taken a few seconds following the electrode removal, or as soon as the camera is positioned correctly and focused on the specimen.



Figure 52. Photograph of the animal skin prior (left) and immediately following a 10-minute FE-DBD treatment at low frequency Setting #1 (right). A mild skin inflammation is visible immediately after the

treatment (shown) which disappears within a few minutes following the treatment (not shown). Black markings on the skin indicate position of the edge of the treatment electrode (for skin sample harvesting purposes).

The inflammation we refer to here is barely visible on the photograph while is more apparent in real life to a human observer directly near the wound. This inflammation disappears quickly following the treatment. The skin is then harvested and sent for H&E histological staining and later sectioning following the same protocols as discussed above for human cadaver and SKH1 mice. Figure 53 shows the result of this staining of the above skin sample treated for 10 minutes. As can be seen from this image, there is no tissue damage and/or inflammation; in other words, this skin sample appears the same as an untreated control sample.

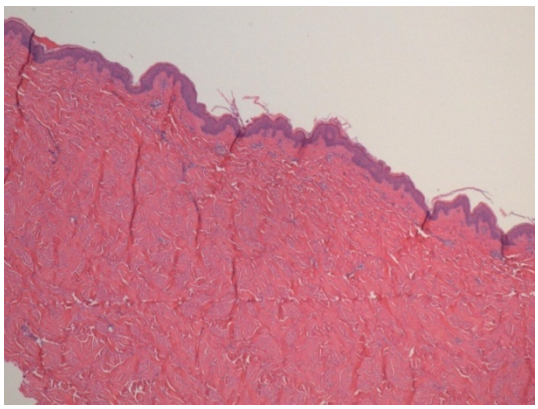


Figure 53. H&E histological stain of the skin sample treated for 10 minutes at low frequency Setting #1 (Figure 52). No microscopic damage to skin can be seen.

The positive control for this treatment is done with the state-of-the-art Bovie® knife which resistively heats up the tissue by passing current through it causing tissue desiccation, inflammation which is immediately visible (compare with 10 minutes of plasma treatment

in Figure 52), and overall severe tissue damage. Figure 54 shows the result of such a treatment where excessive damage is clearly seen.



Figure 54. Photograph of the animal skin immediately following treatment by Bovie® knife (positive control) – excessive skin damage, desiccation, and inflammation are clearly visible.

Overall results of the skin toxicity trials on pigs are similar to those on human cadaver skin and on SKH1 mice – only rather high doses of plasma, those far greater than needed for sterilization or blood coagulation, are able to damage skin; while doses required to achieve desired medically relevant therapeutic effect are significantly below the damage threshold.

4.4. Wound Toxicity Trials on Live Regular Swine

One of the potential applications of FE-DBD plasma treatment is sterilization of wounds and/or coagulation of bleeding capillaries (see end of section 2.2 above). We were able to test the efficacy and toxicity of such treatment on a superficial partial thickness skin wound similar to that of scraping one's knee. Once the animal was anaesthetized the wound was

made with a small hand-held dermatome knife (Zimmer, Franklin County, OH, USA) originally designed to remove precise-thickness skin grafts from a donor patient (Figure 55). Although the hand-held version of this device is difficult to master[4] for precise skin graft removal, the wounds that we were able to create with this blade appear to the eye closer to the actual wounds that FE-DBD plasma would potentially be treating – they have a torn texture similar to that of a deep scrape wound one gets falling from a bicycle, for example (see Figure 55). These are partial thickness wounds with the blade set to cut no deeper than a millimeter into the skin. This exposes the top layer of skin and breaks capillaries located in the skin, but not the bigger vessels. Thus, the bleeding is slow and manageable. The zoom in on the wound demonstrates a typical wound we are able to induce with this procedure. This is not a severe wound and the bleeding would normally self-terminate quickly. Immediately after the wound is made we proceed with the selected treatment.

[4] For taking actual skin grafts, Zimmer recommends their automatic knives which are driven by compressed air and have proven themselves to be quite a bit more precise than the hand-held version.



Figure 55. Photograph of a process of making a partial thickness skin wound with a dermatome knife (left) and a zoomed in photograph of the resulting wound immediately prior to the FE-DBD plasma treatment.

Similar to the intact skin, treatment with Bovie® knife quickly coagulates blood and desiccates the tissue but causes quite significant damage (see Figure 56, left). Although the wound may be closed, there is a significant level of tissue damage which may prolong the wound healing process over that if the wound was simply left with no treatment in this case. While Bovie® electrosurgery knife causes significant tissue damage, FE-DBD plasma treatment can be applied to the tissue for up to 15 minutes with minimal damage to this tissue (Figure 56, right), similar to what was observed above with treatment of intact skin. One other observation is that even after a short treatment, the blood appears to be coagulated and (although this is not visible on the photograph below) the wound looks to be covered with a thin layer of clear coagulum. We have seen such a thin transparent cork formation before with treatment of blood and blood plasma samples [19, 193]. This film was claimed to be a thin layer of coagulated blood plasma – FE-DBD seems to quickly

form a layer of coagulated blood on the surface of the wound which protects the wound from further external disturbances.

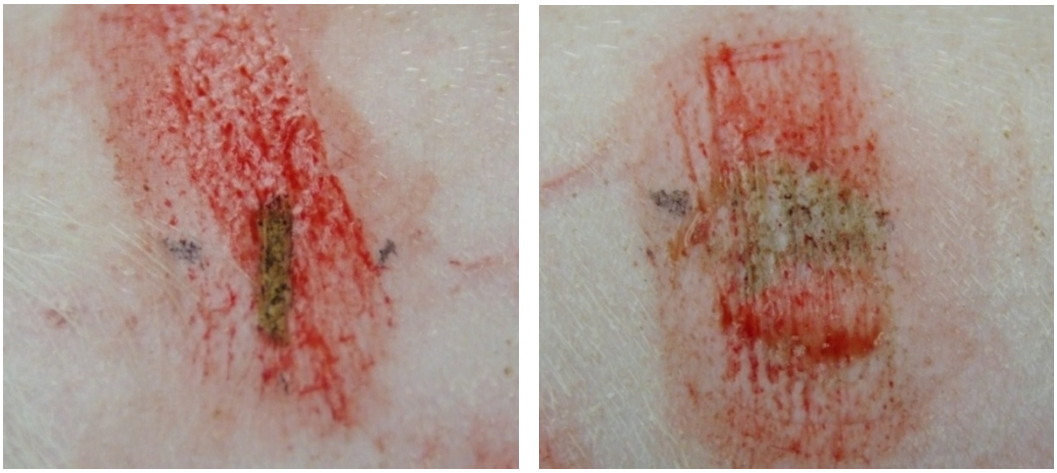


Figure 56. Photograph of a positive control treatment with Bovie® knife (left) where the tissue is clearly desiccated and blood is clotted but the tissue damage is quite extensive. Compared to a photograph of a wound treated by FE-DBD plasma for 15 minutes in low power Setting #1 (right) where no significant tissue damage is observed and a layer of coagulated blood is formed over the wound surface.

Results of the various FE-DBD plasma treatments of wound surface are detailed in Table 6 and Table 7, and histological images of these skin samples are shown in Figure 57 and Figure 58 respectively. The overall observation is that at a low dose rate (Setting #1) we are able to treat the skin surface for prolonged time periods without seeing significant tissue damage; while, as expected, at high dose rates we are able to achieve coagulation and wound closure much faster, along with the tissue damage.

Table 6. Results and analysis of FE-DBD plasma treatment of wound surface.

Label	Treatment Group	Gross observations during surgical treatment (cm)	Histology analysis (blinded to specimens)
1	Bovie knife (positive control)	2.5 x 1.0 area of effect, eroded	Disruption of epidermis and papillary dermis, areas of

			dermis coagulated, no dermal nuclei, hair follicles still intact
2	No treatment (negative control)	No change, normal skin	No change, normal skin
3	3 min, setting 4	2 x 2 area of effect, mottling	Similar to bovie, burn through to dermis
4	3 min, setting 4	2 x 1.5 area of effect, pigmented, irregular, raised	Similar to bovie, burn through to dermis, slightly more than label 3
5	3 min, setting 3	0.5 x 0.7 area of effect, pigmented	Similar to bovie, burn through to dermis
6	3 min, setting 3	1.5 x 1.5 area of effect, some pigmentation, mottling	Burn through to epidermis, small area of congestion in dermis
7	3 min, setting 2	1.5 x 1.2 area of effect, lightly mottled	Small area of burn in epidermis, most skin here is intact
8	3 min, setting 2	2 x 1.5 area of effect, lightly mottled	Small area of burn in epidermis
9	15 min, setting 1	2.5 x 2 area of effect, lightly mottled	Small area of burn in epidermis
10	15 min, setting 1	2.5 x 3 area of effect, lightly mottled	Small area of burn in epidermis
Ends of 1-10	All edges of the specimens (1-10) to assess for zone effect	No change, normal skin	All show normal skin, no zone effect

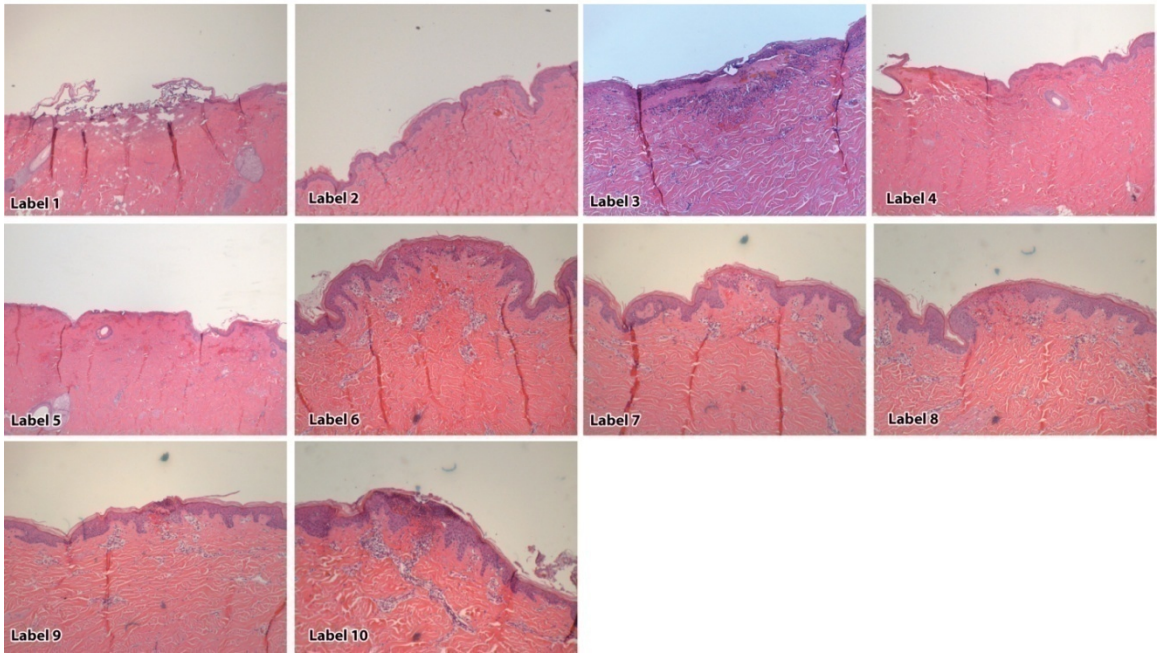


Figure 57. Results of H&E histological stain for samples described in Table 6.

Table 7. Results and analysis of FE-DBD plasma treatment of wound surface.

Label	Treatment Group	Gross observations during surgical treatment	Histology analysis (blinded to specimens)
1	Bovie	Eschar formation, burn formation immediately after treatment Instant blood coagulation Necrotic tissue	Necrosis deep in the dermis. Disruption of the dermis. No dermal nuclei. Hair follicles still intact
1B0	Control wound	Normal wound	No change to wound
2	High Frequency 3 min	Blood clot formation, no necrotic tissue no burn	No damage to dermis. Looks like normal wound. No damage to hair follicles.
3	Low Frequency 3 min	Blood clot formation. No burn	Looks normal. No damage to dermis. Hair follicles intact. Clot formation
4	High Frequency 1	Clot formation. No burn	Looks normal. Practically no

	min	to wound	damage to tissue. No damage in dermis. Hair follicles intact
5	Low frequency 1 min	No burn. Clot formation	No damage. No tissue damage. Hair follicles intact. Clot formation on the surface of the wound
6	High Frequency 30 s	No burn. Clot formation	Practically no damage to tissue. No damage in dermis. Clot formation
7	Low Frequency 30 s	No burn. Clot formation	Practically no change. No damage. Clot formation
8	High Frequency 5 s	No burn. Clot formation	Practically no change. No damage to dermis. No damage to tissue. No clot formation
9	Low frequency 5 s	No burn. Clot formation	No damage. Clot formation. No damage in dermis
10	High Frequency 3 min	Blood coagulation. No burn observed	Practically no damage to dermis. Intact hair follicles
11	Low Frequency 3 min	No burn. Clot formation observed	No damage to dermis. Intact hair follicles. No necrotic tissue
12	High Frequency 1 min	No burn. Clot formation	Clot visible. No damage to dermis. Intact hair follicles.
13	Low frequency 1 min	No burn observed. Clot formation immediately after treatment	No damage to dermis. Practically no change
14	High Frequency 30 s	Clot formation. No burn observed	Clot on the surface. No damage to dermis. No change
15	Low Frequency 30 s	No burn observed. Blood clot formation	Clot on surface. No damage to wound tissue. Intact hair follicles
16	High Frequency 5 s	No change in the wound observed	Clot on the surface of the wound. No damage to wound tissue.
17	Low frequency 5 s	No change in the wound observed	No change. Practically no damage
18	Control wound	Normal wound	No change
18B+	Bovie	Eschar formation. Immediate coagulation	Burn in the dermis. Necrotic tissue. Lack of dermal nuclei. Damaged tissue. Disruption of the dermis

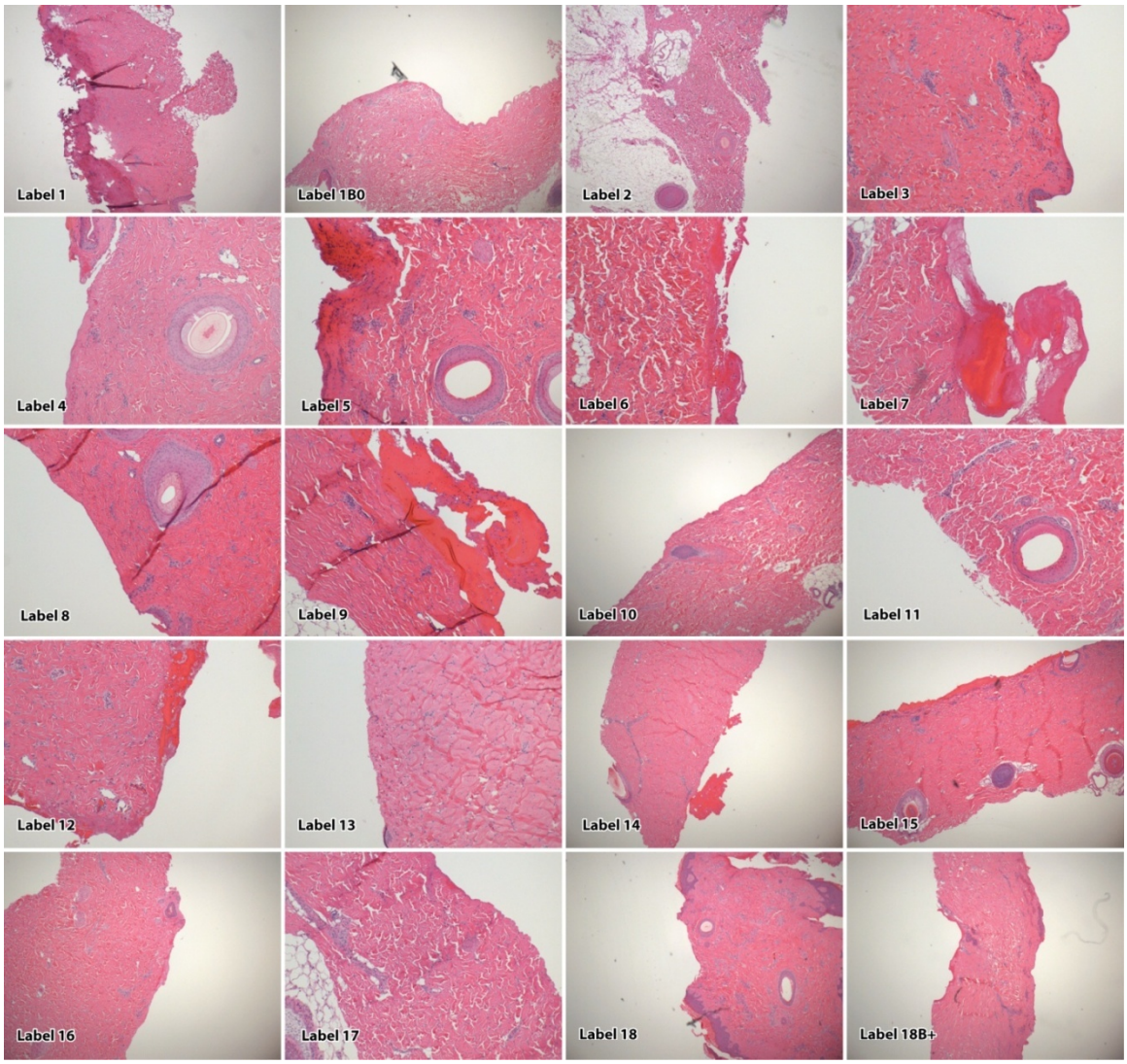


Figure 58. Results of H&E histological stain for samples described in Table 7.

4.5. FE-DBD Treatment of Living Tissue: Next Steps

Application of non-equilibrium plasma to cells and tissues has been shown to be quite selective in inactivation of pathogens, sterilization, and promotion of complex biological responses with minimal or no damage to the treated tissues and cells. Details of such

selectivity with data from many groups around the world are discussed in detail by the authors in a recent review [26]. Based on our own experimental data presented above with cadaver tissue, living mice, living pigs, and data reported on previously with cell cultures of various mammalian cells (macrophages, epithelial cells, b-lymphocytes, fibroblasts, and melanoma cancer cells) we can thus-far deduce three major hypotheses for the reasons of the observed selectivity:

1. Metabolism of reactive oxygen species (ROS) is difference in prokaryotic (i.e. bacteria) and eukaryotic (i.e. mammalian) cells; i.e. while human cells have protection from species like O_2^- (superoxide) bacteria either lack it completely or the resistance is lower.
2. Higher order organisms have developed more resistance mechanisms to external stress (osmotic pressure changes, ROS, chemical and biological poisons, etc); in other words, bacteria usually act as a single cell while mammalian cells, especially those organized into tissues, communicate with each-other possibly lowering the effects of the applied poison.
3. Bacterial cells are usually much smaller than mammalian cells and thus have much higher surface to volume ratio; i.e. simply a lower dose of poison is required to inactivate same number of bacteria vs. mammalian cells.

These hypotheses are of course quite phenomenological and further detailed testing is required to claim them to be true. However, authors are continually receiving evidence in support of these ideas [19, 26, 27, 109, 143, 193-197].

Radiation biology studies biological effects of ionizing and non-ionizing radiation of the whole electromagnetic spectrum. Our concern is primarily with the penetrative ionizing radiation resulting from radioactivity (alpha, beta, and gamma) and x-rays. Here radiobiology claims that the main mechanism of action on a cell is through formation of reactive oxygen species directly in the vicinity of a DNA molecule inside a cell nucleus [198, 199]. The ROS of interest here are hydroxyl radicals (OH), hydrogen peroxide (H_2O_2), and the superoxide anion (O_2^-). A stain for DNA double strand break, the same test used in radiobiology, shows that the damage does, in fact, occur but is repaired by the cell rapidly and the cell recovers [200].

FE-DBD plasma used in this treatment is a gas-phase phenomena and is not generally known to penetrate liquids, unlike radiation does. So, what is it in plasma that is able to go through liquid? Mechanism of action is likely through same ROS as in radiobiology but these ROS are not generated at the vicinity of a DNA molecule but rather are transported to it through a series of mechanisms already present in cells. Example of such a mechanism is as follows. First, a superoxide anion is generated from hydrated electrons deposited into the liquid from plasma: $e_{(H_2O)} + O_{2(H_2O)} \longrightarrow O^-_{2(H_2O)}$. Mammalian cells have a mechanism of defense against superoxide and immediately converts it into less harmful hydrogen peroxide through a reaction termed "superoxide dismutation" which is catalyzed by an enzyme appropriately termed superoxide dismutase (SOD): $2O_2^- + 2H^+ \xrightarrow{[SOD]} H_2O_2 + O_2$. Hydrogen peroxide can then travel through liquid (and we do see quite high concentrations of it in liquid cell growth media). At appropriate conditions, hydrogen peroxide is converted to hydroxyl radicals through a natural reaction chain termed Fenton mechanism

(where M^+ is any ion coming to liquid from plasma, for example N_2^+ which is abundant in air plasma [201]):

$$H_2O_2 + Fe^{2+} \longrightarrow \mathbf{OH} + OH^- + Fe^{3+}$$

$$Fe^{3+} + O_2^- \longrightarrow Fe^{2+} + O_2$$

$$M^+ + H_2O \longrightarrow M + H_2O^+$$

$$H_2O^+ + H_2O \longrightarrow H_3O^+ + \mathbf{OH}$$

Hydroxyl radicals may then react with nearby organics leading to chain oxidation and thus destruction of DNA molecules as well as cellular membranes and other cell components (here R is some organic molecule):

$$OH + RH \longrightarrow \mathbf{R} + H_2O$$

$$\mathbf{R} + O_2 \longrightarrow RO_2$$

$$RO_2 + RH \longrightarrow RO_2H + \mathbf{R}$$

Another potential mechanism is through change of ionic force of solution surrounding the cells by plasma ions. Plasma in this case simply acts as source of excess charges, similar to adding acid or salt in the vicinity of the cell thus changing osmotic pressure which leads to pore formation, cell leakage, and possibly death. We can estimate N_2^+ ion concentration from ionic flux to the treated surface at the electric plasma specific power of 1 W/cm^2:

$$G_{N_2^+} = 0.3\ {}^{1}\!/\!_{100\text{eV}}$$

$$\Phi_{N_2^+} = G \cdot P = \left(0.3\ {}^{1}\!/\!_{100\text{eV}}\right) \cdot \left(1\ {}^{\text{W}}\!/\!_{\text{cm}^2}\right) =$$

$$= \left(0.3\ {}^{1}\!/\!_{100\text{eV}}\right) \cdot \left(\frac{1}{1.6 \cdot 10^{-19}}\ {}^{\text{eV}}\!/\!_{\text{cm}^2 \cdot \text{sec}}\right) \approx 2 \cdot 10^{16}\ \frac{N_2^+\ \text{ions}}{\text{cm}^2 \cdot \text{sec}}$$

here Φ is the ion flux, P is specific power, and G_{N2+} is the "G-factor" for Nitrogen ion production in electric discharge – number of Nitrogen ion produced per 100 electron-Volt (eV). In this simplified model, we are assuming that every N_2^+ ion produced in the plasma volume reaches the liquid surface. Plasma treatment area is a 2 cm diameter circle so the treated area is 3.14 cm^2. From here we can see that the total number of ions produced per second is $6*10^{16}$. This is an excessively high number but gives us an idea of an order of magnitude of ions coming to the vicinity of the bacterial cell during treatment. Although significant further work is needed in this direction, initial indication of a possibility of influence of ionic force of solution in cell's lifecycle is apparent and will be further investigated in the future.

CONCLUDING REMARKS

The main novel contributions of this thesis are:

- Development of a new non-thermal atmospheric pressure plasma discharge which can be applied directly to living tissue without painful sensations or visible damage;
- Demonstration of high efficiency of this discharge in deactivation of bacteria on surfaces of living tissue and those that mimic living tissues;
- Demonstration that the discharge parameters related to its uniformity, temperature, generation of active can be partly controlled via the shape of the applied voltage waveform;
- Demonstration that no visible tissue damage of intact skin and scraped wounds occurs for discharge doses that are much higher than those required to reduce bacterial load by over 6 orders of magnitude; and
- Demonstration that high efficiency of the direct application of the non-thermal plasma is mainly due to contact of infected surfaces with charged species in plasma in the presence of oxygen.

The work carried out in this thesis contributes to the recent trend of using plasma in medicine not only for tissue ablation or cauterization, but also for much more subtle modalities of medical therapy. Medical applications of 'cold' plasmas such as tissue sterilization, treatment of corneal infections, blood coagulation, treatment of cancers,

leishmaniasis, treatment of dental diseases and others are in the beginning stages of their development. Though preliminary results are very promising, bringing 'cold' plasmas into medical practice will not be very easy. Besides the usual safety concerns, the main obstacle remains the lack of understanding on molecular and biological levels of mechanisms of interaction between non-thermal atmospheric pressure plasma and living cells, tissues, organs, and the whole organism. While it is clear that direct interaction with hot plasma occurs mainly through heat transfer, interaction with non-thermal plasma in general may depend on a myriad of variables including various charged species, electric field, UV, radicals, electronically excited atoms and molecules. Complex synergies may be responsible for different effects. Not only dose, but the effects of dose rate may be of critical importance for treatments. Fundamental studies in the area of plasma medicine are further complicated by the true interdisciplinary nature of investigations that are required. Although many challenges remain, this work clearly reveals the enormous potential of the non-thermal plasma technology in medicine. The growth of this technology will probably continue in the near future not only because the payoffs are substantial, but also because plasma is one of the few remaining areas of modern technology whose application in medicine has been barely explored.

LIST OF REFERENCES

1. Compton, K.T. and I. Langmuir, *Electrical Discharges in Gases. Part I. Survey of Fundamental Processes.* Reviews of Modern Physics, 1930. **2**(2): p. 123-242.

2. Laroussi, M., D.A. Mendis, and M. Rosenberg, *Plasma interaction with microbes.* New Journal of Physics, 2003. **5**: p. 41.

3. Ginsberg, G.G., A.N. Barkun, J.J. Bosco, J.S. Burdick, G.A. Isenberg, N.L. Nakao, B.T. Petersen, W.B. Silverman, A. Slivka, and P.B. Kelsey, *The argon plasma coagulator.* Gastrointestinal Endoscopy, 2002. **55**(7): p. 807-810.

4. Lord, M.J., J.A. Maltry, and L.M. Shall, *Thermal injury resulting from arthroscopic lateral retinacular release by electrocautery: report of three cases and a review of the literature.* Arthroscopy, 1991. **7**(1): p. 33-7.

5. Vargo, J.J., *Clinical applications of the argon plasma coagulator.* Gastrointestinal Endoscopy, 2004. **59**(1): p. 81-88.

6. Watson, J.P., S. Jowett, K. Oppong, C.O. Record, and K. Matthewson, *Colonoscopic argon plasma coagulation for benign and malignant rectal tumours.* Gut, 1997. **40**: p. Th156-Th156.

7. Colt, H.G. and S.W. Crawford, *In vitro study of the safety limits of bronchoscopic argon plasma coagulation in the presence of airway stents.* Respirology, 2006. **11**(5): p. 643-647.

8. Raiser, J. and M. Zenker, *Argon plasma coagulation for open surgical and endoscopic applications: state of the art.* Journal of Physics D: Applied Physics, 2006. **39**(16): p. 3520.

9. Tremblay, J., *Plasma skin regeneration (PSR) in the treatment of acne scars.* Journal of the American Academy of Dermatology, 2007. **56**(2, Supplement 2): p. AB1.

10. Bogle, M.A., K.A. Arndt, and J.S. Dover, *Evaluation of plasma skin regeneration technology in low-energy full-facial rejuvenation.* Archives of Dermatology, 2007. **143**(2): p. 168-174.

11. Kronemyer, B., *Portait PSR3 Technology Provides True Skin Regeneration*, in *European Aesthetic Buyers Guide*. Spring 2006.

12. Coulombe, S., V. Leveille, S. Yonson, and R.L. Leask, *Miniature atmospheric pressure glow discharge torch (APGD-t) for local biomedical applications.* Pure and Applied Chemistry, 2006. **78**(6): p. 1147-1156.

13. Leveille, V. and S. Coulombe, *Design and preliminary characterization of a miniature pulsed RF APGD torch with downstream injection of the source of reactive species.* Plasma Sources Science and Technology, 2005. **14**(3): p. 467(10).

14. Coulombe, S. *Live cell permeabilization using the APGD-t*. in *First International Conference on Plasma Medicine (ICPM-1)*. 2007. Corpus Christi, Texas.

15. Kieft, I., D. Darios, A. Roks, and E. Stoffels, *Plasma treatment of mammalian vascular cells: A quantitative description.* Plasma Science, IEEE Transactions on, 2005. **33**(2): p. 771-775.

16. Kieft, I.E., M. Kurdi, and E. Stoffels, *Reattachment and Apoptosis After Plasma-Needle Treatment of Cultured Cells.* Plasma Science, IEEE Transactions on, 2006. **34**(4): p. 1331-1336.

17. Stoffels, E., *Gas plasmas in biology and medicine.* Journal of Physics D: Applied Physics, 2006. **39**(16).

18. Stoffels, E., I. Kieft, R. Sladek, L. Bedem, E. Laan, and M. Steinbuch, *Plasma needle for in vivo medical treatment: recent developments and perspectives.* Plasma Sources Science and Technology, 2006. **15**(4): p. S169.

19. Fridman, G., M. Peddinghaus, H. Ayan, A. Fridman, M. Balasubramanian, A. Gutsol, A. Brooks, and G. Friedman, *Blood coagulation and living tissue sterilization by floating-electrode dielectric barrier discharge in air.* Plasma Chemistry and Plasma Processing, 2006. **26**(4): p. 425-442.

20. Fridman, G., A. Shereshevsky, M. Peddinghaus, A. Gutsol, V. Vasilets, A. Brooks, M. Balasubramanian, G. Friedman, and A. Fridman. *Bio-Medical Applications of Non-Thermal Atmospheric Pressure Plasma*. in *37th AIAA Plasmadynamics and Lasers Conference*. 2006. San Francisco, California.

21. Shekhter, A.B., V.A. Serezhenkov, T.G. Rudenko, A.V. Pekshev, and A.F. Vanin, *Beneficial effect of gaseous nitric oxide on the healing of skin wounds.* Nitric Oxide-Biology and Chemistry, 2005. **12**(4): p. 210-219.

22. Gostev, V. and D. Dobrynin. *Medical microplasmatron*. in *3rd International Workshop on Microplasmas (IWM-2006)*. 2006. Greifswald, Germany.

23. Gostev, V., *Cold Plasma in Biological Investigations*, in *NATO Advanced Study Institute (ASI): Plasma Assisted Decontamination of Biological and Chemical Agents*. 2007: Çeşme, Turkey.

24. Fridman, A., A. Chirokov, and A. Gutsol, *Non-thermal atmospheric pressure discharges.* Journal of Physics D: Applied Physics, 2005. **38**(2): p. R1-R24.

25. Laroussi, M., I. Alexeff, and W.L. Kang, *Biological decontamination by nonthermal plasmas.* Plasma Science, IEEE Transactions on, 2000. **28**(1): p. 184-188.

26. Fridman, G., A.B. Shekhter, V.N. Vasilets, G. Friedman, A. Gutsol, and A. Fridman, *Applied Plasma Medicine.* Plasma Processes and Polymers, 2008. **5**(6): p. 503-533.

27. Fridman, G., A.D. Brooks, M. Balasubramanian, A. Fridman, A. Gutsol, V.N. Vasilets, H. Ayan, and G. Friedman, *Comparison of Direct and Indirect Effects of Non-Thermal Atmospheric Pressure Plasma on Bacteria.* Plasma Processes and Polymers, 2007. **4**: p. 370-375.

28. Rutala, W.A., M.M. Stiegel, and F.A. Sarubbi, *Decontamination of laboratory microbiological waste by steam sterilization.* Applied and Environmental Microbiology, 1982. **43**(6): p. 1311-1316.

29. Lemieux, P., R. Sieber, A. Osborne, and A. Woodard, *Destruction of Spores on Building Decontamination Residue in a Commercial Autoclave?* Applied and Environmental Microbiology, 2006. **72**(12): p. 7687-7693.

30. Sheldrake, M.A., C.D. Majors, D.J. Gaines, and C.J. Palenik, *Effectiveness of three types of sterilization on the contents of sharps containers.* Quintessence Int, 1995. **26**(11): p. 771-8.

31. Palenik, C.J., M.L. Adams, and C.H. Miller, *Effectiveness of steam autoclaving on the contents of sharps containers.* Am J Dent, 1990. **3**(6): p. 239-44.

32. Prolo, D.J., P.W. Pedrotti, and D.H. White, *Ethylene oxide sterilization of bone, dura mater, and fascia lata for human transplantation. Journal Article Neurosurgery. 6 (5): 529-39, May 1980.* Neurosurgery, 1980. **6**(5): p. 529-39.

33. Gilbert, G.L., V.M. Gambill, D.R. Spiner, R.K. Hoffman, and C.R. Phillips, *Effect of Moisture on Ethylene Oxide Sterilization 1.* Applied and Environmental Microbiology, 1964. **12**(6): p. 496-503.

34. Ohmi, T., T. Isagawa, T. Imaoka, and I. Sugiyama, *Ozone Decomposition in Ultrapure Water and Continuous Ozone Sterilization for a Semiconductor Ultrapure Water System.* Journal of The Electrochemical Society, 1992. **139**: p. 3336.

35. Burleson, G.R., T.M. Murray, and M. Pollard, *Inactivation of Viruses and Bacteria by Ozone, With and Without Sonication.* Applied and Environmental Microbiology, 1975. **29**(3): p. 340-344.

36. Jeng, D.K. and A.G. Woodworth, *Chlorine Dioxide Gas Sterilization under Square-Wave Conditions.* Applied and Environmental Microbiology, 1990. **56**(2): p. 514-519.

37. Dennis Jr, M.B., D.R. Jones, and F.C. Tenover, *Chlorine dioxide sterilization of implanted right atrial catheters in rabbits.* Lab Anim Sci, 1989. **39**(1): p. 51-5.

38. Moisan, M., J. Barbeau, S. Moreau, J. Pelletier, M. Tabrizian, and L.H. Yahia, *Low-temperature sterilization using gas plasmas: a review of the experiments and an analysis of the inactivation mechanisms.* International Journal of Pharmaceutics, 2001. **226**(1-2): p. 1-21.

39. Lerouge, S., M.R. Wertheimer, and L.H. Yahia, *Plasma Sterilization: A Review of Parameters, Mechanisms, and Limitations.* Plasmas and Polymers, 2001. **6**(3): p. 175-188.

40. Laroussi, M., I. Alexeff, J.P. Richardson, and F.F. Dyer, *The resistive barrier discharge.* IEEE Transactions on Plasma Science, 2002. **30**(1): p. 158-159.

41. Thiyagarajan, M., I. Alexeff, S. Parameswaran, and S. Beebe, *Atmospheric pressure resistive barrier cold plasma for biological decontamination.* IEEE Transactions on Plasma Science, 2005. **33**(2): p. 322-323.

42. Laroussi, M., *Nonthermal decontamination of biological media by atmospheric-pressure plasmas: Review, analysis, and prospects.* Plasma Science, IEEE Transactions on, 2002. **30**(4): p. 1409-1415.

43. Laroussi, M. and F. Leipold, *Evaluation of the roles of reactive species, heat, and UV radiation in the inactivation of bacterial cells by air plasmas at atmospheric pressure.* International Journal of Mass Spectrometry, 2004. **233**(1-3): p. 81-86.

44. Laroussi, M., O. Minayeva, F.C. Dobbs, and J. Woods, *Spores Survivability After Exposure to Low-Temperature Plasmas.* Plasma Science, IEEE Transactions on, 2006. **34**(4): p. 1253-1256.

45. Lu, X.P. and M. Laroussi, *Optimization of ultraviolet emission and chemical species generation from a pulsed dielectric barrier discharge at atmospheric pressure.* Journal of Applied Physics, 2005. **98**(2).

46. Lu, X.P. and M. Laroussi, *Temporal and spatial emission behaviour of homogeneous dielectric barrier discharge driven by unipolar sub-microsecond square pulses.* Journal of Physics D-Applied Physics, 2006. **39**(6): p. 1127-1131.

47. Laroussi, M. and X. Lu, *Room-temperature atmospheric pressure plasma plume for biomedical applications.* Applied Physics Letters, 2005. **87**(11).

48. Lu, X.P. and M. Laroussi, *Dynamics of an atmospheric pressure plasma plume generated by submicrosecond voltage pulses.* Journal of Applied Physics, 2006. **100**(6): p. 063302-6.

49. Laroussi, M., X.P. Lu, and C.M. Malott, *A non-equilibrium diffuse discharge in atmospheric pressure air.* Plasma Sources Science & Technology, 2003. **12**(1): p. 53-56.

50. Lu, X.P. and M. Laroussi, *Atmospheric pressure glow discharge in air using a water electrode.* IEEE Transactions on Plasma Science, 2005. **33**(2): p. 272-273.

51. Boudam, M.K., M. Moisan, B. Saoudi, C. Popovici, N. Gherardi, and F. Massines, *Bacterial spore inactivation by atmospheric-pressure plasmas in the presence or absence of UV photons as obtained with the same gas mixture.* Journal of Physics D: Applied Physics, 2006. **39**(16): p. 3494.

52. Massines, F., N. Gherardi, N. Naude, and P. Segur, *Glow and Townsend dielectric barrier discharge in various atmosphere.* Plasma Physics and Controlled Fusion, 2005. **47**: p. B577-B588.

53. Massines, F., A. Rabehi, P. Decomps, R.B. Gadri, P. Segur, and C. Mayoux, *Experimental and theoretical study of a glow discharge at atmospheric pressure controlled by dielectric barrier.* Journal of Applied Physics, 1998. **83**(6): p. 2950-2957.

54. Becker, K., A. Koutsospyros, S.M. Yin, C. Christodoulatos, N. Abramzon, J.C. Joaquin, and G. Brelles-Marino, *Environmental and biological applications of microplasmas.* Plasma Physics and Controlled Fusion, 2005. **47**: p. B513-B523.

55. Becker, K.H., K.H. Schoenbach, and J.G. Eden, *Microplasmas and applications.* Journal of Physics D-Applied Physics, 2006. **39**(3): p. R55-R70.

56. Ben Gadri, R., J.R. Roth, T.C. Montie, K. Kelly-Wintenberg, P.P.Y. Tsai, D.J. Helfritch, P. Feldman, D.M. Sherman, F. Karakaya, and Z.Y. Chen, *Sterilization and plasma processing of room temperature surfaces with a one atmosphere uniform glow discharge plasma (OAUGDP).* Surface & Coatings Technology, 2000. **131**(1-3): p. 528-542.

57. Kelly-Wintenberg, K., A. Hodge, T.C. Montie, L. Deleanu, D. Sherman, J.R. Roth, P. Tsai, and L. Wadsworth, *Use of a one atmosphere uniform glow discharge plasma to kill a broad spectrum of microorganisms.* Journal of Vacuum Science & Technology a-Vacuum Surfaces and Films, 1999. **17**(4): p. 1539-1544.

58. Kelly-Wintenberg, K., D.M. Sherman, P.P.Y. Tsai, R.B. Gadri, F. Karakaya, C. Zhiyu, J.R. Roth, and T.C. Montie, *Air filter sterilization using a one atmosphere*

uniform glow discharge plasma (the volfilter). Plasma Science, IEEE Transactions on, 2000. **28**(1): p. 64-71.

59. Montie, T.C., K. Kelly-Wintenberg, and J.R. Roth, *An overview of research using the one atmosphere uniform glow discharge plasma (OAUGDP) for sterilization of surfaces and materials.* Plasma Science, IEEE Transactions on, 2000. **28**(1): p. 41-50.

60. Roth, J.R., S. Nourgostar, and T.A. Bonds, *The one atmosphere uniform glow discharge plasma (OAUGDP) - A platform technology for the 21st century.* IEEE Transactions on Plasma Science, 2007. **35**(2): p. 233-250.

61. Roth, J.R., J. Rahel, X. Dai, and D.M. Sherman, *The physics and phenomenology of one atmosphere uniform glow discharge plasma (OAUGDP (TM)) reactors for surface treatment applications.* Journal of Physics D-Applied Physics, 2005. **38**(4): p. 555-567.

62. Roth, J.R., D.M. Sherman, R.B. Gadri, F. Karakaya, C. Zhiyu, T.C. Montie, K. Kelly-Wintenberg, and P.P.Y. Tsai, *A remote exposure reactor (RER) for plasma processing and sterilization by plasma active species at one atmosphere.* Plasma Science, IEEE Transactions on, 2000. **28**(1): p. 56-63.

63. Redlich, C.A., J. Sparer, and M.R. Cullen, *Sick-building syndrome.* The Lancet, 1997. **349**(9057): p. 1013-1016.

64. Chalise, P.R., S. Perni, G. Shama, B.M. Novac, I.R. Smith, and M.G. Kong, *Lethality mechanisms in Escherichia coli induced by intense sub-microsecond electrical pulses.* Applied Physics Letters, 2006. **89**(15).

65. Deng, X., J. Shi, and M.G. Kong, *Physical Mechanisms of Inactivation of Bacillus subtilis Spores Using Cold Atmospheric Plasmas.* Plasma Science, IEEE Transactions on, 2006. **34**(4): p. 1310-1316.

66. Deng, X.T., J.J. Shi, H.L. Chen, and M.G. Kong, *Protein destruction by atmospheric pressure glow discharges.* Applied Physics Letters, 2007. **90**(1).

67. Deng, X.T., J.J. Shi, and M.G. Kong, *Protein destruction by a helium atmospheric pressure glow discharge: Capability and mechanisms.* Journal of Applied Physics, 2007. **101**(7).

68. Nie, Q.Y., C.S. Ren, D.Z. Wang, S.Z. Li, J.L. Zhang, and M.G. Kong, *Self-organized pattern formation of an atmospheric pressure plasma jet in a dielectric barrier discharge configuration.* Applied Physics Letters, 2007. **90**(22).

69. Perni, S., X.T. Deng, G. Shama, and M.G. Kong, *Modeling the Inactivation Kinetics of Bacillus subtilis Spores by Nonthermal Plasmas.* Plasma Science, IEEE Transactions on, 2006. **34**(4): p. 1297-1303.

70. Perni, S., G. Shama, J.L. Hobman, P.A. Lund, C.J. Kershaw, G.A. Hidalgo-Arroyo, C.W. Penn, X.T. Deng, J.L. Walsh, and M.G. Kong, *Probing bactericidal mechanisms induced by cold atmospheric plasmas with Escherichia coli mutants.* Applied Physics Letters, 2007. **90**(7).

71. Shi, J., D. Liu, and M. Kong, *Effects of dielectric barriers in radio frequency atmospheric glow discharges.* IEEE Transactions on Plasma Science, 2007. **35**(2): p. 137-142.

72. Vleugels, M., G. Shama, X.T. Deng, E. Greenacre, T. Brocklehurst, and M.G. Kong, *Atmospheric plasma inactivation of biofilm-forming bacteria for food safety control.* Plasma Science, IEEE Transactions on, 2005. **33**(2): p. 824-828.

73. Walsh, J.L. and M.G. Kong, *Sharp bursts of high-flux reactive species in submicrosecond atmospheric pressure glow discharges.* Applied Physics Letters, 2006. **89**(23).

74. Walsh, J.L., J.J. Shi, and M.G. Kong, *Contrasting characteristics of pulsed and sinusoidal cold atmospheric plasma jets.* Applied Physics Letters, 2006. **88**: p. 171501.

75. Glover, J., P. Bendick, and W. Link, *The use of thermal knives in surgery: electrosurgery, lasers, plasma scalpel.* Curr Probl Surg., 1978. **15**(1): p. 1-78.

76. Shekhter, A.B., R.K. Kabisov, A.V. Pekshev, N.P. Kozlov, and Y.L. Perov, *Experimental and clinical validation of plasmadynamic therapy of wounds with*

nitric oxide. Bulletin of Experimental Biology and Medicine, 1998. **126**(2): p. 829-834.

77. Pekshev, A.V., *Use of a novel biological factor - exogenic nitrogen oxide - in surgical treatment of paradontitis.* Stomatology, 2001. **1**: p. 80-83.

78. Furchgott, R.F., *Endothelium-Derived Relaxing Factor: Discovery, Early Studies, and Identifcation as Nitric Oxide (Nobel Lecture).* Angewandte Chemie International Edition, 1999. **38**(13-14): p. 1870-1880.

79. Shulutko, A.M., N.V. Antropova, and Y.A. Kryuger, *No-therapy in the treatment of purulent and necrotic lesions of lower extremities in diabetic patients.* Surgery, 2004. **12**: p. 43-46.

80. Seeger, W., *Pneumology - From phthisiology to regenerative medicine.* Deutsche Medizinische Wochenschrift, 2005. **130**(25-26): p. 1543-1546.

81. Efimenko, N.A., V.I. Hrupkin, L.A. Marahonich, V.I. Iashenko, V.I. Moskalenko, and E.V. Lykianenko, *Air-Plasma Flows and NO-therapy - a Novel Technology in a Clinical Setting of the Military Treatment and Profilactic Facilities (Experimental and Clinical Study).* Journal of Military Medicine (Voenno-Meditsinskii Jurnal), 2005. **5**: p. 51-54.

82. Davydov, A.I., S.T. Kuchukhidze, A.B. Shekhter, A.G. Khanin, A.V. Pekshev, and V.V. Pankratov, *Clinical evaluation of intraoperative application of air-plasma flow enriched by nitrogen monoxide in operations on the uterus and adnexa.* Problems of Gynecology, Obstetrics and Perinatology, 2004. **3**(4): p. 12-17.

83. Davydov, A.I., A.N. Strijakov, A.V. Pekshev, S.T. Kuchukhidze, and I.A. Klihdukhov, *Possibilities and prospectives in plasma endosurgery with generation of nitrogen monoxide in vaginal surgeries.* Questions in Obstetrics and Gynaecology (OB/GYN), 2002. **1**(2): p. 57-60.

84. Kuchukhidze, S.T., I.A. Klihdukhov, K.R. Bakhtiarov, and V.V. Pankratov, *High energy applications in modern gynaecology* Questions in Obstetrics and Gynaecology (OB/GYN), 2004. **3**(2): p. 76-82.

85. Grigoryan, A.S., A.I. Grudyanov, O.A. Frolova, Z.P. Antipova, A.I. Yerokhin, A.B. Shekhter, and A.V. Pekshev, *New biological factor, exogenous nitrogen oxide, in treatment of chronic periodontitis.* Stomatology, 2001(1): p. 80-83.

86. Chesnokova, N.V., R.A. Gundorova, O.I. Krvasha, V.P. Bakov, and N.G. Davydova, *Experimental investigation of the influence of gas flow containing nitrogen oxide in treatment of corneal wounds.* Vestnik RAMN, 2003. **5**: p. 40-44.

87. Golubovskii, G.A., V.G. Zenger, A.N. Nasedkin, E.I. Prokofieva, and A.A. Borojtsov. *Use of exogenic NO-therapy in regenerative surgery of bronchial tubes*. in *IV'th Army Medical Conference on Intensive Therapy and Profilactic Treatments of Surgical Infections*. 2004. Moscow, Russia.

88. Zaitsev, V.M., *Comparative analysis of effectiveness of treatment of chronic supporated ulcers by NO-therapy with addition of ultrasound implantation of miramistine with treatment by ultrasound implantation alone.* Russian Journal of Otorinolaringology, 2003. **1**: p. 58-59.

89. Chernekhovskaia, N.E., V.K. Shishlo, B.D. Svistunov, and A.S. Svitunova. *Intra-bronchial NO-therapy in treatment of wound complications in tuberculosis patients*. in *IV'th Army Medical Conference on Intensive Therapy and Profilactic Treatments of Surgical Infections*. 2004. Moscow, Russia.

90. Misyn, F., E. Besedin, V. Gostev, and O. Komkova. *Experimental studying of bactericidal action of cold plasma*. in *Diagnostics and treatment of infectious diseases*. 2000. Petrozavodsk, Russia.

91. Misyn, F.A., E.V. Besedin, O.P. Komkova, and V.A. Gostev. *Experimental investigation of bactericidal influence of "cold" plasma and its interaction with cornea*. in *Diagnostics and treatment of infectious diseases*. 2000. Petrozavodsk, Russia.

92. Misyn, F.A., E.V. Besedin, A.M. Obraztsova, and V.A. Gostev. *Experimental curing of bacterial ulcerous keratitis with "cold" plasma*. in *Diagnostics and treatment of infectious diseases*. 2000. Petrozavodsk, Russia.

93. Misyn, F.A. and V.A. Gostev. *"Cold" plasma application in eyelid phlegmon curing*. in *Diagnostics and treatment of infectious diseases*. 2000. Petrozavodsk, Russia.

94. Choudhuri, M., R. McQueen, S. Inoue, and R.C. Gordon, *Efficiency of skin sterilization for a venipuncture with the use of commercially available alcohol or iodine pads.* Am J Infect Control, 1990. **18**(2): p. 82-5.

95. Laan, E., E. Stoffels, and M. Steinbuch, *Development of a smart positioning sensor for the plasma needle.* Plasma Sources Science and Technology, 2006. **15**(3): p. 582.

96. Kieft, I.E., E.P. Laan, and E. Stoffels, *Electrical and optical characterization of the plasma needle.* New Journal of Physics, 2004. **6**(1): p. 149.

97. Stoffels, E., A.J. Flikweert, W.W. Stoffels, and G.M.W. Kroesen, *Plasma needle: a non-destructive atmospheric plasma source for fine surface treatment of (bio)materials.* Plasma Sources Science and Technology, 2002. **11**(4): p. 383-388.

98. Stoffels, E. *Cold atmospheric plasma for wound healing: in vitro assessment*. in *First International Conference on Plasma Medicine (ICPM-1)*. 2007. Corpus Christi, Texas.

99. Kieft, I.E., J.L.V. Broers, V. Caubet-Hilloutou, D.W. Slaaf, F.C.S. Ramaekers, and E. Stoffels, *Electric discharge plasmas influence attachment of cultured CHO k1 cells.* Bioelectromagnetics, 2004. **25**(5): p. 362-368.

100. Kieft, I.E., D. Darios, A.J.M. Roks, and E. Stoffels, *Plasma treatment of mammalian vascular cells: A quantitative description.* IEEE Transactions on Plasma Science, 2005. **33**(2): p. 771-775.

101. Kieft, I.E., N.A. Dvinskikh, J.L.V. Broers, D.W. Slaaf, and E. Stoffels, *Effect of plasma needle on cultured cells [5483-31]*. Proceedings of SPIE, 2004. **5483**: p. 247-251.

102. Sladek, R.E.J., E. Stoffels, R. Walraven, P.J.A. Tielbeek, and R.A. Koolhoven, *Plasma treatment of dental cavities: A feasibility study.* Plasma Science, IEEE Transactions on, 2004. **32**(4): p. 1540-1543.

103. Sladek, R.E.J. and E. Stoffels, *Deactivation of Escherichia coli by the plasma needle.* Journal of Physics D: Applied Physics, 2005. **38**(11): p. 1716-1721.

104. Pompl, R., T. Shimizu, H.U. Schmidt, W. Bunk, F. Jamitzky, B. Steffes, K. Ramrath, B. Peters, W. Stolz, T. Urayama, R. Ramasamy, S. Fujii, and G.E. Morfill. *Efficiency and Medical Compatibility of Low-Temperature Plasma Sterilization*. in *6th Int. Conf. Reactive Plasmas*. 2006. Matsushima, Japan.

105. Shimizu, T., B. Steffes, R. Pompl, F. Jamitzky, W. Bunk, K. Ramrath, B. Peters, W. Stolz, H.U. Schmidt, T. Urayama, K. Fujioka, R. Ramasamy, S. Fujii, and G.E. Morfill. *Microwave Plasma Torch for Bacterial Sterilization*. in *6th Int. Conf. Reactive Plasmas*. 2006. Matsushima, Japan.

106. Elaine L. Chao, S., *Controlling Electrical Hazards, OSHA 3075*, U.S.D.o. Labor, Editor. 2002 (Revised).

107. Bayrashev, A. and B. Ziaie, *Silicon wafer bonding through RF dielectric heating.* Sensors & Actuators: A. Physical, 2003. **103**(1-2): p. 16-22.

108. Ikediala, J., J. Hansen, J. Tang, S. Drake, and S. Wang, *Development of saline-water-immersion technique with RF energy as a postharvest treatment against codling moth in cherries.* Postharvest Biology and Technology, 2002. **24**(2): p. 209-221.

109. Cooper, M., Y. Yang, D. Dobrynin, H. Ayan, A. Fridman, A. Gutsol, V. Vasilets, and G. Fridman, *Observations of Filament Behavior and Plasma Uniformity in Continuous and Pulsed Dielectric Barrier Discharges*, in *Drexel University Ninth Annual Research Innovation Scholarship and Creativity (RISC) Day*. 2007: Philadelphia, USA.

110. Cooper, M., Y. Yang, G. Fridman, H. Ayan, V.N. Vasilets, A. Gutsol, G. Friedman, and A. Fridman. *Uniform and Filamentary Nature of Continuous-Wave and Pulsed Dielectric Barrier Discharge Plasma*. in *NATO Advanced Study Institute on Plasma Assisted Decontamination of Biological and Chemical Agents*. 2007. Cesme-Izmir, Turkey: Springer.

111. Dee Unglaub Silverthorn, W.C.O., Claire W. Garrison, Andrew C. Silverthorn, Bruce R. Johnson, *Human Physiology, an Integrated Approach*. 3rd ed. 2004: Benjamin-Cummings Publishing Company. 912.

112. Henry, J.B., *Clinical Diagnosis and Management by Laboratory Methods*. 20 ed. 2001: W.B. Saunders Company. 1512.

113. Cheng, C., P. Liu, L. Xu, L. Zhang, R. Zhan, and W. Zhang, *Development of a new atmospheric pressure cold plasma jet generator and application in sterilization.* Chinese Physics, 2006. **15**(7): p. 1544.

114. Herbold, K., B. Flehmig, and K. Botzenhart, *Ozone application for sterilization.* Appl Enviromental Microbiology, 1989. **11**: p. 2949-2953.

115. Sharma, A., A. Pruden, O. Stan, and G.J. Collins, *Bacterial Inactivation Using an RF-Powered Atmospheric Pressure Plasma.* Plasma Science, IEEE Transactions on, 2006. **34**(4): p. 1290-1296.

116. Abramzon, N., J.C. Joaquin, J. Bray, and G. Brelles-Marino, *Biofilm Destruction by RF High-Pressure Cold Plasma Jet.* Plasma Science, IEEE Transactions on, 2006. **34**(4): p. 1304-1309.

117. Efremov, N.M., B.Y. Adamiak, V.I. Blouchin, S.J. Dadashev, K.J. Dmitriev, O.P. Gryaznova, and V.F. Jusbashev, *Action of a self-sustained glow discharge in atmospheric pressure air on biological objects.* Plasma Science, IEEE Transactions on, 2000. **28**(1): p. 238-241.

118. Stoffels, E., *Biomedical applications of electric gas discharge.* High Temperature Material Processes, 2000. **5**(2): p. 191-202.

119. Chu, P.K., J.Y. Chen, L.P. Wang, and N. Huang, *Plasma-surface modification of biomaterials.* Materials Science & Engineering R-Reports, 2002. **36**(5-6): p. 143-206.

120. Zhang, R., L. Wang, Y. Wu, Z. Guan, and Z. Jia, *Bacterial Decontamination of Water by Bipolar Pulsed Discharge in a Gas-Liquid-Solid Three-Phase Discharge Reactor.* Plasma Science, IEEE Transactions on, 2006. **34**(4): p. 1370-1374.

121. Tarasenko, O., S. Nourbakhsh, S.P. Kuo, A. Bakhtina, P. Alusta, D. Kudasheva, M. Cowman, and K. Levon, *Scanning Electron and Atomic Force Microscopy to Study Plasma Torch Effects on B. cereus Spores.* Plasma Science, IEEE Transactions on, 2006. **34**(4): p. 1281-1289.

122. Soloshenko, I.A., V.Y. Bazhenov, V.A. Khomich, V.V. Tsiolko, and N.G. Potapchenko, *Comparative Research of Efficiency of Water Decontamination by UV Radiation of Cold Hollow Cathode Discharge Plasma Versus That of Low- and Medium-Pressure Mercury Lamps.* Plasma Science, IEEE Transactions on, 2006. **34**(4): p. 1365-1369.

123. Sladek, R.E.J., T.A. Baede, and E. Stoffels, *Plasma-Needle Treatment of Substrates With Respect to Wettability and Growth of Escherichia coli and Streptococcus mutans.* Plasma Science, IEEE Transactions on, 2006. **34**(4): p. 1325-1330.

124. Sarra-Bournet, C., S. Turgeon, D. Mantovani, and G. Laroche, *A study of atmospheric pressure plasma discharges for surface functionalization of PTFE used in biomedical applications.* Journal of Physics D: Applied Physics, 2006. **39**(16): p. 3461.

125. Sakiyama, Y. and D.B. Graves, *Finite element analysis of an atmospheric pressure RF-excited plasma needle.* Journal of Physics D: Applied Physics, 2006. **39**(16): p. 3451.

126. Narsetti, R., R.D. Curry, K.F. McDonald, T.E. Clevenger, and L.M. Nichols, *Microbial Inactivation in Water Using Pulsed Electric Fields and Magnetic Pulse Compressor Technology.* Plasma Science, IEEE Transactions on, 2006. **34**(4): p. 1386-1393.

127. Kuo, S.P., O. Tarasenko, S. Popovic, and K. Levon, *Killing of Bacterial Spores Contained in a Paper Envelope by a Microwave Plasma Torch.* Plasma Science, IEEE Transactions on, 2006. **34**(4): p. 1275-1280.

128. Cvelbar, U., D. Vujosevic, Z. Vratnica, and M. Mozetic, *The influence of substrate material on bacteria sterilization in an oxygen plasma glow discharge.* Journal of Physics D: Applied Physics, 2006. **39**(16): p. 3487.

129. Goree, J., B. Liu, D. Drake, and E. Stoffels, *Killing of S. mutans Bacteria Using a Plasma Needle at Atmospheric Pressure.* Plasma Science, IEEE Transactions on, 2006. **34**(4): p. 1317-1324.

130. Gaunt, L.F., C.B. Beggs, and G.E. Georghiou, *Bactericidal Action of the Reactive Species Produced by Gas-Discharge Nonthermal Plasma at Atmospheric Pressure: A Review.* Plasma Science, IEEE Transactions on, 2006. **34**(4): p. 1257-1269.

131. Moisan, M., J. Barbeau, J. Pelletier, and B. Saoudi, *Low-pressure cold plasma sterilization at atmospheric pressure.* Vide-Science Technique Et Applications, 2002. **57**(303): p. 71.

132. Krishnamurthy, K., A. Demirci, and J. Irudayaraj, *Inactivation of Staphylocloccus aureus by pulsed UV-light sterilization.* Journal of Food Protection, 2004. **67**(5): p. 1027-1030.

133. Sosnin, E.A., E. Stoffels, M.V. Erofeev, I.E. Kieft, and S.E. Kunts, *The effects of UV irradiation and gas plasma treatment on living mammalian cells and bacteria: A comparative approach.* Plasma Science, IEEE Transactions on, 2004. **32**(4): p. 1544-1550.

134. Erofeev, M.V., I.E. Kieft, E.A. Sosnin, and E. Stoffels, *UV Excimer Lamp Irradiation of Fibroblasts: The Influence on Antioxidant Homeostasis.* Plasma Science, IEEE Transactions on, 2006. **34**(4): p. 1359-1364.

135. Craik, S.A., D. Weldon, G.R. Finch, J.R. Bolton, and M. Belosevic, *Inactivation of Cryptosporidium parvum oocysts using medium- and low-pressure ultraviolet radiation.* Water Research, 2001. **35**(6): p. 1387-1398.

136. Stoffels, E., I.E. Kieft, R.E. Sladek, E.P. van der Laan, and D.W. Slaaf, *Gas plasma treatment: a new approach to surgery?* Crit Rev Biomed Eng, 2004. **32**(5-6): p. 427-60.

137. Stoffels, E., I.E. Kieft, and R.E.J. Sladek, *Superficial treatment of mammalian cells using plasma needle.* Journal of Physics D Applied Physics, 2003. **36**(23): p. 2908-2913.

138. Stoffels, E., R.E.J. Sladek, and I.E. Kieft, *Gas Plasma Effects on Living Cells.* Physica Scripta, 2004. **107**: p. 79.

139. Laroussi, M., C. Tendero, X. Lu, S. Alla, and W.L. Hynes, *Inactivation of Bacteria by the Plasma Pencil.* Plasma Processes and Polymers, 2006. **3**(6-7): p. 470-473.

140. Leveille, V. and S. Coulombe, *Atomic oxygen production and exploration of reaction mechanisms in a He-O-2 atmospheric pressure glow discharge torch.* Plasma Processes and Polymers, 2006. **3**(8): p. 587-596.

141. Yonson, S., S. Coulombe, V. Leveille, and R.L. Leask, *Cell treatment and surface functionalization using a miniature atmospheric pressure glow discharge plasma torch.* Journal of Physics D-Applied Physics, 2006. **39**(16): p. 3508-3513.

142. Leveille, V. and S. Coulombe, *Design and preliminary characterization of a miniature pulsed RF APGD torch with downstream injection of the source of reactive species.* Plasma Sources Science & Technology, 2005. **14**(3): p. 467-476.

143. Ayan, H., G. Fridman, D. Staack, A. Gutsol, V. Vasilets, A. Fridman, and G. Friedman, *Heating effect of dielectric barrier discharges in direct medical treatment.* IEEE Transactions on Plasma Science, 2007(submitted).

144. Schoenbach, K., R. Barker, and S. Liu, *Special issue on nonthermal medical/biological treatments using electromagnetic fields and ionized gases.* Plasma Science, IEEE Transactions on, 2000. **28**(1): p. 2-5.

145. Kotov, Y.A. and S.Y. Sokovnin, *Overview of the application of nanosecond electron beams for radiochemical sterilization.* Plasma Science, IEEE Transactions on, 2000. **28**(1): p. 133-136.

146. Kolb, J.F., M.G. Kong, and P.F. Blackmore, *Special Issue on Nonthermal Medical/Biological Applications Using Ionized Gases and Electromagnetic Fields.* Plasma Science, IEEE Transactions on, 2006. **34**(4): p. 1250-1252.

147. Chirokov, A., A. Gutsol, A. Fridman, K. Sieber, J. Grace, and K. Robinson, *Self-organization of microdischarges in dielectric barrier discharge plasma.* Plasma Science, IEEE Transactions on, 2005. **33**(2): p. 300-301.

148. Chirokov, A., A. Gutsol, A. Fridman, K.D. Sieber, J.M. Grace, and K.S. Robinson, *Analysis of two-dimensional microdischarge distribution in dielectric-barrier discharges.* Plasma Sources Science and Technology, 2004. **13**(4): p. 623.

149. Laux, C.O., T.G. Spence, C.H. Kruger, and R.N. Zare, *Optical diagnostics of atmospheric pressure air plasmas.* Plasma Sources Science and Technology, 2003. **12**(2): p. 125.

150. Lin, C.K., C.C. Wu, Y.S. Wang, Y.T. Lee, H.C. Chang, J.L. Kuo, and M.L. Klein, *Vibrational predissociation spectra and hydrogen-bond topologies of H+ (H2O)(9-11).* Physical Chemistry Chemical Physics, 2005. **7**(5): p. 938-944.

151. Fozza, A.C., J.E. Klemberg-Sapieha, and M.R. Wertheimer, *Vacuum Ultraviolet Irradiation of Polymers.* Plasmas and Polymers, 1999. **4**(2): p. 183-206.

152. Lerouge, S., A.C. Fozza, M.R. Wertheimer, R. Marchand, and L.H. Yahia, *Sterilization by Low-Pressure Plasma: The Role of Vacuum-Ultraviolet Radiation.* Plasmas and Polymers, 2000. **5**(1): p. 31-46.

153. Wilken, R., A. Holländer, and J. Behnisch, *Vacuum Ultraviolet Photolysis of Polyethylene, Polypropylene, and Polystyrene.* Plasmas and Polymers, 2002. **7**(2): p. 185-205.

154. Sosnin, E.A., E. Stoffels, M.V. Erofeev, I.E. Kieft, and S.E. Kunts, *The effects of UV irradiation and gas plasma treatment on living mammalian cells and bacteria: A comparative approach.* Ieee Transactions on Plasma Science, 2004. **32**(4): p. 1544-1550.

155. MacGregor, S.J., N.J. Rowan, L. McIlvaney, J.G. Anderson, R.A. Fouracre, and O. Farish, *Light inactivation of food-related pathogenic bacteria using a pulsed power source.* Letters in Applied Microbiology, 1998. **27**(2): p. 67-70.

156. Amr, A.G. and K.H. Schoenbach, *Biofouling prevention with pulsed electric fields.* Plasma Science, IEEE Transactions on, 2000. **28**(1): p. 115-121.

157. El-Hag, A.H., S.H. Jayaram, and M.W. Griffiths, *Inactivation of Naturally Grown Microorganisms in Orange Juice Using Pulsed Electric Fields.* Plasma Science, IEEE Transactions on, 2006. **34**(4): p. 1412-1415.

158. Tekle, E., H. Oubrahim, S.M. Dzekunov, J.F. Kolb, K.H. Schoenbach, and P.B. Chock, *Selective field effects on intracellular vacuoles and vesicle membranes with nanosecond electric pulses.* Biophysical Journal, 2005. **89**(1): p. 274-284.

159. Frey, W., J.A. White, R.O. Price, P.F. Blackmore, R.P. Joshi, R. Nuccitelli, S.J. Beebe, K.H. Schoenbach, and J.F. Kolb, *Plasma membrane voltage changes during nanosecond pulsed electric field exposure.* Biophysical Journal, 2006. **90**(10): p. 3608-3615.

160. Hu, Q., V. Sridhara, R.P. Joshi, J.F. Kolb, and K.H. Schoenbach, *Molecular Dynamics Analysis of High Electric Pulse Effects on Bilayer Membranes Containing DPPC and DPPS.* Plasma Science, IEEE Transactions on, 2006. **34**(4): p. 1405-1411.

161. Nuccitelli, R., U. Pliquett, X. Chen, W. Ford, R. James Swanson, S.J. Beebe, J.F. Kolb, and K.H. Schoenbach, *Nanosecond pulsed electric fields cause melanomas to self-destruct.* Biochem. Biophys. Res. Commun, 2006. **343**: p. 351–360.

162. Chirokov, A., A. Gutsol, A. Fridman, K. Sieber, J. Grace, and K. Robinson, *A Study of Two-Dimensional Microdischarge Pattern Formation in Dielectric Barrier Discharges.* Plasma Chemistry and Plasma Processing, 2006. **26**(2): p. 127-135.

163. Fridman, A., *Plasma Chemistry*. 2008: Cambridge University Press. 1024.

164. Fridman, A. and Y.I. Cho, *Transport Phenomena in Plasma (Advances in Heat Transfer)*. Vol. 40. 2007: Academic Press. 668.

165. Ayan, H., G. Fridman, A.F. Gutsol, V. Vasilets, A. Fridman, and G. Friedman, *Nanosecond-Pulsed Uniform Dielectric-Barrier Discharge.* Plasma Science, IEEE Transactions on, 2008. **36**(2): p. 504-508.

166. Yalin, A.P., C.O. Laux, C.H. Kruger, and R.N. Zare, *Spatial profiles of N2+ concentration in an atmospheric pressure nitrogen glow discharge.* Plasma Sources Science and Technology, 2002. **11**(3): p. 248.

167. Packan, D., C.O. Laux, R.J. Gessman, L. Pierrot, and C.H. Kruger, *Measurement and Modeling of OH, NO, and CO2 infrared radiation at 3400 K.* Journal of Thermophysics and Heat Transfer, 2003. **17**(4): p. 450-456.

168. Ayan, H., G. Fridman, A. Gutsol, V.N. Vasilets, A. Fridman, and G. Friedman, *Nanosecond Pulsed Uniform Dielectric Barrier Discharge.* IEEE Transactions on Plasma Science, 2007(submitted).

169. Chan, C.M., T.M. Ko, and H. Hiraoka, *Polymer surface modification by plasmas and photons.* Surface Science Reports, 1996. **24**(1-2): p. 3-54.

170. Farrar, L.C., D.P. Haack, S.E. McGrath, J.C. Dickens, E.A. O'Hair, and J.A. Fralick, *Rapid decontamination of large surface areas.* Plasma Science, IEEE Transactions on, 2000. **28**(1): p. 173-179.

171. Gibalov, V.I. and G.J. Pietsch, *The development of dielectric barrier discharges in gas gaps and on surfaces.* Journal of Physics D: Applied Physics, 2000. **33**(20): p. 2618.

172. Laskarakis, A., C. Gravalidis, and S. Logothetidis, *FTIR and Vis–FUV real time spectroscopic ellipsometry studies of polymer surface modifications during ion beam bombardment* Nuclear Instruments and Methods in Physics Research Section B: Beam Interactions with Materials and Atoms 2004. **216**: p. 131-136.

173. McDonald, K.F., R.D. Curry, T.E. Clevenger, B.J. Brazos, K. Unklesbay, A. Eisenstark, S. Baker, J. Golden, and R. Morgan, *The development of photosensitized pulsed and continuous ultraviolet decontamination techniques for surfaces and solutions.* Plasma Science, IEEE Transactions on, 2000. **28**(1): p. 89-96.

174. Strobel, M. and C.S. Lyons, *Plasma Surface Modification of Polymers - Relevance to Adhesion - Guest Editorial.* Journal of Adhesion Science and Technology, 1994. **8**(4): p. 303-304.

175. Vasilets, V.N., L.A. Tikchomirov, and A.N. Ponomarev, *The study of the action of high frequency discharge plasma on polyethylene surface.* High Energy Chemistry, 1978. **12**(N5): p. 442-447.

176. Vasilets, V.N., L.A. Tikchomirov, and A.N. Ponomarev, *The study of continues HF low pressure discharge plasma action on the polyethylene surface.* High Energy Chemistry, 1981. **15**(N1): p. 77-81.

177. Wagner, H.E., R. Brandenburg, K.V. Kozlov, A. Sonnenfeld, P. Michel, and J.F. Behnke, *The barrier discharge: basic properties and applications to surface treatment.* Vacuum, 2003. **71**(3): p. 417-436.

178. Mancini, A., *Skin.* Pediatrics, 2004. **113**(4): p. 1114.

179. Breneman, D., M. Duvic, T. Kuzel, R. Yocum, J. Truglia, and V. Stevens, *Phase 1 and 2 Trial of Bexarotene Gel for Skin-Directed Treatment of Patients With Cutaneous T-Cell Lymphoma*. 2002, Am Med Assoc. p. 325-332.

180. Belden, L. and A. Blaustein, *UV-B Induced Skin Darkening in Larval Salamanders Does Not Prevent Sublethal Effects of Exposure on Growth.* Copeia, 2002. **2002**(3): p. 748-754.

181. VELLA BRIFFA, D., S. ROGERS, M. GREAVES, J. MARKS, S. SHUSTER, and A. WARIN, *A randomized, controlled clinical trial comparing photochemotherapy with dithranol in the initial treatment of chronic plaque psoriasis.* Clinical and Experimental Dermatology, 1978. **3**(4): p. 339-339.

182. Vella-Briffa, D., S. Rogers, M. Greaves, J. Marks, S. Shuster, and A. Warin, *A randomized, controlled clinical trial comparing photochemotherapy with dithranol in the initial treatment of chronic plaque psoriasis.* Clinical and Experimental Dermatology, 1978. **3**(4): p. 339-339.

183. Fridman, A. and L. Kennedy, *Plasma Physics and Engineering*. 1 ed. 2004: Taylor & Francis Group. 860.

184. Yurgelenas, Y.V. and H.E. Wagner, *A computational model of a barrier discharge in air at atmospheric pressure: the role of residual surface charges in microdischarge formation.* Journal of Physics D: Applied Physics, 2006. **39**(18): p. 4031.

185. Fridman, G., S. Kalghatgi, R. Sensenig, A. Shereshevsky, R. Stoddard, G. Friedman, A. Gutsol, V. Vasilets, A. Fridman, and A.D. Brooks, *Non-Equilibrium Dielectric Barrier Discharge Plasma Promoting Apoptotic Behavior in Melanoma Skin Cancer Cells*, in *NATO Advanced Study Institute (ASI), Plasma Assisted Decontamination of Biological and Chemical Agents*. 2007: Çesme, Turkey.

186. Bronaugh, R., R. Stewart, and E. Congdon, *Methods for in vitro percutaneous absorption studies II. Animal models for human skin.* Toxicology and Applied Pharmacology, 1982. **62**(3): p. 481-488.

187. Schmook, F., J. Meingassner, and A. Billich, *Comparison of human skin or epidermis models with human and animal skin in in-vitro percutaneous absorption.* International Journal of Pharmaceutics, 2001. **215**(1-2): p. 51-56.

188. Bartek, M., J. Labudde, and H. Maibach, *Skin Permeability in vivo: Comparison in Rat, Rabbit, Pig and Man.* Journal of Investigative Dermatology, 1972. **58**(3): p. 114-123.

189. Zhang, Z. and N. Monteiro-Riviere, *Comparison of integrins in human skin, pig skin, and perfused skin: An in vitro skin toxicology model.* Journal of Applied Toxicology, 1997. **17**(4): p. 247-253.

190. Aguilella, V., K. Kontturi, L. Murtomaki, and P. Ramirez, *Estimation of the pore size and charge density in human cadaver skin.* Journal of controlled release, 1994. **32**(3): p. 249-257.

191. Wester, R., J. Christoffel, T. Hartway, N. Poblete, H. Maibach, and J. Forsell, *Human Cadaver Skin Viability for In Vitro Percutaneous Absorption: Storage and Detrimental Effects of Heat-Separation and Freezing.* Pharmaceutical Research, 1998. **15**(1): p. 82-84.

192. Kealey, G., J. Aguiar, R. Lewis 2nd, M. Rosenquist, R. Strauss, and J. Bale Jr, *Cadaver skin allografts and transmission of human cytomegalovirus to burn patients.* J Am Coll Surg, 1996. **182**(3): p. 201-5.

193. Kalghatgi, S.U., G. Fridman, M. Cooper, G. Nagaraj, M. Peddinghaus, M. Balasubramanian, V.N. Vasilets, A. Gutsol, A. Fridman, and G. Friedman, *Mechanism of Blood Coagulation by Non-Thermal Atmospheric Pressure Dielectric Barrier Discharge Plasma.* IEEE Transactions on Plasma Science, 2007(accepted: Jul 13, 2007).

194. Fridman, G. *Medical applications of Floating Electrode Dielectric Barrier Discharge (FE-DBD)*. in *First International Conference on Plasma Medicine (ICPM-1)*. 2007. Corpus Christi, Texas.

195. Fridman, G., A. Shereshevsky, M. Jost, A. Brooks, A. Fridman, A. Gutsol, V. Vasilets, and G. Friedman, *Floating Electrode Dielectric Barrier Discharge Plasma in Air Promoting Apoptotic Behavior in Melanoma Skin Cancer Cell Lines.* Plasma Chemistry and Plasma Processing, 2007. **27**(2): p. 163-176.

196. Gallagher, M.J., N. Vaze, S. Gangoli, V.N. Vasilets, A.F. Gutsol, T.N. Milovanova, S. Anandan, D.M. Murasko, and A.A. Fridman, *Rapid Inactivation of Airborne*

Bacteria Using Atmospheric Pressure Dielectric Barrier Grating Discharge. Plasma Science, IEEE Transactions on, 2007. **35**(5): p. 1501-1510.

197. Staak, D., B. Farouk, A. Gutsol, and A. Fridman, *Characterization of a dc atmospheric pressure normal glow discharge.* Plasma Sources Science and Technology, 2005. **14**: p. 700-711.

198. Wiseman, H. and B. Halliwell, *Damage to DNA by reactive oxygen and nitrogen species: role in inflammatory disease and progression to cancer.* Biochem J, 1996. **313**(Pt 1): p. 17-29.

199. Riley, P.A., *Free Radicals in Biology: Oxidative Stress and the Effects of Ionizing Radiation.* International Journal of Radiation Biology, 1994. **65**(1): p. 27-33.

200. Kalghatgi, S.U., G. Fridman, A. Fridman, G. Friedman, and A. Morss-Clyne, *Non-Thermal Dielectric Barrier Discharge Plasma Treatment of Endothelial Cells*, in *30th Annual International Conference of the IEEE Engineering in Medicine and Biology Society (IEEE EMBS)*. 2008: Vancouver, British Columbia, Canada.

201. Kogelschatz, U., *Dielectric-barrier discharges: Their history, discharge physics, and industrial applications.* Plasma Chemistry and Plasma Processing, 2003. **23**(1): p. 1-46.

VITA

Education

Ph.D. candidate, Biomedical Engineering, June, 2006 – 2008, expected
School of Biomedical Engineering, Science, and Health Systems,
Drexel University, Philadelphia, Pennsylvania

M.S., Biomedical Science, January, 2003 – June, 2006
School of Biomedical Engineering, Science, and Health Systems,
Drexel University, Philadelphia, Pennsylvania

B.S., Math, Stats and Comp Sci, September, 1995 – June, 2003
College of Liberal Arts and Sciences,
University of Illinois at Chicago (UIC), Chicago, Illinois

Professional Experience

Graduate Research Fellow, primary appointment, January, 2003 – present
Department of Electrical and Computer Engineering,
Drexel University, Philadelphia, Pennsylvania

Graduate Assistant, partial appointment, March, 2004 – present
Department of Mechanical Engineering and Mechanics,
Drexel University, Philadelphia, Pennsylvania

Senior Software Developer, consultant, November, 1999 – July, 2002
Compuware Corporation, Rosemont, Illinois.

Teaching assistant, August, 1996 – December, 1996
University of Illinois at Chicago (UIC), Chicago, Illinois.

Field of research

- Non-equilibrium plasma for processing of biomaterials;
- Polymer treatment and surface modification for wettability and biocompatibility;
- Applications of non-equilibrium discharges in medicine and biology;
- Characterization of physical, biochemical, and mechanical properties of the treated material;
- Plasma characterization;
- Plasma power supply design and development.

Publications

- Peer-reviewed journal publications – 11;
- Invited talks at international conferences – 4;
- Invited talks at international conferences, presented by co-authors – 8;
- Conference proceedings – 12;
- Conference oral and poster presentations – 94;
- Patents and patent applications – 2.